OCEAN SYSTEMS RESEARCH REPORT 4-90

Rapid Thermal Ice Penetration:
Feasibility Study for an
"A" Size Sensor

James K. Andersen, Dr. Kent T.S. Tzou, and Dr. Ching-Jen Chen
Ocean Systems Research, Inc.
580 Bellerive Drive Suite 5C
Annapolis, Maryland 21401

16 November 1990

Final Report Contract No. N62269-90-0546
Contract Dollar Amount: $132,194.00

Prepared for:
Dr. Arthur Horbach
Naval Air Development Center
Code 5031
Warminster, PA 18974-5000

19950120 066

SECURITY CLASSIFICATION OF THIS PAGE

REPORT DOCUMENTATION PAGE

Form Approved
OMB No. 0704-0188

1a. REPORT SECURITY CLASSIFICATION Unclassified	1b. RESTRICTIVE MARKINGS
2a. SECURITY CLASSIFICATION AUTHORITY	3. DISTRIBUTION/AVAILABILITY OF REPORT Approved for public release; distribution unlimited
2b. DECLASSIFICATION/DOWNGRADING SCHEDULE	
4. PERFORMING ORGANIZATION REPORT NUMBER(S)	5. MONITORING ORGANIZATION REPORT NUMBER(S)
6a. NAME OF PERFORMING ORGANIZATION Ocean Systems Research 6b. OFFICE SYMBOL *(If applicable)*	7a. NAME OF MONITORING ORGANIZATION Naval Air Development Center
6c. ADDRESS *(City, State, and ZIP Code)* 580 Bellerive Drive Suite 5C Annapolis, Maryland 21401	7b. ADDRESS *(City, State, and ZIP Code)* Warminster, PA 18974-5000
8a. NAME OF FUNDING/SPONSORING ORGANIZATION 8b. OFFICE SYMBOL *(If applicable)*	9. PROCUREMENT INSTRUMENT IDENTIFICATION NUMBER N62269-90C-0546
8c. ADDRESS *(City, State, and ZIP Code)*	10. SOURCE OF FUNDING NUMBERS PROGRAM ELEMENT NO. / PROJECT NO. / TASK NO. / WORK UNIT ACCESSION NO.

11. TITLE *(Include Security Classification)*
Rapid Thermal Ice Penetration: Feasibility Study for an "A" size sensor (U)

12. PERSONAL AUTHOR(S)
James K. Andersen, Dr. Kent T.S. Tzou and Dr. Ching-Jen Chen

13a. TYPE OF REPORT	13b. TIME COVERED	14. DATE OF REPORT *(Year, Month, Day)*	15. PAGE COUNT
Final	FROM 6/90 TO 10/90	11/19/90	113

16. SUPPLEMENTARY NOTATION

17. COSATI CODES			18. SUBJECT TERMS *(Continue on reverse if necessary and identify by block number)*
FIELD	GROUP	SUB-GROUP	Ice Penetration Arctic Sensors

19. ABSTRACT *(Continue on reverse if necessary and identify by block number)*

Ocean Systems Research, Inc. has developed a Rapid Thermal Ice Penetrator (patent pending) with a demonstrated capability to penetrate thick Arctic ice at rates in excess of 6 feet per minute. This report addresses research and testing performed to determine the feasibility of the concept for rapid delivery of "A" size (4 7/8 inch) environmental sensors through 10 feet of ice in under 2 minutes. Two prototype "A" size penetrators were built and successfully tested. A prototype autonomous uprighting device was also built and tested. An analytical model was also developed to provide the capability to predict the affect of various parameters such as payload diameter, weight, etc. on penetrator performance. Three additional payload sizes were evaluated, these being 10, 14, and 21 inch diameters.

20. DISTRIBUTION/AVAILABILITY OF ABSTRACT ☐ UNCLASSIFIED/UNLIMITED ☒ SAME AS RPT. ☐ DTIC USERS	21. ABSTRACT SECURITY CLASSIFICATION Unclassified
22a. NAME OF RESPONSIBLE INDIVIDUAL Dr. Arthur Horbach	22b. TELEPHONE *(Include Area Code)* (215) 441-1485 22c. OFFICE SYMBOL NADC (Code5031)

DD Form 1473, JUN 86 — Previous editions are obsolete. — SECURITY CLASSIFICATION OF THIS PAGE

S/N 0102-LF-014-6603

Table of Contents

1.0 Summary

In May of 1989 Ocean Systems Research (OSR) built and tested its Rapid Thermal Ice Penetrator (patent pending). It created a 9-10 inch diameter hole in a 42 inch thick block of ice in approximately 1.5 minutes.

Based upon the tremendous success of the above test, and the enormous potential for improvements, OSR received a research contract (N62269-90-C-0546) from the Naval Air Development Center in Warminster, PA to assess the feasibility of adapting their ice penetrator technology to an "A" size configuration (5 inch diameter) for an Arctic environmental sensor. As part of this research effort two ice penetrators were built and tested. Both penetrators achieved penetration rates in excess of 5 feet per minute, representing a greater than threefold increase in speed as compared to the 1989 testing.

Also developed under this contract was a numerical model for predicting the penetration rate, efficiency, and resultant hole diameter for various penetrator configurations. The analytical results generated by the model have shown good correlation with experimental data to date. The analytical model was also used to test the feasibility of applying the OSR ice penetrator concept to several other payload sizes ranging from 5 to 21 inches in diameter. In all of the cases analyzed, predicted results indicated that penetrating 10 feet of ice in 2 minutes can be easily achieved.

The feasibility of adapting the autonomous uprighting concept to an "A" size configuration was also studied as part of this research effort. A prototype "A" size uprighting device was built that successfully demonstrated the capability to upright an "A" size canister from horizontal to vertical.

2.0 Background

There is a critical need for a rapid means of delivering payloads of various sizes through thick Arctic ice. A vast amount of research and testing has been performed in recent years to develop a viable system expressly for this purpose. Presently one is faced with two basic choices when attempting to deliver a payload through thick Arctic ice:

- melt through the ice
- penetrate via fracturing the ice (eg., kinetic penetrator)

Numerous melt-through methods have been tested by DOD labs/contractors. One method that has been the subject of significant research utilizes a lithium thermochemical contact reaction to melt a hole through the ice. This technology was demonstrated as feasible, however, it proved to be unreliable in practice as well as not being cost effective.(1) In addition, times well in excess of 30 minutes were required to penetrate 10 feet of ice. Competing melt-through technologies are also currently being investigated including, the pumping of an antifreeze type solution around a penetrating nozzle. Whereas this approach shows potential for achieving penetration of 10 feet of

ice in approximately 20 minutes, it appears that the mechanical configuration required to implement this technology may be somewhat complex.

The alternate (i.e. kinetic) approach uses a high velocity shaped projectile to penetrate the ice. In this case, the penetration is very rapid, however, there are two major drawbacks:

1. The tremendous deceleration upon impact with the ice appears incompatible with the delicate sensors/electronics currently in use.
2. It is difficult to maintain communications with the device once it penetrates the ice (i.e., in the case of a sensor) because the object tends to penetrate deeply into the water, never returning to the original point of penetration.

OSR developed the solid propellant ice penetrator to incorporate the best features from both of the above mentioned methods while eliminating their drawbacks. The OSR penetrator utilizes the melt through approach relying on directed, hot, high velocity exhaust gases to provide the high heat transfer coefficient required for rapid penetration.

The concept of operation of the OSR penetrator is as follows: The entire unit will be dropped from a maritime patrol aircraft and, upon reaching the surface of the ice, will automatically right itself to the proper orientation with respect to the ice for penetration. The solid propellant will then be ignited such that the hot gases impinge upon the ice thereby melting it. As the ice

is penetrated, the penetrator will follow the receding ice surface by gravity, its own motive force, or both (depending upon the weight of the payload). The uprighting mechanism also functions as a guide to maintain vertically of the penetrator during the initial stages of penetration. Upon fully penetrating the ice, the penetrator and payload will separate, enabling the payload to carry out its mission.

3.0 HARDWARE DESCRIPTION

3.1 Test Motors

In order to minimize fabrication costs and complete the testing in the allotted four months, the motors were proposed in a heavyweight design. Whereas the external diameter of the test motor matches the final design, the interior volume available for propellant was reduced by the heavy wall steel casings, the thick insulation, and the use of heavy duty threaded closures on either end. Reduced prints of the manufacturing drawings are shown in Figures 1a-e.

The two identically designed motors were designed for an approximate 40 second burn time using a Thiokol TP-H-3443 propellant. The energy content of the propellant was 2250 Btu/Lbm. Chamber pressure of the motors was designed to be 500 psia. The motors employed 5 nozzles. The center nozzle was directed parallel to the longitudinal axis of the motor, whereas the four remaining nozzles were canted 15 degrees to impart rotation. The motors contained 8.3 pounds of propellant each. The net axial thrust of

4 | 3 | E43894 | 2 | 1

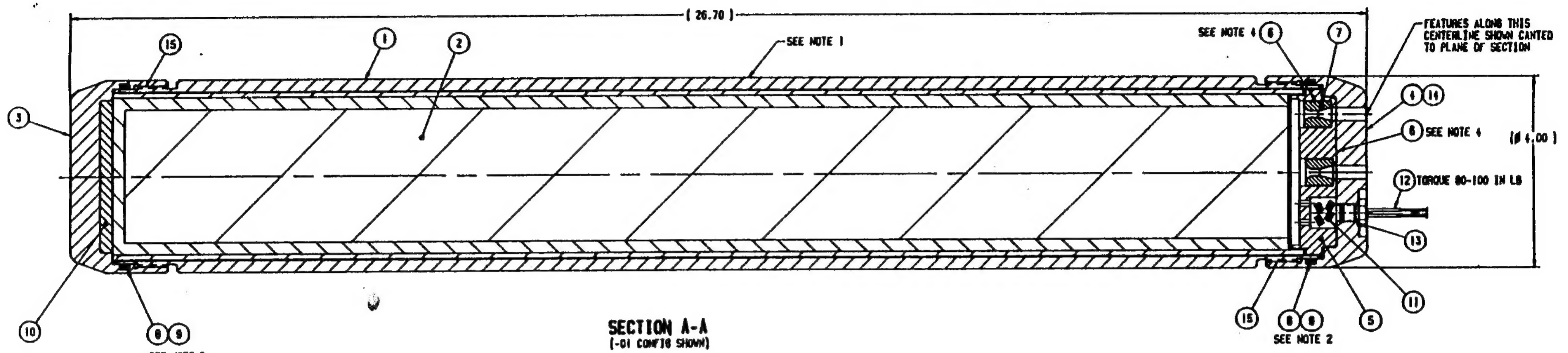

SECTION A-A
(-01 CONFIG SHOWN)

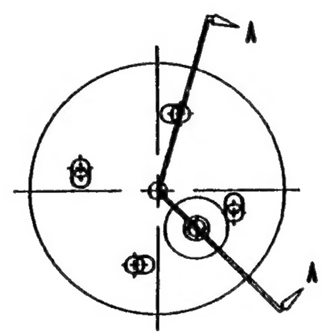

VIEW LOOKING FWD

NOTES:

1. MARK ASSY NO. AND REV LTR PER P-10001-7.
2. APPLY GREASE TO ENTIRE SURFACE OF O-RING PRIOR TO INSTALLING.
3. COPPER. SIZE: .500 OD X .380 ID X .030 THK.
4. CURE ADHESIVE FOR 16 HOURS MINIMUM AT 70°-100° F.
5. PROOF PRESSURE TEST -02 CONFIG TO THE REQUIREMENTS OF DWG E43891.

-02	-01	ITEM NO.	CAGE NO.	PART NO. OR IDENTIFYING NO.	NOMENCLATURE OR DESCRIPTION	MATERIAL	SPECIFICATION
AR	AR	15			THD COMPOUND		MIL-T-5544
1	-	14		E43891-04	CLOSURE, PROOF TEST		
-	1	13			BASKET	SEE NOTE 3	
-	1	12	10640	1196A	SQUIB		
-	8	11	27934	2A	PELLETS, IGNITER	$BKNO_3$	TC ESMN-13, CLASS I
-	AR	10			INHIBITOR	TA-D-308	ESPR-80
AR	AR	9			GREASE		MIL-G-4343
2	2	8		AS 568-239	O-RING	SYNTH RBR	TC SE-2000, CL C
-	5	7		E43892-02	INSERT, NOZZLE		
-	AR	6	33564	EA 934NA	ADHESIVE		TC ESMN-06
-	1	5		E43892-01	INSULATOR, NOZZLE CLOSURE		
-	1	4		E43891-02	CLOSURE, NOZZLE		
1	1	3		E43891-03	HEAD CAP		
-	1	2		E43893-03	GRAIN ASSY		
1	1	1		E43891-01	CHAMBER		

QTY REQUIRED PER DASH NO.

PARTS LIST

DASH NO.	USED ON	NEXT ASSY
-02	TE-N-913-2	
-01	TE-N-913-2	FINAL

APPLICATION

GAS GENERATOR ASSY

MODEL NO. OR DESIGNATION: ICE PENETRATOR

SIZE D | CAGE NO. 07299 | DWG. NO. E43894

SCALE 1/1 | SHEET 1 OF 1

REDUCED PRINT

Figure 1a

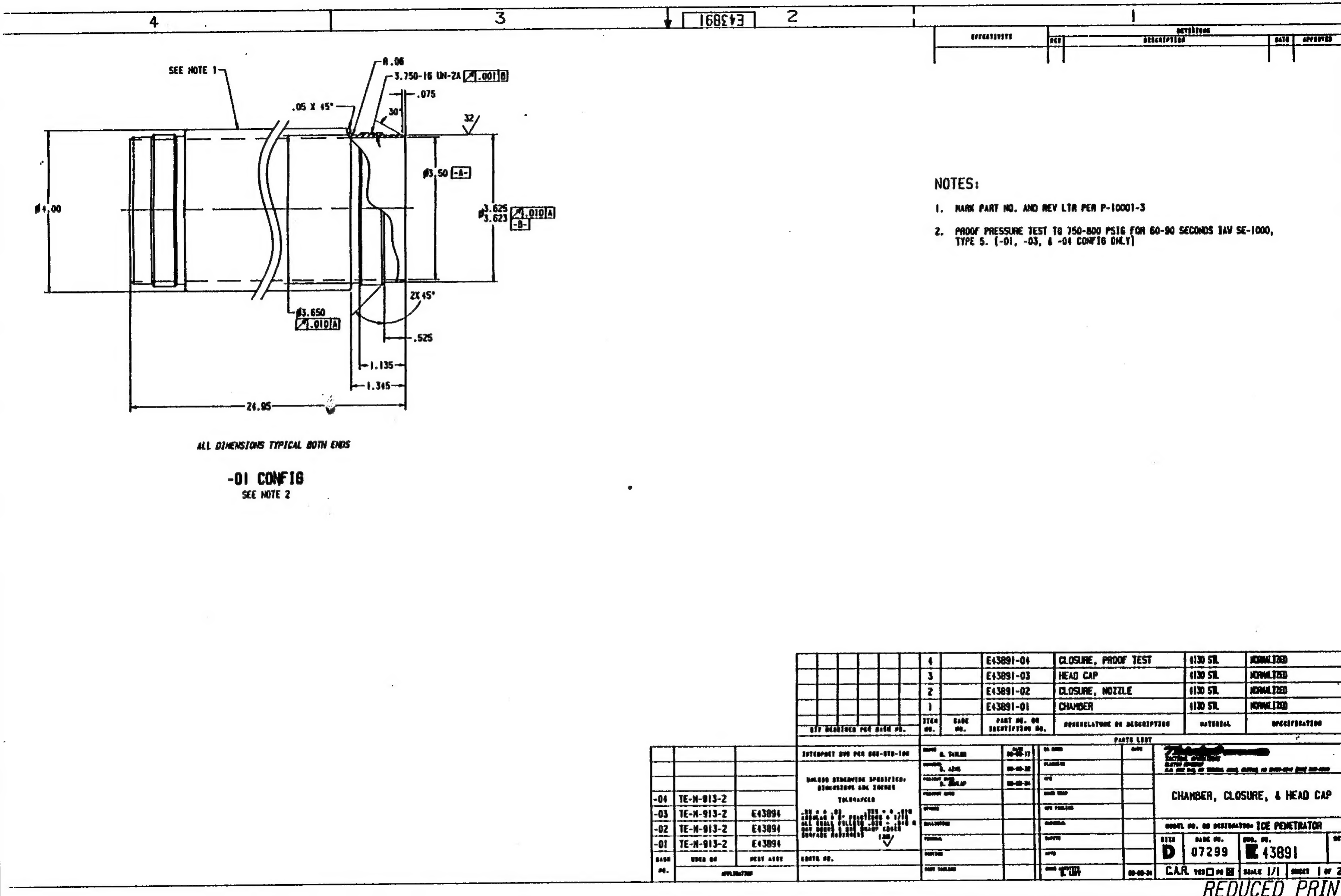
E43891
SEE NOTE 1
R.06
3.750-16 UN-2A .001 B
.075
.05 X 45°
30°
32
ø3.50 -A-
ø4.00
ø3.625 3.623 .010 A -B-
ø3.650 .010 A
2X 45°
.525
1.135
1.345
24.85
ALL DIMENSIONS TYPICAL BOTH ENDS
-01 CONFIG
SEE NOTE 2
NOTES:
1. MARK PART NO. AND REV LTR PER P-10001-3
2. PROOF PRESSURE TEST TO 750-800 PSIG FOR 60-90 SECONDS IAW SE-1000, TYPE 5. (-01, -03, & -04 CONFIG ONLY)
4 E43891-04 CLOSURE, PROOF TEST 4130 STL NORMALIZED
3 E43891-03 HEAD CAP 4130 STL NORMALIZED
2 E43891-02 CLOSURE, NOZZLE 4130 STL NORMALIZED
1 E43891-01 CHAMBER 4130 STL NORMALIZED
PARTS LIST
-04 TE-M-913-2
-03 TE-M-913-2 E43894
-02 TE-M-913-2 E43894
-01 TE-M-913-2 E43894
CHAMBER, CLOSURE, & HEAD CAP
ICE PENETRATOR
D 07299 E43891
C.A.R.
SCALE 1/1 SHEET 1 OF 2
REDUCED PRINT

Figure 1b

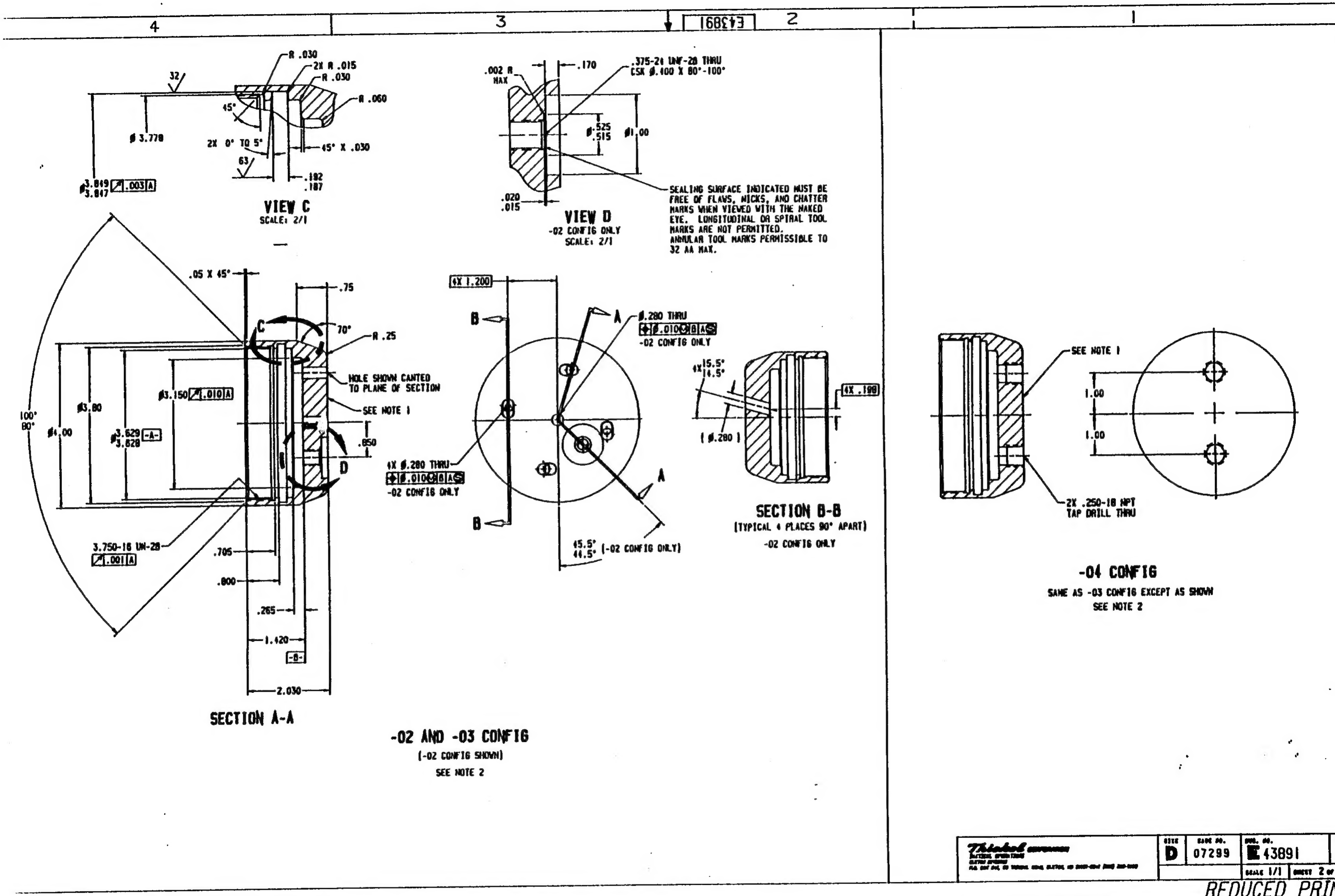

VIEW C
SCALE: 2/1
VIEW D
-02 CONFIG ONLY
SCALE: 2/1
.375-24 UNF-2B THRU
CSK ⌀.400 X 80°-100°
SEALING SURFACE INDICATED MUST BE FREE OF FLAWS, NICKS, AND CHATTER MARKS WHEN VIEWED WITH THE NAKED EYE. LONGITUDINAL OR SPIRAL TOOL MARKS ARE NOT PERMITTED. ANNULAR TOOL MARKS PERMISSIBLE TO 32 AA MAX.
HOLE SHOWN CANTED TO PLANE OF SECTION
SEE NOTE 1
SECTION A-A
-02 AND -03 CONFIG
(-02 CONFIG SHOWN)
SEE NOTE 2
⌀.280 THRU
-02 CONFIG ONLY
4X ⌀.280 THRU
-02 CONFIG ONLY
SECTION B-B
(TYPICAL 4 PLACES 90° APART)
-02 CONFIG ONLY
SEE NOTE 1
2X .250-18 NPT TAP DRILL THRU
-04 CONFIG
SAME AS -03 CONFIG EXCEPT AS SHOWN
SEE NOTE 2
D
07299
E43891
SCALE 1/1
SHEET 2 OF 2
REDUCED PRINT

Figure 1c

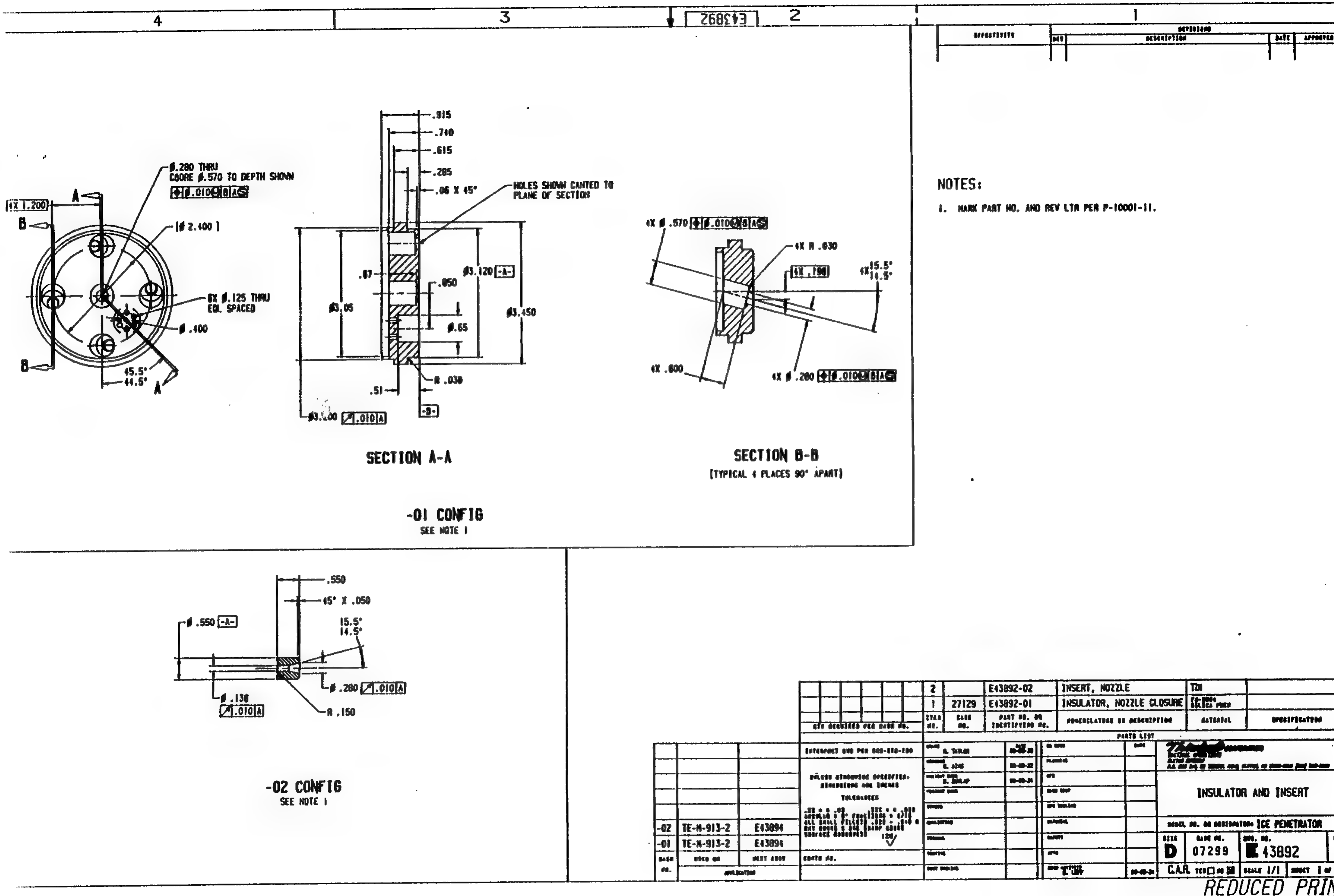
E43892
NOTES:
1. MARK PART NO. AND REV LTR PER P-10001-11.
SECTION A-A
SECTION B-B
(TYPICAL 4 PLACES 90° APART)
-01 CONFIG
SEE NOTE 1
-02 CONFIG
SEE NOTE 1
HOLES SHOWN CANTED TO PLANE OF SECTION
ø.280 THRU
CBORE ø.570 TO DEPTH SHOWN
6X ø.125 THRU
EQL SPACED
E43892-02
INSERT, NOZZLE
27129
E43892-01
INSULATOR, NOZZLE CLOSURE
INSULATOR AND INSERT
ICE PENETRATOR
D
07299
43892
TE-M-913-2
E43894
REDUCED PRINT

Figure 1d

NOTES:

1. MARK PART NO. AND REV LTR PER P-10001-11.
2. RADIOGRAPHIC INSPECT GRAIN ASSY 4 PLACES 90° APART. SEPARATIONS AND VOID CRITERIA TO BE DETERMINED BY TC ENGINEER.

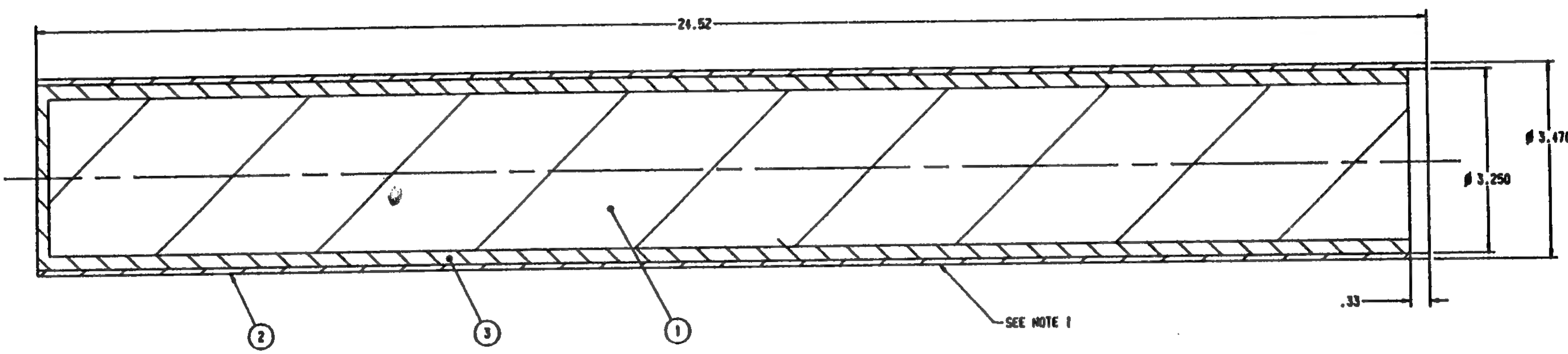

QTY REQUIRED PER DASH NO. -03	ITEM NO.	CAGE NO.	PART NO. OR IDENTIFYING NO.	NOMENCLATURE OR DESCRIPTION	MATERIAL	SPECIFICATION
AR	3			INHIBITOR	TI-H-3000	ESPR-100
1	2		E43893-02	INSULATOR, CASE	PAPER PHEN	SEE F/B
1	1		E43893-01	PROPELLANT	TP-H-3413	ø2.75 X 24.00 LG

PARTS LIST

DASH NO.	USED ON	NEXT ASSY
-03	TE-H-913-2	E43894

APPLICATION

GRAIN ASSY

ICE PENETRATOR

SIZE D | CAGE NO. 07299 | DWG. NO. E43893

SCALE 1/1

REDUCED PRIN

Figure 1e

the motors, as well as the total weight of each motors was approximately 40 pounds.

3.2 Uprighting Device

In order for the penetrator to function properly it must be oriented somewhat normal to the ice surface prior to penetration. The uprighting device, which surrounds the penetrator and sensor payload, carries out this function. The entire sensor package, including the uprighter, is designed to fit within the standard envelope dimensions for an "A" size sonobuoy, namely 4 7/8 inch O.D. and 36 inches in length. In addition, the "A" size package has a weight limit of 50 lbs, and must upright itself in under 4 seconds. The I.D. of the uprighting device is 4.00 inches (nominal).

3.2.1 Prototype Fabrication

As part of the research effort a prototype uprighting device meeting the above requirements was built and tested (See Figure 1 & 2). It consisted of a 4.25 inch diameter O.D. aluminum cylinder, approximately 36 inches in length. Mounted around the outer periphery of the cylinder are 6 retractable legs, that when collapsed give the device an O.D. of 4 7/8 inches. A combination of multiple leaf springs and a coil spring provide the motive force for uprighting the unit.

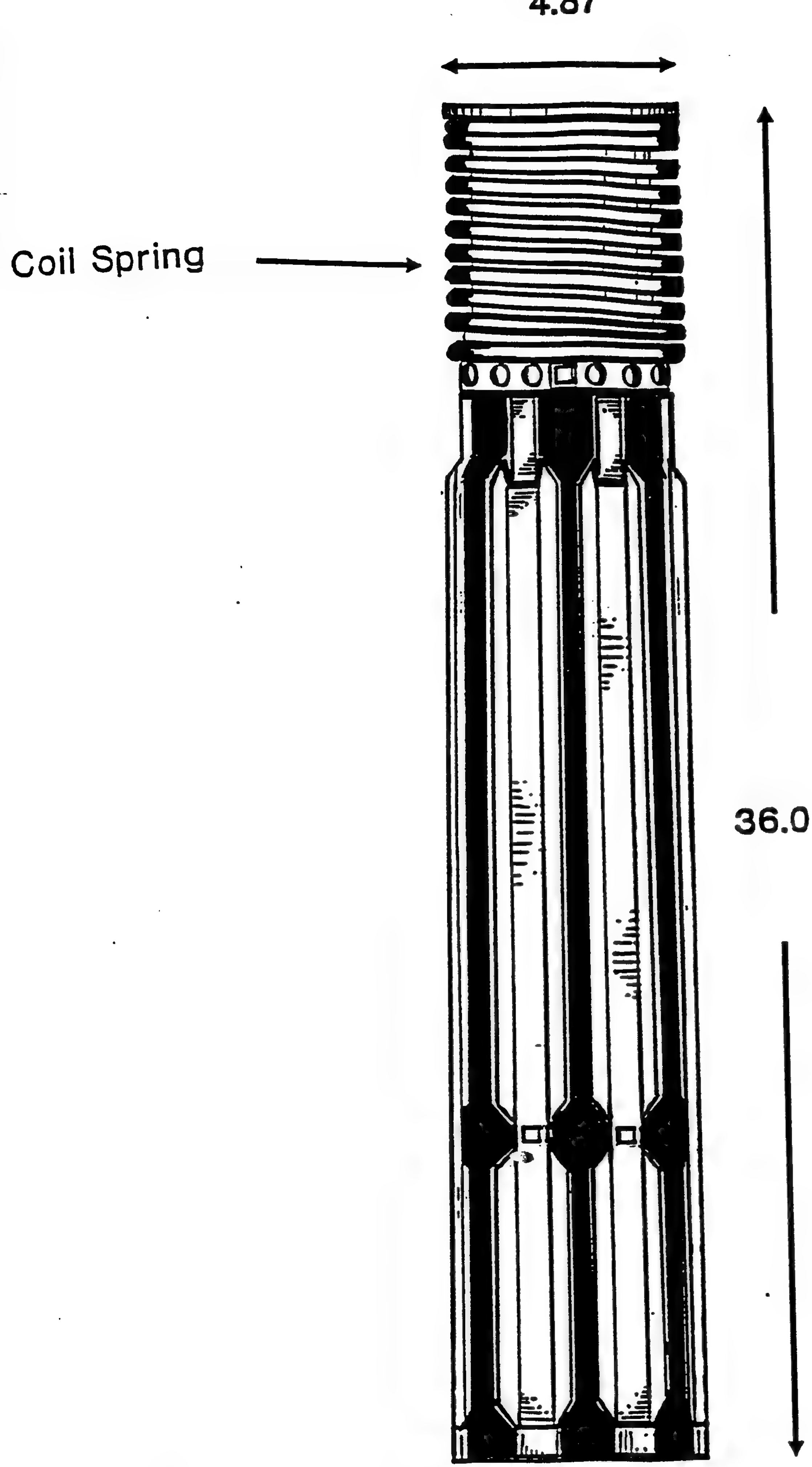

Figure 1 OSR Uprighting Device (closed)

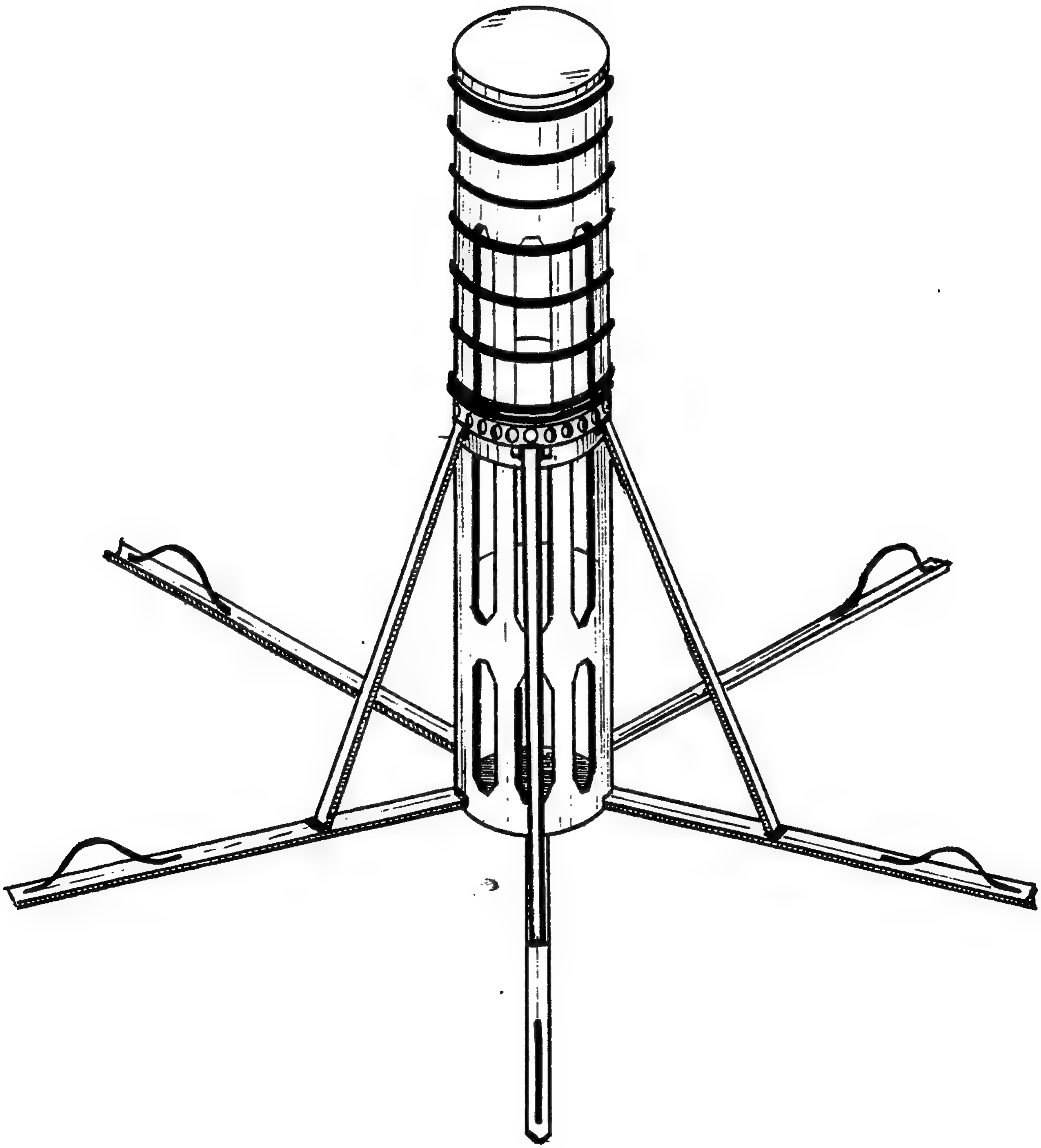

Figure 2 OSR Uprighting Device (open)

The device is designed to operate as follows (see Figure 3):

1. Unit comes to rest horizontally on the surface of the ice.
2. Release mechanism unleashes springs, leaf springs open legs to approximately 12 - 15 degrees.
3. Coil spring provides the remaining motive force required to bring the unit to vertical.

The spring constant (k) of the coil spring used in the prototype was 13.5 lbs/inch. The total travel of the coil spring was approximately 10 inches (closed to open) still remaining slightly compressed at full extension.

For exhibition purposes only, the prototype unit incorporated a manual lead screw device for opening and closing rather than an instantaneous release mechanism.

3.3 Testing

The test apparatus was set up as shown in Figures 4 and 6. To overcome thrust with an adequate safely margin, weight was added at the top of the tubular guide rod (69 pounds for test #1, 30 pounds for test 2). A 41 inch thick ice block was used in test 1 and a 62.5 inch thick block was used in test 2. Three video cameras (two high speed black and white and one standard color videp recorder) were positioned at various angles to monitor and record ice penetrator performance during the test. Fans were strategically positioned to remove smoke/vapor thus allowing better video coverage. Figures 5 and 7 depict test results from tests 1 and 2 respectively.

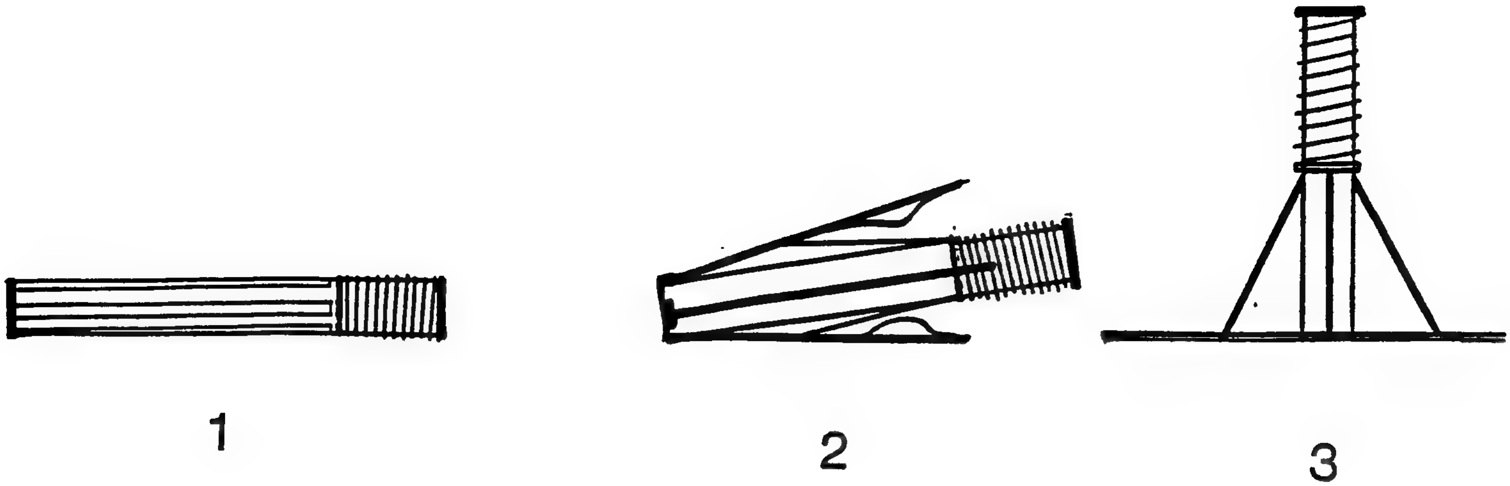

Figure 3 OSR Uprighting Device Operation

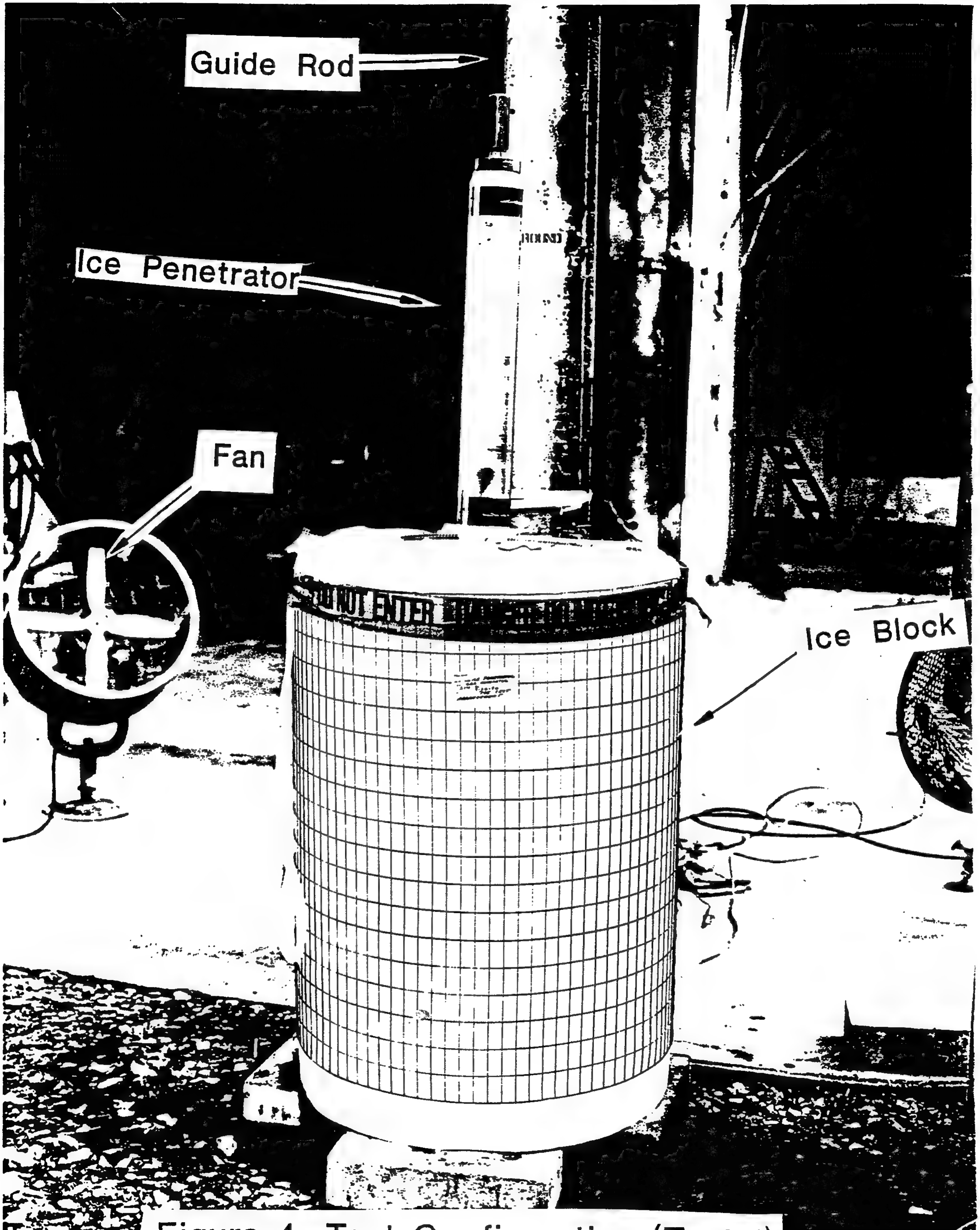

Figure 4 Test Configuration (Test 1)

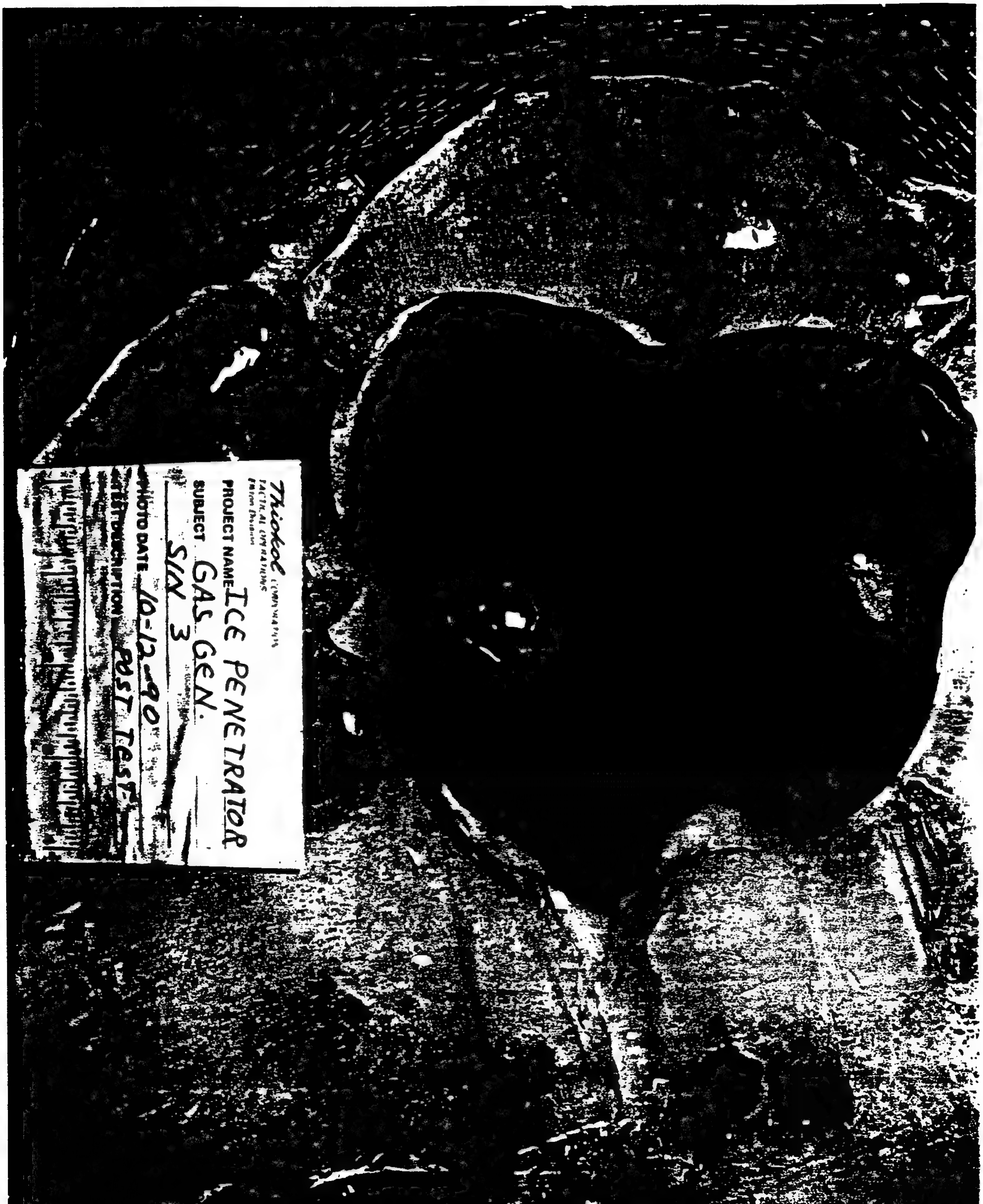

Figure 5 Test Results (Test 1

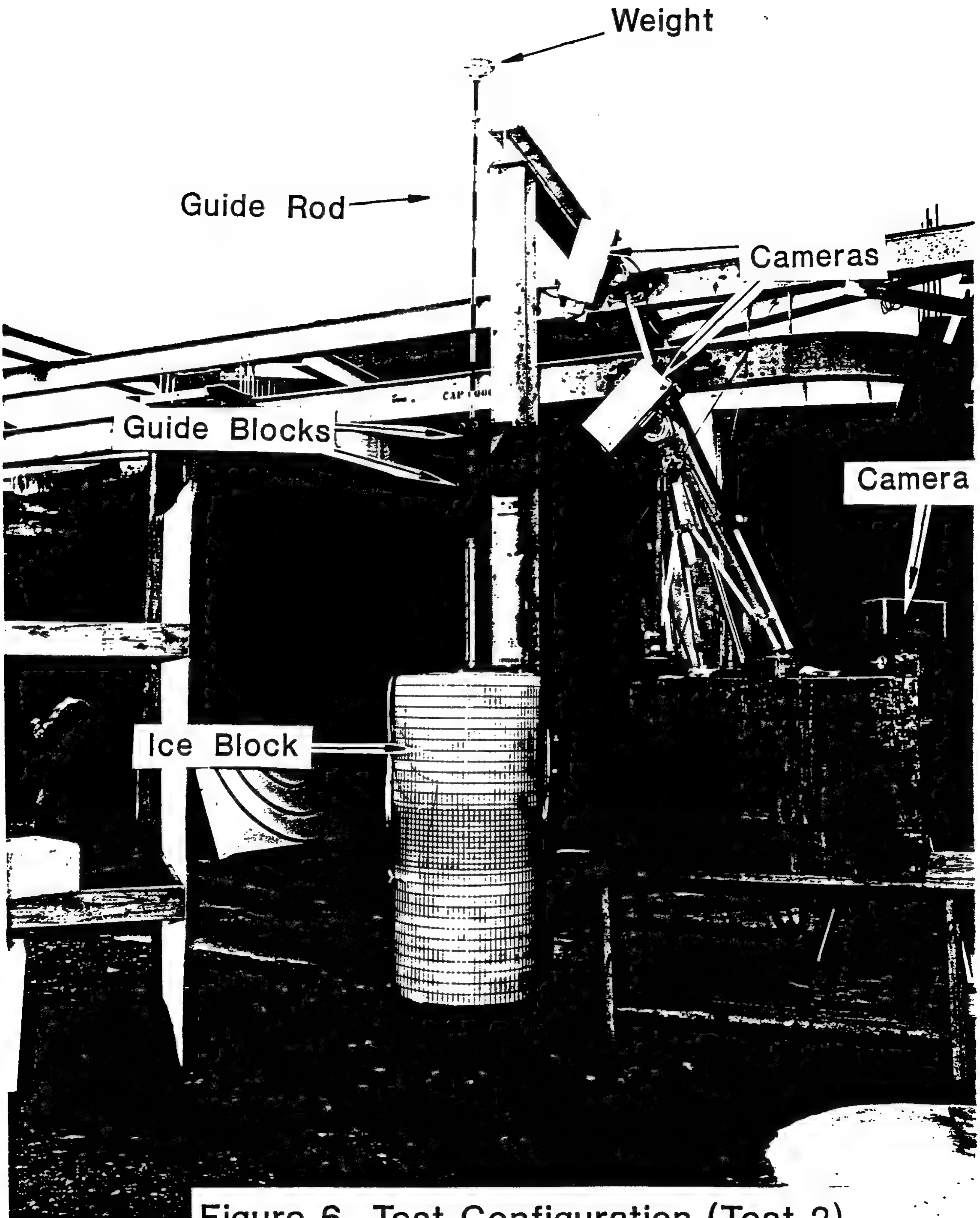

Figure 6 Test Configuration (Test 2)

Figure 7 Test Results (Test 2)

Analytical Models
Section 4 Table of Contents

4.0 Summary and Conclusions

A simple lumped parameter analysis was used to develop an analytical model for predicting the performance of our Rapid Thermal Ice Penetrator. Based on empirical formula and test data, we confirmed the model. Results from the tests and the predictions are in good agreement. Aso investigated are the effects of various parameters on the performance of the system. Applications to other sizes, 10, 14 and 21 inches in diameter are possible. For a 4-inch penetrator having weight limitation, we propose a reverse jet to balance the thrust force. The proposed system has a total of 9 nozzles with 4 reverse acting nozzles. We predict that it can penetrate 10 feet of ice in 100 seconds.

4.1 Introduction

For many applications, there is a need to deliver sensors or weapons through thick Arctic ice. Therefore, a requirement exists to develop a rapid ice penetrating system. Reference [2], discusses a technique using a solid-fuel rocket to drill through the glacier ice. In 1989, OSR has designed and tested a solid propellant ice penetrator. The system penetrated 42 inches of ice in 89 seconds. That is 0.46 inch per second. [3] [4].

Now, there are two basic methods for delivering a payload through thick Arctic ice [3]. One method is using a slow melt-through approach. It will take up to 30 minutes to penetrate 10 feet of ice. That is only 0.07 inch per second. The other method is using a high speed kinetic penetrator. Slow penetrating rate and high impact force during penetration are the key drawbacks for the first and second methods respectively. The goal of this program is to develop a new solid propellant ice penetrator. It requires that the system penetrate 10 feet of ice in 2 minutes. Appendices [2] and [3] present the results from tests conducted by Thiokol. This report presents our analytical study of the program.

4.2 Analytical Approaches

4.2.1 Physical Model for Thermal Ice Penetration

The rapid thermal ice penetration system is essentially a device capable of issuing high temperature gases down toward the ice surface to provide a rapid thermal heating to the ice surface. When the ice surface encounters the rapid heating, a layer of ice, due to thermal expansion and stress, may begin to crack and simultaneously melt, forming a liquid layer on top of the ice. Figure 8 shows a sketch of the rapid thermal ice penetration system. The device moves downward due to its own weight thereby penetrating as the melted and/or cracked ice is removed by the jet impinging on the surface.

Before a mathematical model can be formulated to predict the penetration rate of the rapid thermal ice penetration system, a proper account and discussion of the physical processes involved is necessary. In order to present a clear picture of the physical process, the physical process of the cyclic phenomenon has been divided into four stages.

<u>Stage 1- Rapid Heating of Ice Layer</u>

In this stage, the physical process is dominated by the rapid transient conduction in the ice where the heat is provided at the ice surface. Preliminary analysis shows that the time spent on heating the ice surface to melting point is on the order of milliseconds.

<u>Stage 2- Rapid Thermal Expansion and Initial Crack</u>

The ice property that has the dominant influence on cracking

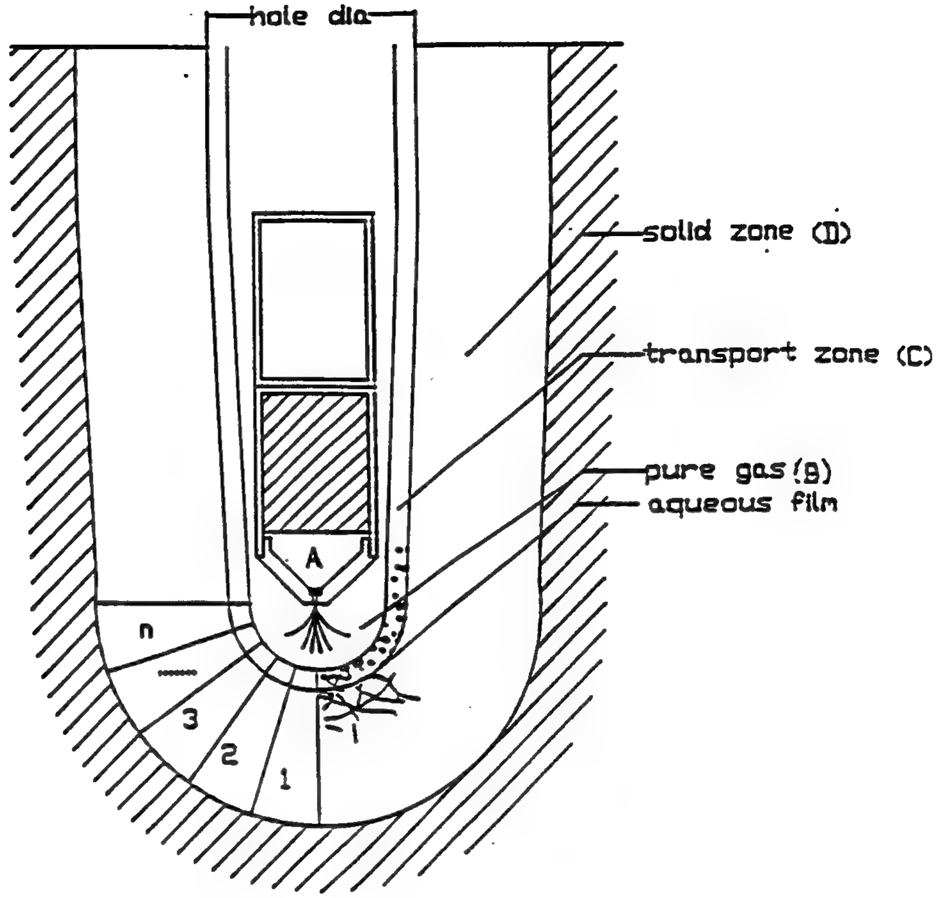

Figure 8

Sketch of a Rapid Thermal Ice Penetrator

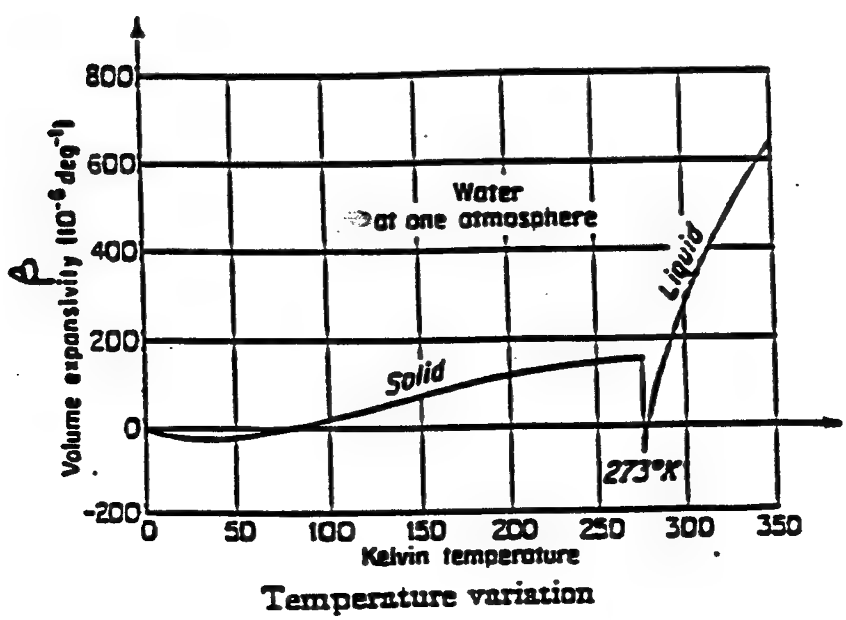

Figure 9

is the thermal expansion coefficient or expansivity, ß. It is defined as:

$$\beta = \frac{1}{\rho}\frac{\partial \rho}{\partial T} \qquad \begin{array}{l} T = \text{Temperature (°Kelvin)} \\ \rho = \text{density of ice} \end{array}$$

For ice near the melting point, 32° (273°K), the thermal expansion coefficient has a peculiar behavior in that it changes from $\beta = 158\times10^{-6}$ (1/K°) as solid ice at 273°K (32°F) to $\beta = -67\times10^{-6}$ (1/K°) as liquid water at 273°K (32°F). Therefore, cracking is initiated by rapid contraction as the ice changes from solid to liquid. Figure 9 shows the variation of ice expansivity or expansion coefficient as a function of temperature in Kelvin (1 deg K = 1 deg C).

<u>Stage 3 - Rapid Melting and Continuous Cracking</u>

In this period the heat begins to penetrate around the crack line made in Stage 2 causing the ice to melt and continuously to crack into further small pieces. During this stage, some of the cracked ice may become movable due to melting and fragmentation of the fracture such that the impinging jet may lift and move the fractured ice. This stage will take a much longer time since the heat transfer coefficient in the cracks will be, in general, less than the heat transfer coefficient at the ice surface facing the thermal ice penetration system. Also, the heating at the deeper crack gap would take a longer time since it take longer for the heat to reach it.

<u>Stage 4 - Removal of the Gas/Liquid/Ice Mixture</u>

In this stage the melting of the ice through the crack becomes substantial and the ice may begin to mix with the liquid, and possibly, to become mixed with the vapor that is generated due to the superheating from the high temperature gas issuing from the penetrator. The removal of the gas/liquid/ice mixture is accomplished by the pressure difference between the atmosphere and that of propellant gas issuing from the penetrator. It is reasonable to expect that the deeper the thermal ice penetrator penetrates, the longer it takes for the gas/liquid/ice/mixture to be removed.

When the gas/liquid/ice mixture is removed, the ice layer again becomes solid and faces the rapid heating again. Therefore, the physical process will be to repeat Stage 1 of transient thermal conduction of the ice layer again.

4.2.2 Mathematical Model

For the analytical approach, we consider a simple lumped parameter analysis as follows.

The governing equation for transient thermal response of a fixed volume can be expressed as:

$$h\ A\ (T - T_f) = -\rho V C_p \frac{dT}{dt} \qquad (1)$$

Where h = heat transfer coefficient

A_s = exposed surface area

T = average ice/water temperature

T_f = temperature of the fluid film

ρ = density of ice

V = volume of ice $\underline{\pi}\ D_i^2$

D_i = diameter of ice hole

z = depth of ice column

C_p = specific heat of ice

t = thermal response time

Integrating equation (1) and evaluating the constant to satisfy the initial condition, $t = 0$, $T =$ we have the following solution:

$$\frac{T - T_f}{T_i - T_f} = \frac{-h\ A_s}{\rho\ C_p V} \tag{2}$$

Since thermal diffusivity $\alpha = \frac{k}{C_p}$, where k is thermal conductivity, equation (2) becomes:

$$\frac{T - T_f}{T_i - T_f} = \mathrm{Exp}\left[- \frac{h\alpha A_s}{kV} \cdot t\right] = \mathrm{Exp}\ [- t/\tau] \tag{3}$$

$$\text{where } \tau = \frac{kV}{h\alpha A_s}$$

The parameter τ is the so-called time constant of the body. The larger the value of τ, the slower the body responds to the changes in temperature. Equation (3) can be arranged to:

$$\ln\left[\frac{T - T_f}{T_i - T_f}\right] = \left[\frac{h\ A_s}{kz}\right] \cdot \left(\frac{4}{\pi}\right) \cdot \left[\frac{\alpha t}{Di^2}\right] = \mathbb{B} \cdot \left(\frac{4}{\pi}\right) \mathbb{F} \tag{4}$$

Where $\mathbb{B}$ is Biot Number and $\mathbb{F}$ is Fourier Time.

For this analysis, we are interested in the thermal response time,

therefore we have:

$$t = \frac{kz \frac{\pi}{4} Di^2}{\alpha h A_s} \ln\left[\frac{T - T_f}{T_i - T_f}\right] \qquad (5)$$

$$V = \frac{\pi}{4} Di^2 z$$

Evaluation of Heat Transfer Coefficient (h)

Correlation of space-average heat transfer coefficient between a plate & arrays of jets has been studied by Gardon & Cobonque (1961-1962). They have reached a correlation formula as:

$$N_u = C_{Nu} \, R_e^{C_{Re}} \qquad \text{with} \quad \begin{aligned} C_{Nu} &= 0.286 \\ C_{Re} &= 0.625 \end{aligned}$$

where $N_u = h\, S_j/k$ is Nusselt Number, and

$$R_e = \frac{u_a \; S_j \; \rho}{\mu}$$ is Reynolds Number,

u_a is arrival velocity, it is defined as $u_a = C_u \frac{u_e d}{z_n}$ with $C_u = 6.63$

where u_e is jet velocity, d is jet diameter, and z_n is the distance from the jet to the plate. S_j is the jet spacing.

In order to apply their correlation formula to this analysis, I define S_j as a characteristic length with

$$S_j = \frac{\pi}{4} \frac{D^2}{N_j}$$

where D is diameter of the bottom of the ice penetrator, N_j is number of jets. Therefore the correlation formula for heat transfer coefficient can be expressed as:

$$h_{gas} = C_{Nu} \quad k_{gas} \quad \frac{4N_j}{\pi D_2} \quad Re^{\,Cre}$$

$$\text{with } R_e = Cu \cdot \frac{U_e d}{Z_i} \sqrt{\frac{\pi D^2}{4N_j}} \cdot \frac{\rho}{\mu}.$$

Furthermore, I assume $h_{water} = C_{gw} \ h_{gas}$ and also assume it varies with time

$$h_{water} = h_{water} \ \text{Exp} \ [-T/C_{time}]$$

where C_{gw} and C_{time} are coefficients, T is total elapsed time in seconds.

Evaluation of Exposed Surface Area A_s

The exposed surface area A_s includes the ice surface facing the propellant jet and the crack channels. In this analysis, I assume

$$A_s = C_{crack} \ \frac{\pi}{4} \ D_i^2$$

Evaluation of the Distance from the jet to the Ice, Z_n

The actual weight (W_{actual}) of the system is supported by the jet impinging on the surface. For N vertical jets, the force can be expressed by

$$F_{jet} = W_{actual} = N_{jet} \ \rho \left[\frac{\pi}{4} d^2 \ u_e\right]\left[C_u \ \frac{u_e d}{Z_n}\right]$$

$$W_{actual} = W_{total} - F_{buoy} - T_{time} \ B_{rate}$$

Where

W_{total} = Initial total weight

W_{buoy} = Buoyancy force due to gas water mixture

T_{time} = Total elapse time

B_{rate} = Propellant burning rate

$$Z_n = N_{jet} \ \rho \left[\frac{\pi}{4} d^2 \ \ ue\right] \left[C_u \ \ u_e \ \cdot d\right] / W_{actual}$$

4.3 Results and Discussions

The mathematical model described in section 3 has been coded into a simple Fortran computer program. Inputs and outputs for two test cases are presented in Attachment A. Required fluid and chemical parameters are provided by Thiokol as shown in Attachment B. In this report, we present results in form of the penetration depth versus time. Variation parameters in the Figures are 3 and 4 explained as follows:

W_{total}	=	Total weight of the system in lbs.
W_{propel}	=	Total propellant weight in lbs.
B_{rate}	=	Propellant burning rate in lb/sec.
N_{cjet}	=	Number of center jet (downward)
N_{djet}	=	Number of downward jet
N_{ujet}	=	Number of upward jet
ang_{jet}	=	Incline angle of the jet
c_{gw}	=	Ratio of heat transfer coefficient in the ice crack channel to the hot gas.
c_{crack}	=	Ratio of the crack surface to the circular surface area of the ice penetrator
C_{time}	=	Decrease in heat transfer coefficient according to the formula $\exp[-T/C_{time}]$ where T is the total elapsed time.

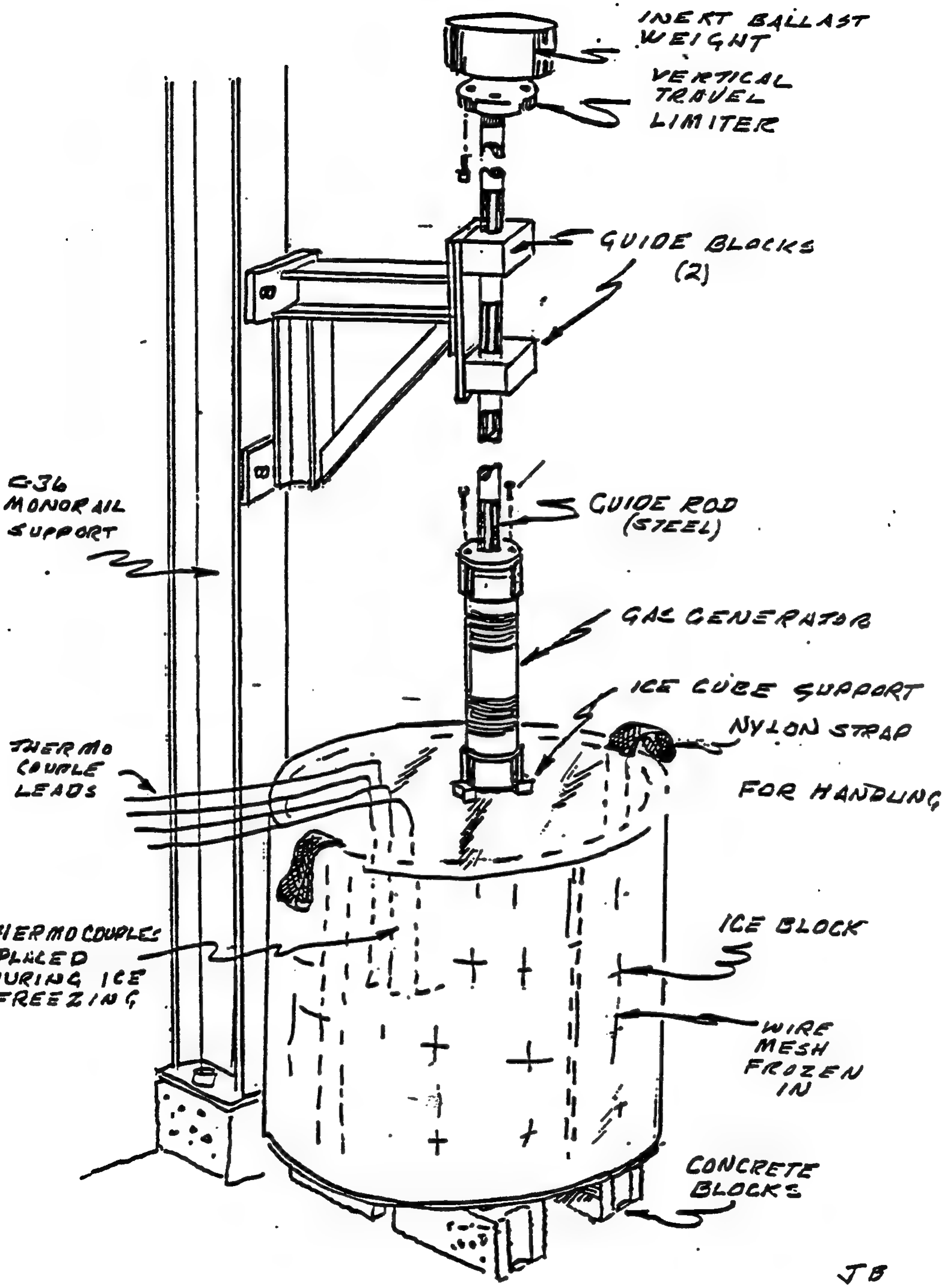

Figure 10

Test Arrangement (Sep. 20 & Oct. 12, 1990)

4.3.1 Validation of the Model

Two tests have been conducted in this program. Figure 10 shows the test arrangement. Figure 11 shows the motor cross section and the jet-hole pattern for the 4-inch penetration. Detail descriptions and results of the test are presented in Appendices [2] and [3].

Figures 12 and 13 present the comparisons of test data and the predictions. For test on September 20, 1990, we have the following results:

Total Weight: 131 lbs.

Total Propellant: 8.3 lbs.

Propellant Burning Rate: 0.180 lb/sec.

Coefficients for the Model:

$C_{gw} = 0.85$

$C_{crack} = 3.0$

$C_{time} = 80$

The penetration rate varies from 1.58 in/sec at depth of 1 inch to 1.01 at depth of 41 inches. The average rate is 1.21 in/sec. Two curves from the test and from the prediction are in good agreement

For test of October 12, 1990 we have the following results:

Total Weight: 90 lbs.

Total Propellant: 8.24 lbs.

Propellant Burning Rate: 0.179 lb/sec.

Coefficients for the Model:

$C_{gw} = 0.85$

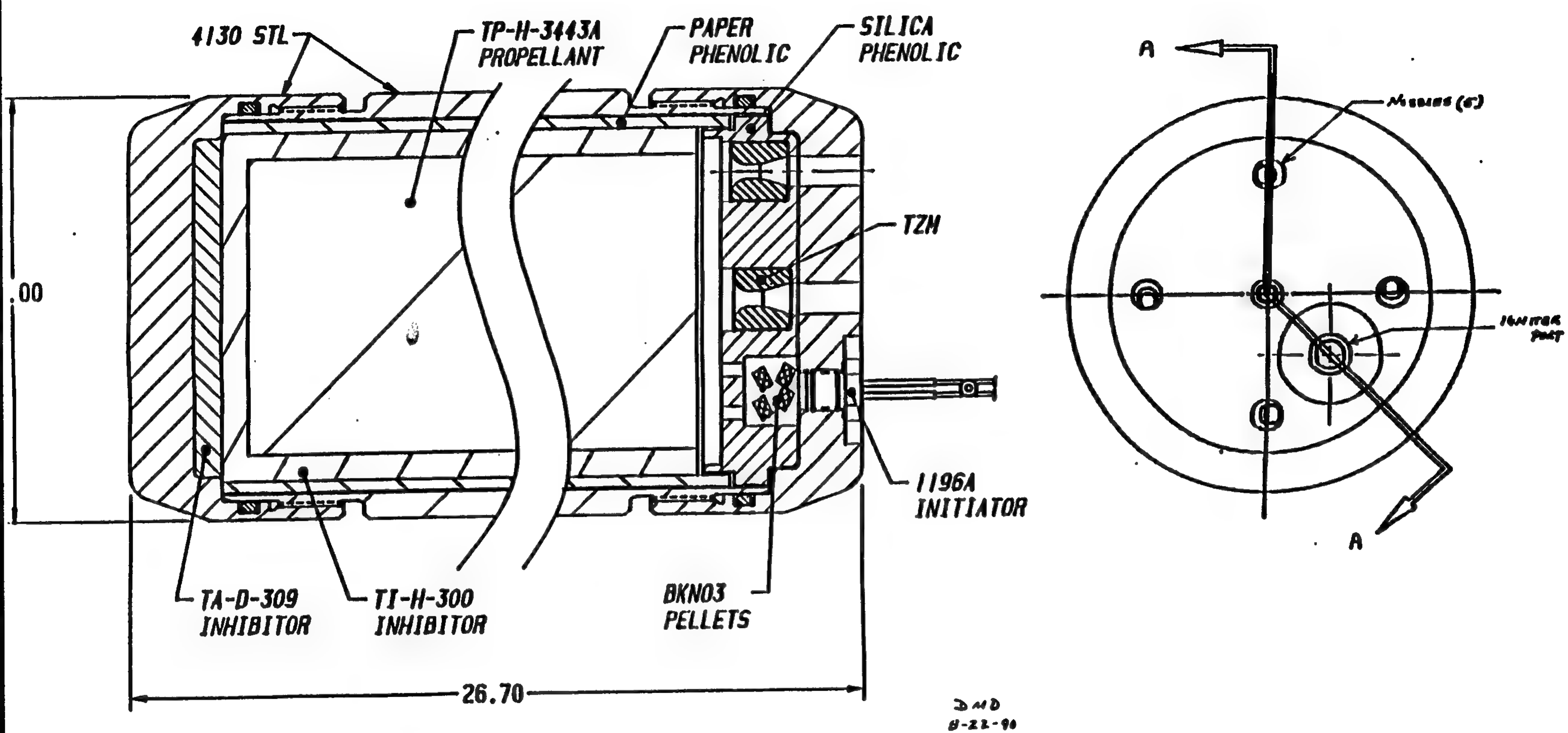

Figure 11

5-Hole Pattern for The Test Ice Penetrator - 4-inch Diameter

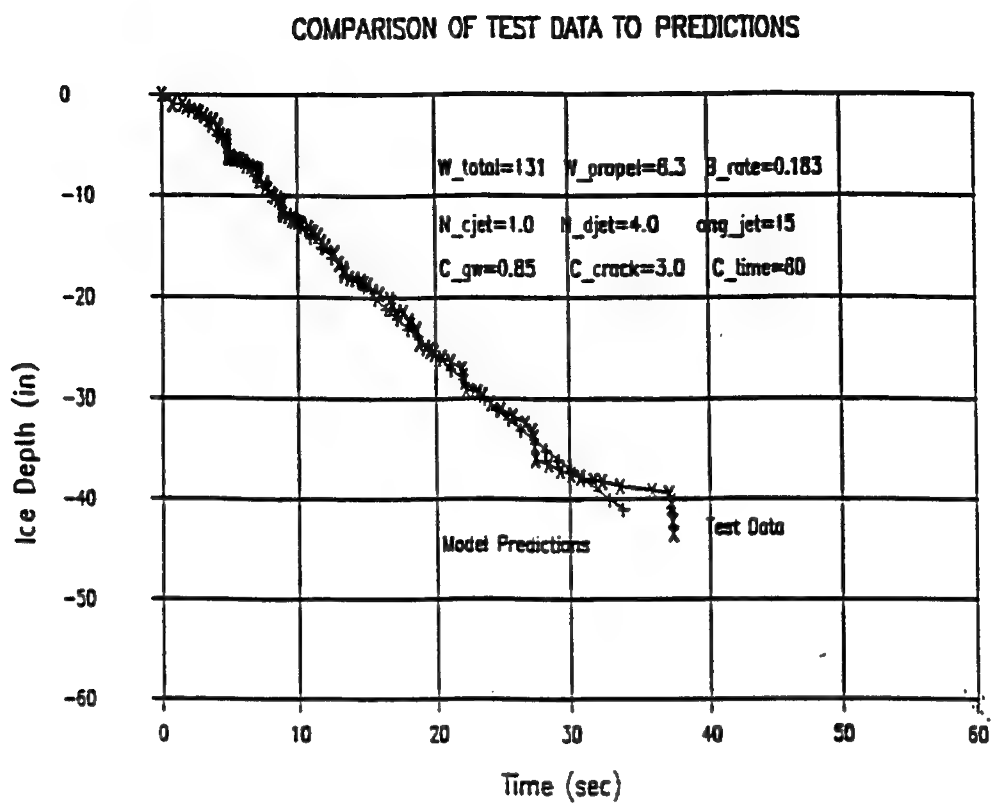

TEST DATE: 20 SEPTEMBER 1990

Figure 12

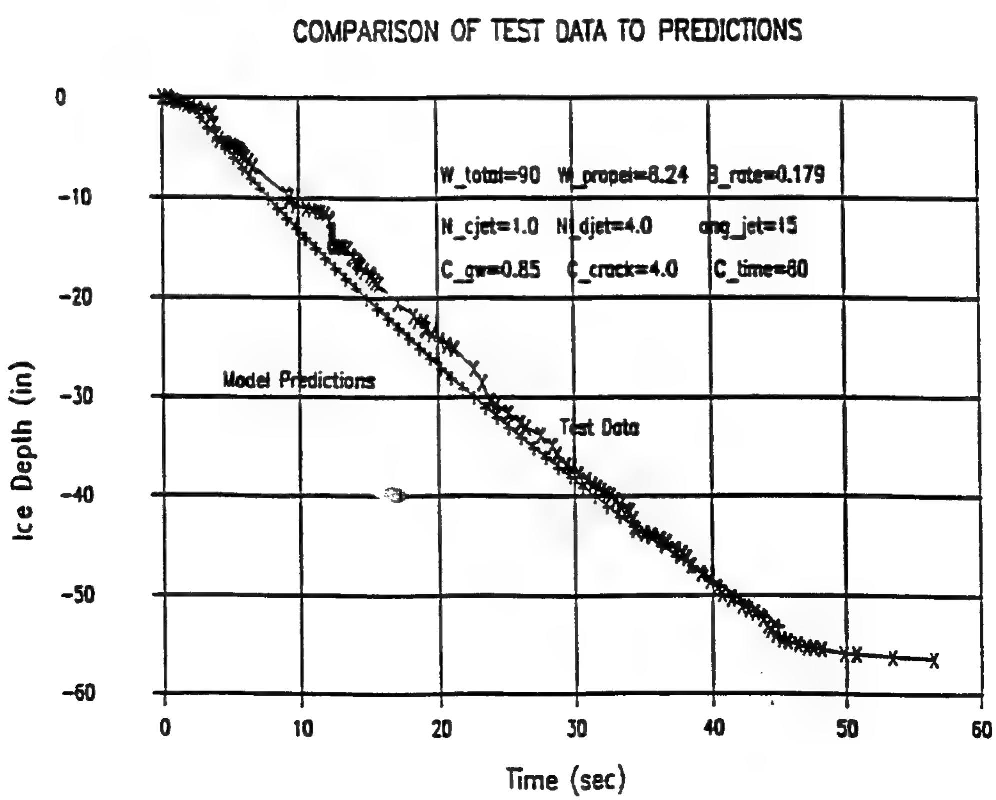

TEST DATE: 12 OCTOBER 1990

Figure 13

$C_{crack} = 4.0$

$C_{time} = 80$

The penetration rate varies from 1.66 in/sec at depth of 1 inch to 0.89 at depth of 53 inches. The average rate is 1.18 in/sec. Results from the test and the predictions are also in good agreement. Spinning action of the ice penetrator was improved in the second test. Therefore the crack coefficient increase from $C_{crack} = 3$ to $C_{crack} = 4$. It was also observed that the decrease in total weight did appear to slow down the penetration rate at greater depth.

4.3.2 Effect of Various Parameters

In order to evaluate the sensitivity of the various parameters, we have performed the following analysis:

Effect of C_{gw}:

Figure 14 presents the variation of C_{gw} from 0.60 to 1.0. It is clear that the penetration rate increases with the increasing C_{gw} value.

Effect of C_{crack}:

Figure 15 presents the variation of C_{crack} from 2 to 5. It shows that the larger the crack area, the faster the penetration rate.

Effect of C_{time}:

Figure 16 presents the variation of C_{time} on penetration. The lower the C_{time} value, the slower the penetration rate. As shown in the figure, effects are more profound at greater depth.

Effect of total weight (W_{total}):

Figure 17 presents the penetration depth versus time for the systems having total weight of 180, 131, 90, and 60 lbs. It shows that the total weight can have a tremendous effect on the penetration rate. For total weight of 131 lbs., the penetration rate decreases from 2.10 in/sec. at 1 inch to 0.46 in/sec. at 120 inches. The system is capable of penetration 10 ft. of ice in 114.38 seconds with average rate of 1.05 in/sec.

For total weight of 60 lbs., the penetration rate decreases from 1.29 in/sec at 1 inch to 0.22 in/sec at 69 inches. With 120 seconds, time limit, the system only can penetrate 69 inches at the

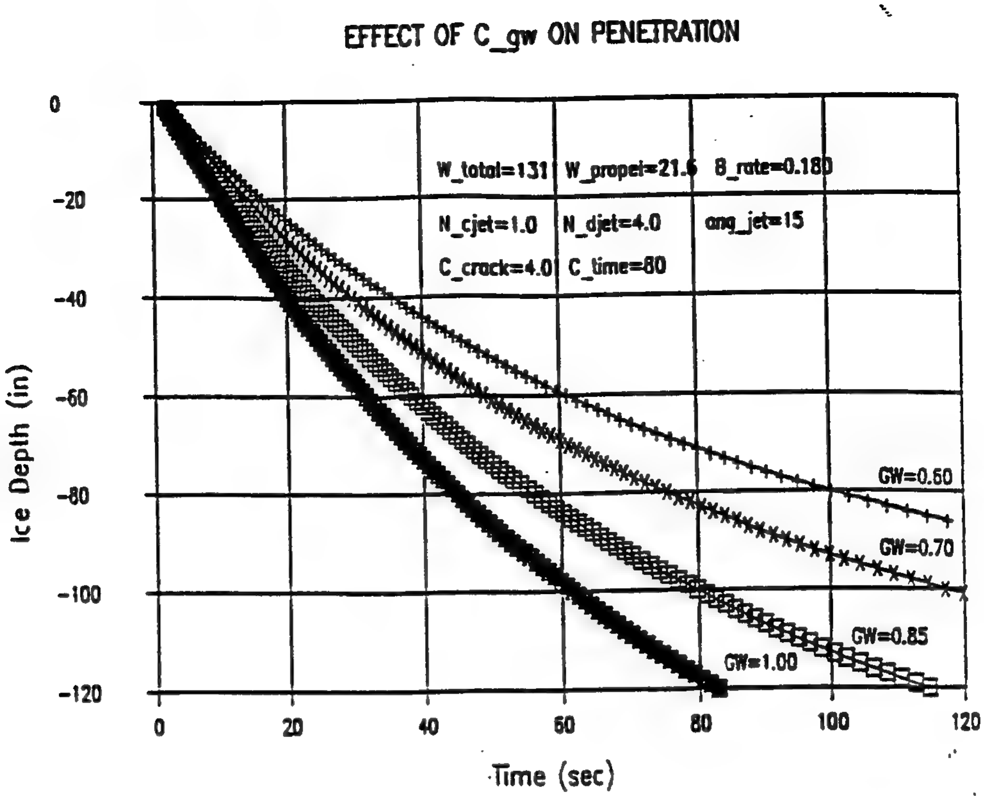

Figure 14

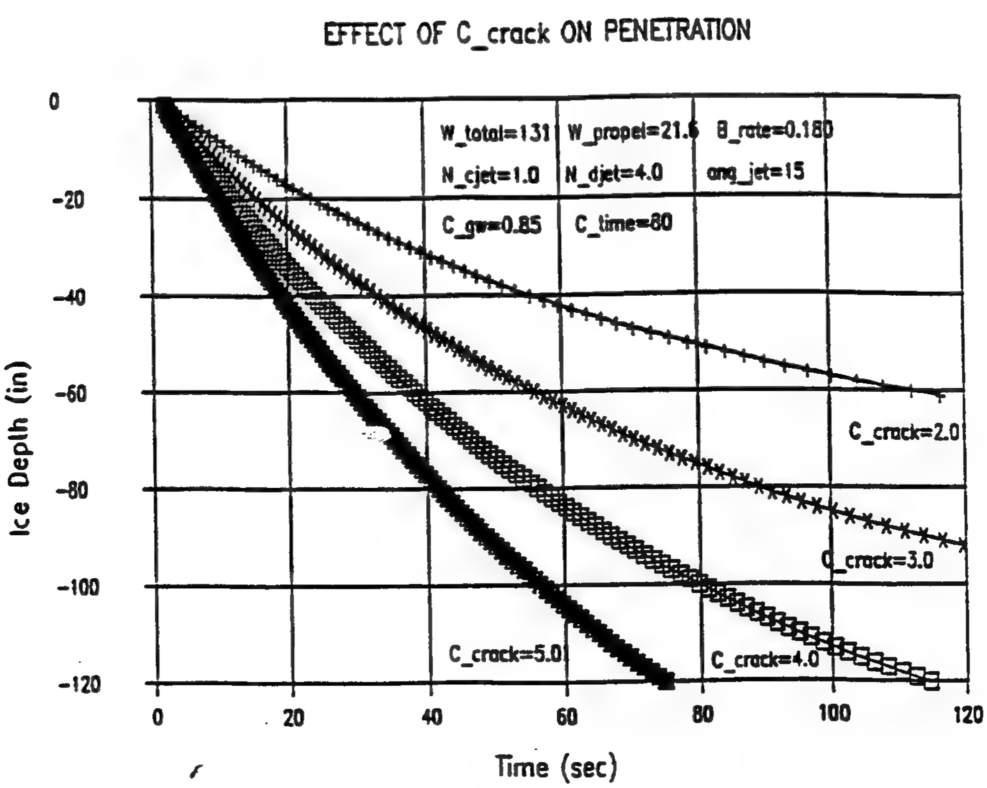

Figure 15

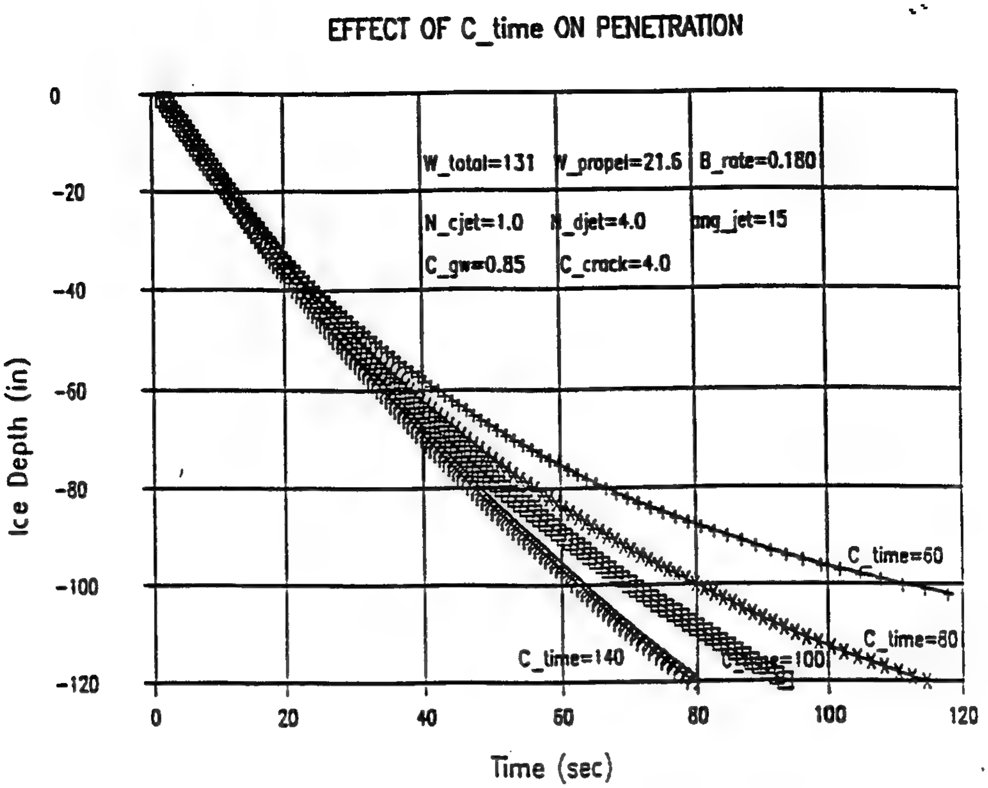

Figure 16

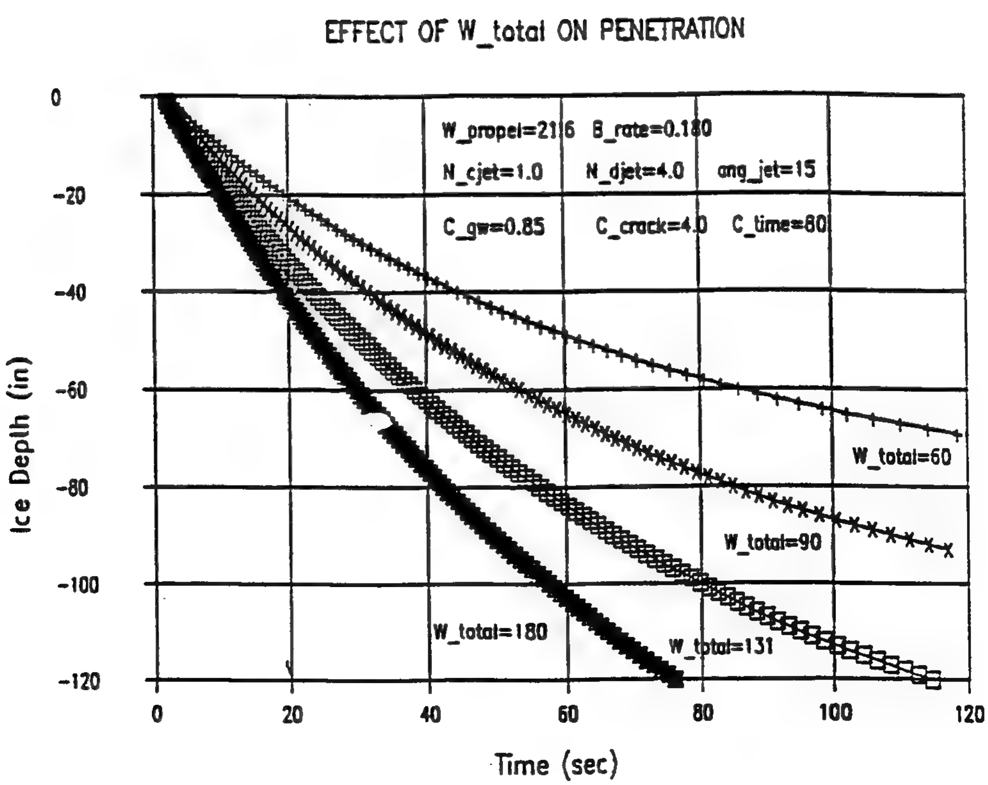

Figure 17

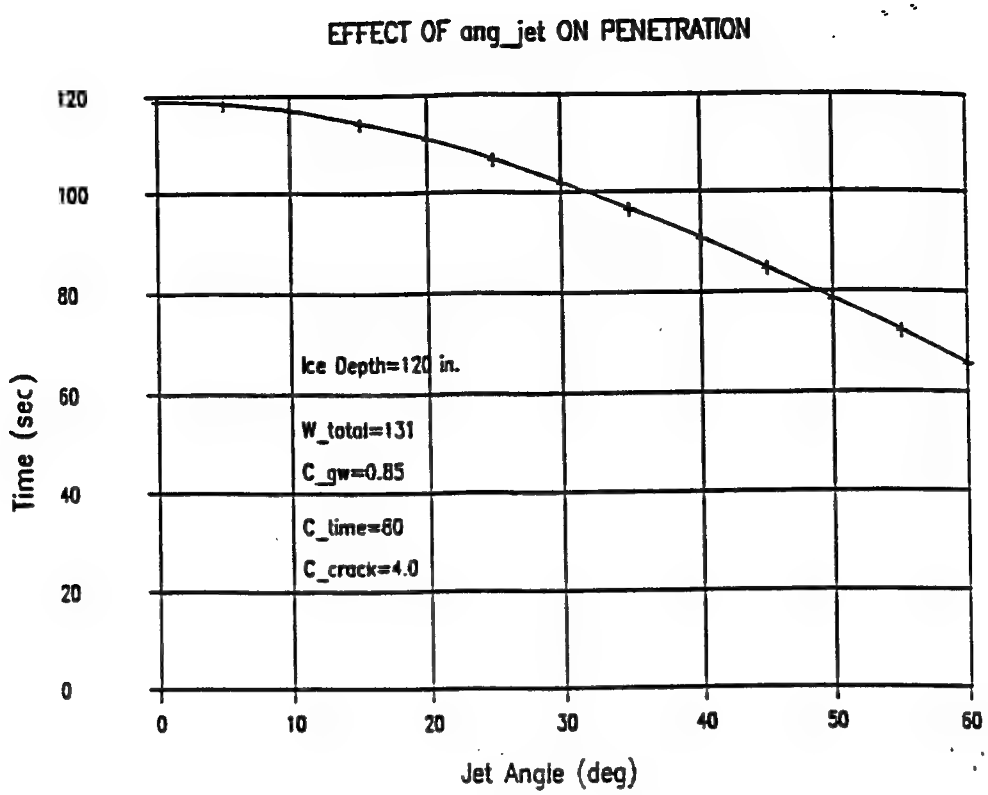
EFFECT OF ang_jet ON PENETRATION
Ice Depth=120 in.
W_total=131
C_gw=0.85
C_time=80
C_crack=4.0
Time (sec)
Jet Angle (deg)
0
20
40
60
80
100
120
0
10
20
30
40
50
60

Figure 18

average rate of 0.58 in/sec. (This assumes a penetrator thrust of approximately 40 lbs and the system weight decreasing as propellant is burned.)

A method to overcome the weight effect will be discussed in section 4.3.

Effect of Jet Incline Angle (ang_{jet}):

Figure 18 shows the effect of incline jet angle on the penetration time for 10 feet ice. Because of the reducing thrust force, increase in the incline jet angle can reduce the total penetrating time.

4.3.3 Modified Nozzle Design for Reducing Thrust

From our discussions in the previous section, the total weight to compensate the jet thrust force is one of the key parameters. In order to achieve our goal of penetrating 10 feet of ice in 2 minutes with a limiting weight of 50 lbs., we propose the use of reverse nozzles for this application. A 9-hole ice penetrator, consisting of downward center jet, 4 downward 45 degree jets and 4 upward 45 degree jets as shown in Figure 19 is one of the candidates. Analytical prediction based on the coefficients, C_{gw}, = 0.50, C_{crack} = 4.0 and C_{time} = 60 is presented in Figure 20. The prediction shows that the system will be able to penetrate 10 feet of ice in 100 seconds at the average rate of 1.20 in/sec.

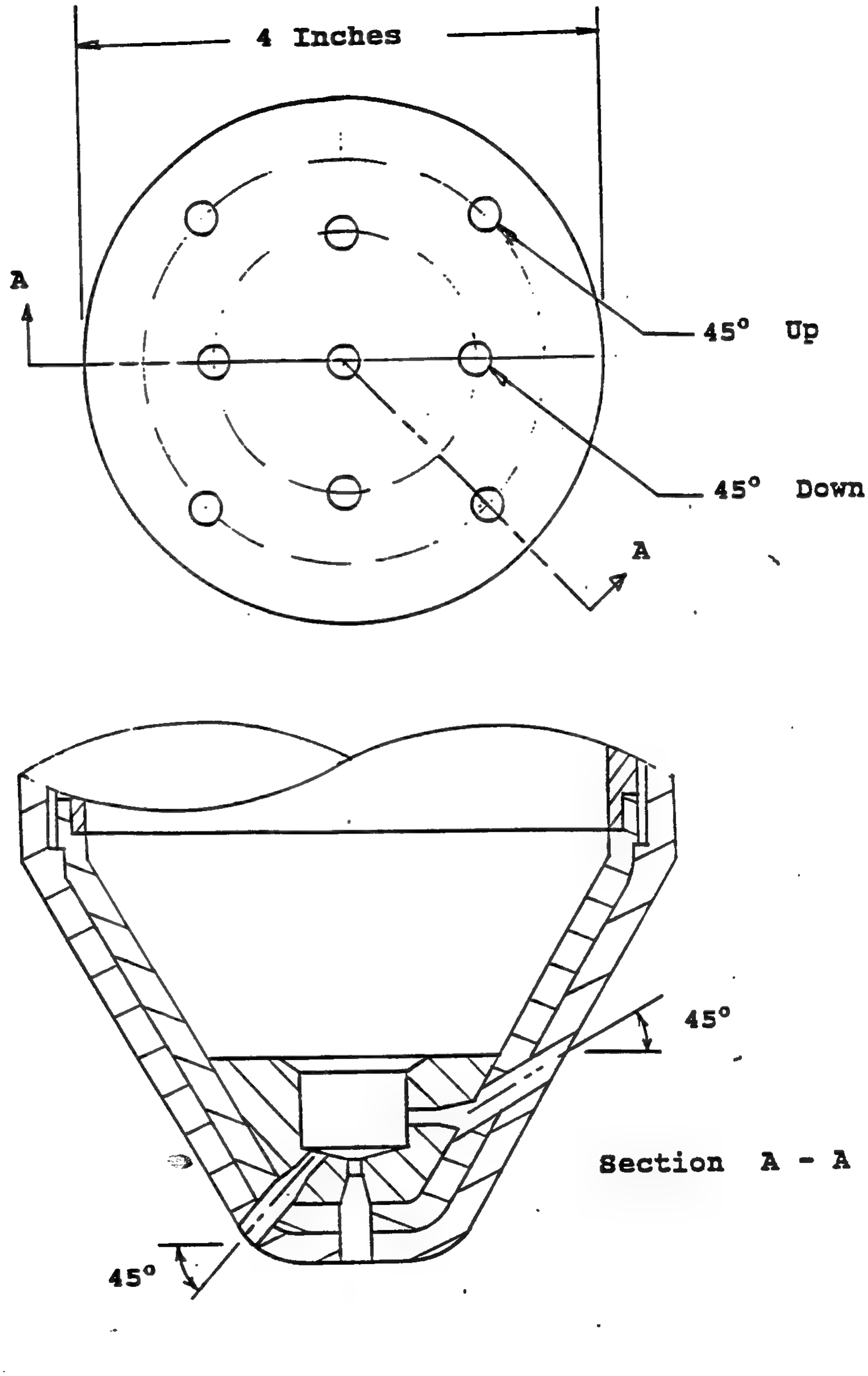

Figure 19

Proposed 9-Hole Pattern for a 4-inch Diameter Ice Penetrator

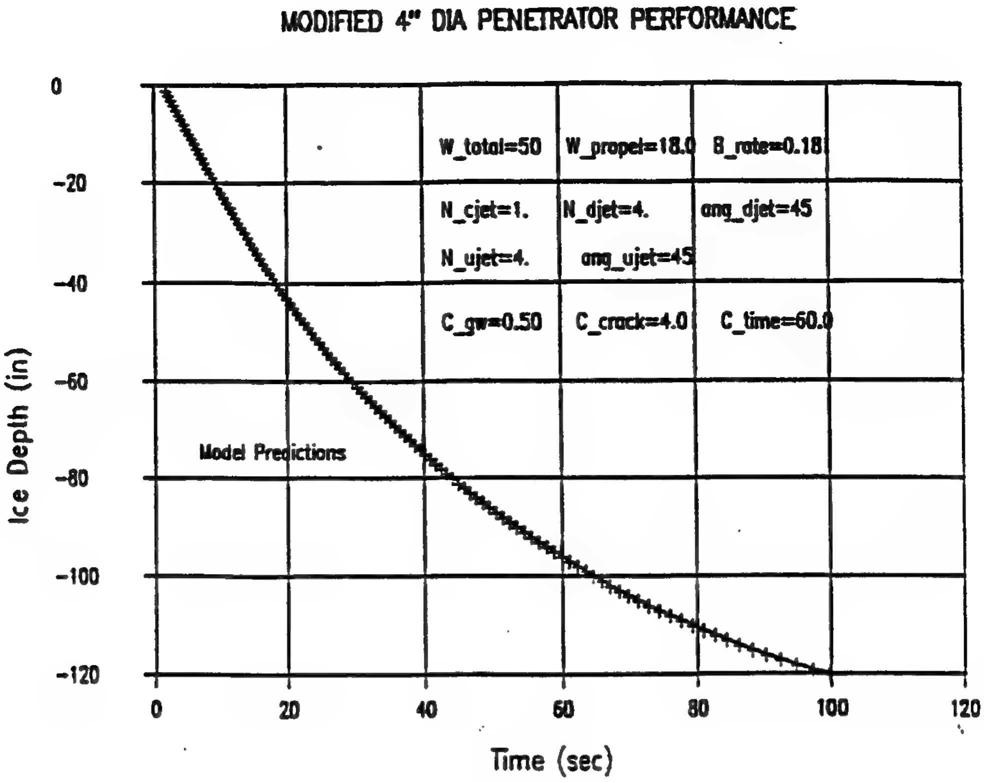
MODIFIED 4" DIA PENETRATOR PERFORMANCE
W_total=50
W_propel=18.0
B_rate=0.18
N_cjet=1.
N_djet=4.
ang_djet=45
N_ujet=4.
ang_ujet=45
C_gw=0.50
C_crack=4.0
C_time=60.0
Model Predictions
Ice Depth (in)
0
-20
-40
-60
-80
-100
-120
Time (sec)
0
20
40
60
80
100
120

Figure 20

4.3.4 Applications to Other Size of the Penetrators

Three other sizes of the ice penetrators have been studied for future applications. Figure 21, 22 and 23 present the hole-pattern and predicted results for 10, 14 and 21 inches diameter respectively. Results can be summarized in the following table.

<u>Summary of Performance</u>

Diameter of the Penetrator (in)	10	14	21
Total Weight (lbs)	1046	1503	2360
Payload (lbs)	800	1200	2000
Total Number of jets	19	16	13
Number of Center Jets	1	1	1
Incline Angle of Side Jet	45°	45°	45°
Required Penetrating Time (for 10 ft of ice)	111	112	106
Average Penetrating Rate (in/sec.)	1.08	1.07	1.14

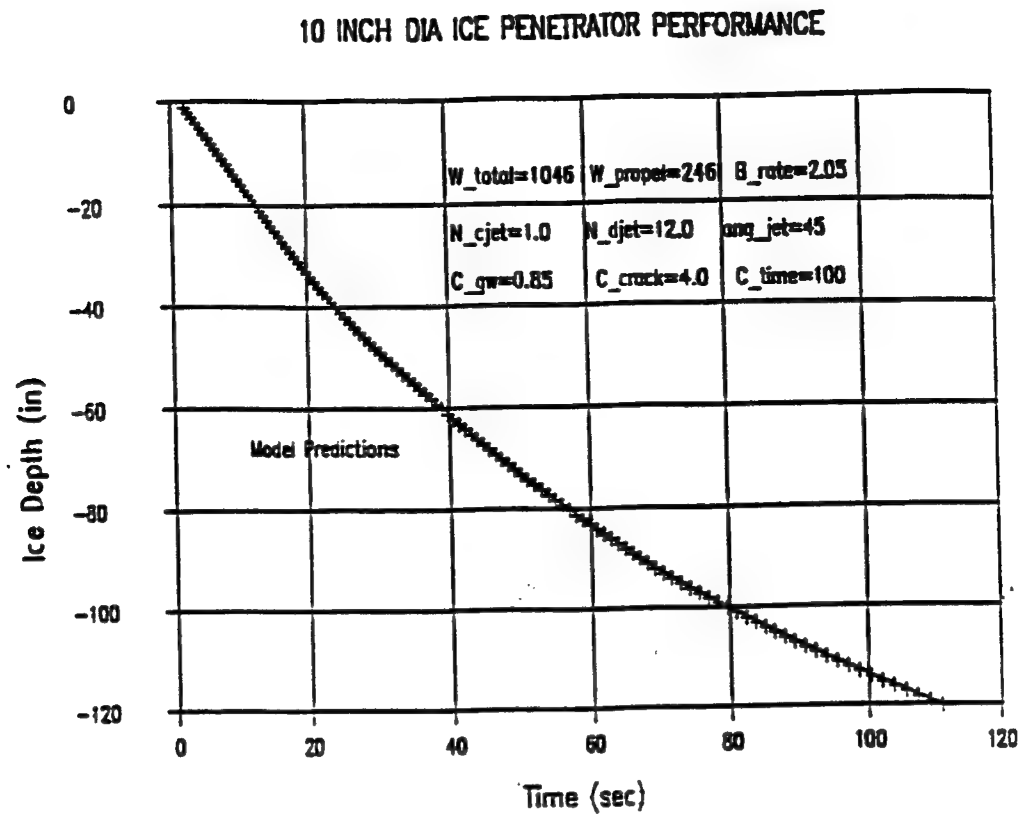

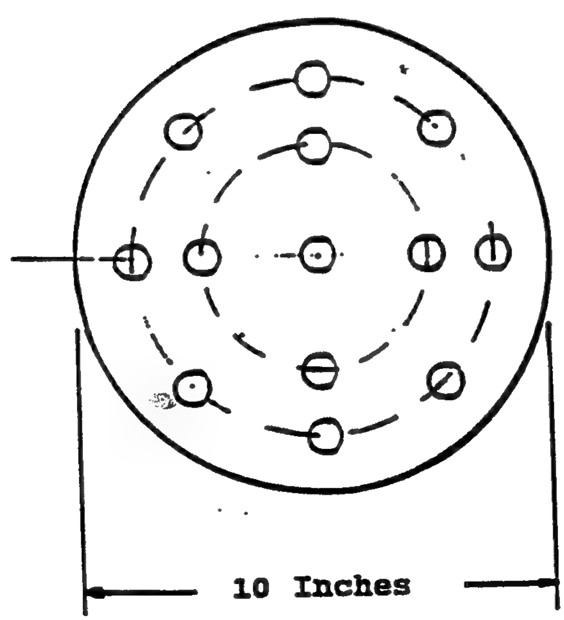

A 13-Hole Pattern for A 10-inch Diameter Ice Penetrator

Figure 21

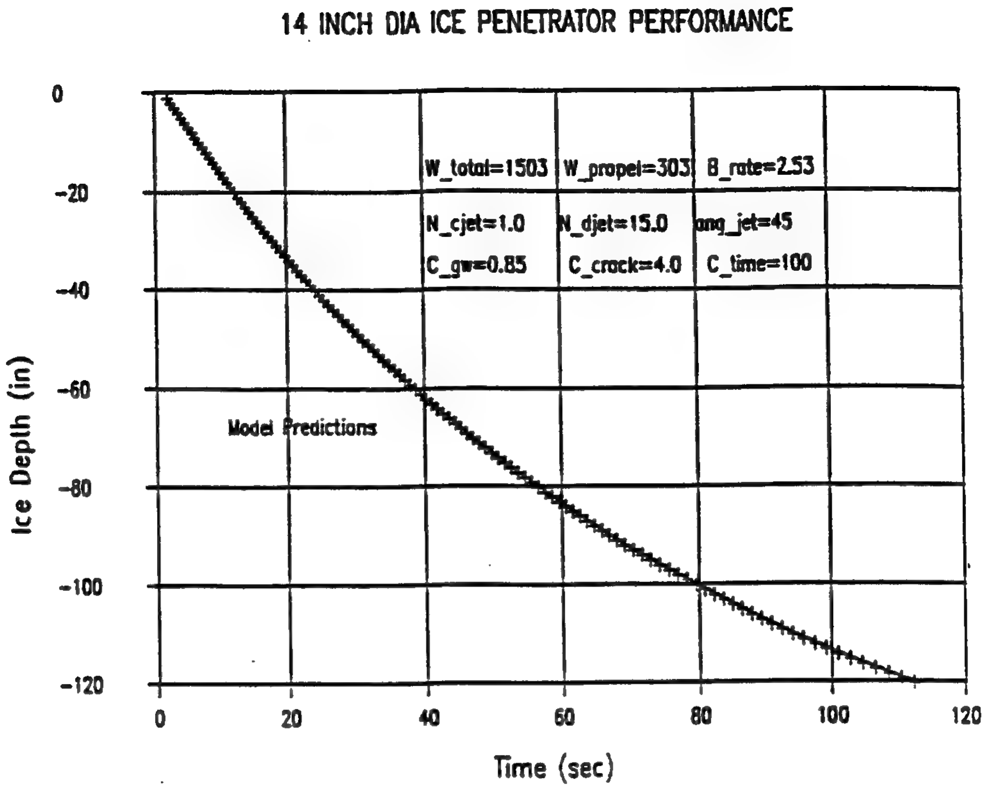

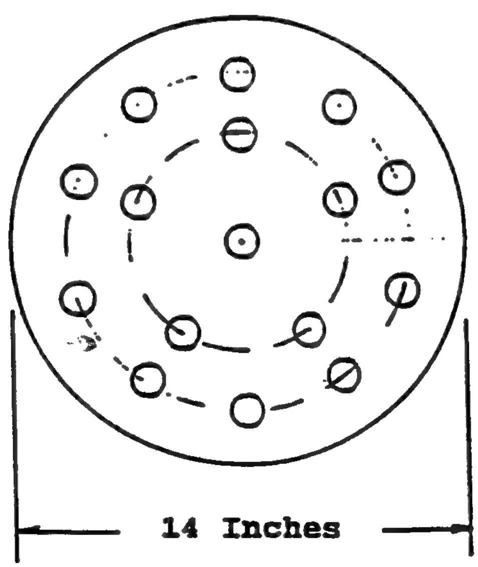

A 16-Hole Pattern for A 14-inch Diameter Ice Penetrator

Figure 22

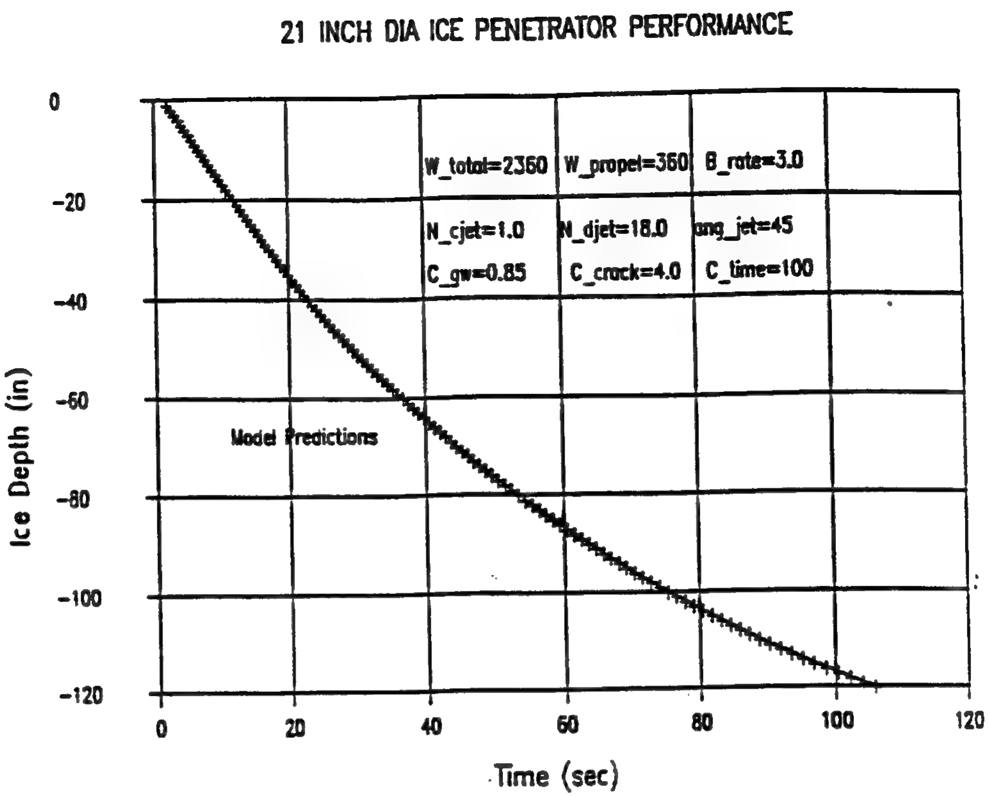

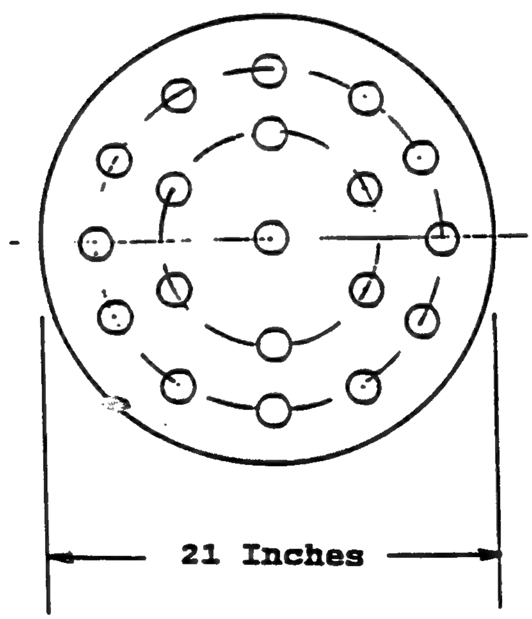

A 19-Hole Pattern for A 21-inch Diameter Ice Penetrator

Figure 23

4.4 References

1. Selsor, Harry D., Ice Penetrating Arctic Oceanographic Buoy, Proceedings Arctic Technology Workshop, June 1989, p. 101.

2. Zotikov, I.A., The Thermophysics of Glaciers, Institute of Geography, U.S.S.R., Academy of Sciences, Moscow, U.S.S.R., 1986.

3. Andersen, James K., Rapid Thermal Ice Penetration System, Proceedings Arctic Technology Workshop, June 1989, p. 224.

4. White, James W., Rapid Thermal Ice Penetrator, Test Report, Ocean Systems Research, Inc., August 1989.

5.0 TEST RESULTS

5.1 TEST # 1

The total burn time of the gas generator was 45.5 seconds. The measured penetrator rate was approximately 6.46 feet per minute. The resultant hole diameter measured approximately 7.0 inches across the top of the ice block and approximately 5.0 inches at the bottom (exit point). The estimated efficiency (based upon the average hole diameter versus amount of propellant used) is calculated below:

1. Volume of ice melted: $\frac{(3.14)(6.25\ \text{in.})^2 \times 41.0\ \text{in}}{4} = 1257\ \text{in}^2$
$= 0.73\text{ft}^3$

2. Weight of ice melted: $0.73\ \text{ft}^3 \times 57.2\ \text{Lbs/ft}^3 = 41.7\ \text{Lbs}$

3. Amount of propellant: $\frac{28.8\ \text{sec.}}{44.5\ \text{sec.}} \times 8.3\text{Lbs} = 5.3\ \text{Lbs}$

4. Energy expended by motor: $5.3\ \text{Lb} \times 2250\ \text{Btu/Lb} = 11{,}876\ \text{Btu}$

5. Energy required to melt ice:
$\frac{36\ \text{in.}}{41\ \text{in.}}(41.7\text{Lbs})(167.5\text{Btu/Lb}) = 6132\ \text{Btu}$

6. Melting Efficiency: $\frac{6132\ \text{Btu}}{11876\ \text{Btu}}$ **= 51.6%**

5.2 Test # 2

The total burn time of the gas generator was 45.5 seconds, which was identical to the first test. The measured penetration rate was approximately 6.0 feet per minute. The resultant hole diameter measured approximately 7.0 inches across the top of the ice block and approximately 4.50 inches across at the lowest point of penetration. The estimated efficiency (based upon the average hole diameter versus amount of propellant used) is calculated below:

1. Volume of ice melted: $\frac{(3.14)(6.25\text{ in.})^2 \times 54.5\text{ in}}{4}$ $= 1672\text{ in}^3$

   $= 0.97\text{ft}^3$

2. Weight of ice melted: $.97\text{ ft}^3 \times 57.2\text{ Lbs/ft}^3$ $= 55.50\text{ Lbs}$

3. Amount of propellant: $= 8.24\text{ Lbs}$

4. Energy expended by motor: $8.24\text{Lbs} \times 2250\text{ Btu/Lb}$ $= 18{,}540\text{ Btu}$

5. Energy required to melt ice: $(55.50\text{Lbs})(167.5\text{Btu/Lb})$ $= 9296\text{ Btu}$

6. Melting Efficiency: $\frac{9296\text{ Btu}}{18540\text{ Btu}}$ $= 50.1\%$

6.0 CONCLUSIONS/LESSONS LEARNED

Based upon successful test results, the use of solid propellant to rapidly penetrate thick Arctic ice appears very feasible. The penetration rate achieved on these two tests was 15-20 times faster than the best thermochemical type penetrators, which have seen many years of development and testing. It appears that based upon the average penetration rate achieved during these two tests (6.25 feet/minute), penetration of 10 feet of ice in under two minutes is easily achievable. Further optimization of nozzle design, burn rate, and propellant selection should lead to additional improvements in efficiency and/or penetration rate. Additional testing and analysis is required, however, in order to characterize the critical design parameters for performance optimization. The goal of the optimization process will be to develop the simplest and most effective ice penetrator design while staying within the volume, weight, and penetration constraints.

The nozzle configurations tested as part of this feasibility demonstration are ideally suited for large , heavy payloads. Little additional design effort would be required to design a penetrator for such devices. For smaller, lighter weight devices (such as environmental sensors) some means of thrust negation/reversal is necessary in order to achieve rapid penetration. There are several ways in which this can be accomplished, one of which is presented in Section 4 of this report. Whereas the optimization of the nozzle configuration for this application requires additional developmental testing, our

analysis show that penetration of 10 feet of ice in under two minutes can be achieved.

The propellant used in this feasibility demonstration had an energy content of 2250 Btu/lbm. In order to reduce the propellant/volume weight requirements, future penetrators will use a propellant with a 40% higher energy content per Lb. The higher energy propellant will reduce the propellant weight by 40% and since the specific gravity of the proposed propellant is slightly higher, the volume will be reduced by more than 40%.

Two thicknesses of ice were used for the feasibility demonstration, 41 inches and 62.5 inches. The 62.5 inch-thick block was formed by joining two smaller blocks of ice. During test 2, which utilized the 62.5 inch block, the seam ruptured and energy (i.e. hot gases) was diverted through the seam, thereby affecting the penetration efficiency. In future tests we will design the ice blocks to prevent seam rupture.

Attachments A

Analytical Prediction for Ice Penetration (test1012)

(Test Date : October 12, 1990)

Ice (in)	W_total	W_Propel	B_rate	
-60.0	90.0	8.24	.179	
N_cjet	N_djet	ang_djet		
1.	4.	15.		
Dia(in)	Height	d_jet(in)	son_vel	Mach
4.0	26.7	.2800	806.9	2.657
Rho	Vis	Cp	Pr	C_gw
.2150E-03	.1128E-05	.4062	.5663	.85
C_Nu	C_Re	C_u	C_crack	C_time
.268	.625	6.630	4.0	80.0
k_ice	alpha	T (F)	Tf (F)	Ti (F)
1.2500	.0450	32.00	212.00	-15.00

time(sec)	Depth(in)	h_water	Weight(Lb)	V(in/sec)
2.10	-1.00	804.	90.00	1.6630
2.71	-2.00	796.	89.89	1.6468
3.94	-4.00	780.	89.67	1.6145
5.20	-6.00	765.	89.45	1.5822
6.48	-8.00	749.	89.22	1.5499
7.79	-10.00	734.	88.99	1.5177
9.13	-12.00	718.	88.75	1.4855
10.50	-14.00	702.	88.51	1.4534
11.90	-16.00	687.	88.26	1.4213
13.33	-18.00	671.	88.01	1.3893
14.80	-20.00	656.	87.75	1.3573
16.30	-22.00	641.	87.49	1.3254
17.83	-24.00	625.	87.21	1.2935
19.41	-26.00	610.	86.94	1.2617
21.02	-28.00	596.	86.65	1.2326
22.67	-30.00	582.	86.36	1.2050
24.36	-32.00	569.	86.06	1.1774
26.09	-34.00	556.	85.75	1.1497
27.86	-36.00	542.	85.44	1.1221
29.68	-38.00	529.	85.12	1.0945
31.54	-40.00	516.	84.79	1.0668
33.45	-42.00	502.	84.45	1.0392
35.42	-44.00	489.	84.11	1.0115
37.44	-46.00	475.	83.75	.9838
39.51	-48.00	462.	83.38	.9561
41.65	-50.00	449.	83.01	.9285
42.74	-51.00	442.	82.81	.9146
43.85	-52.00	435.	82.62	.9008
44.98	-53.00	429.	82.42	.8869

Analytical Prediction for Ice Penetration (test920)

(Test Data : September 20, 1990)

Ice (in)	W_total	W_Propel	B_rate	
-41.0	131.0	8.30	.180	

N_cjet	N_djet	ang_djet		
1.	4.	15.		

Dia(in)	Height	d_jet(in)	son_vel	Mach
4.0	26.7	.2800	806.9	2.657

Rho	Vis	Cp	Pr	C_gw
.2150E-03	.1128E-05	.4062	.5663	.85

C_Nu	C_Re	C_u	C_crack	C_time
.268	.625	6.630	3.0	80.0

k_ice	alpha	T (F)	Tf (F)	Ti (F)
1.2500	.0450	32.00	212.00	-15.00

time(sec)	Depth(in)	h_water	Weight(Lb)	V(in/sec)
2.13	-1.00	1017.	131.00	1.5778
2.77	-2.00	1007.	130.89	1.5629
4.07	-4.00	988.	130.65	1.5330
5.40	-6.00	969.	130.42	1.5032
6.75	-8.00	950.	130.18	1.4735
8.12	-10.00	930.	129.93	1.4438
9.53	-12.00	911.	129.68	1.4141
10.97	-14.00	892.	129.43	1.3844
12.44	-16.00	873.	129.16	1.3548
13.94	-18.00	854.	128.90	1.3253
15.47	-20.00	835.	128.62	1.2958
17.04	-22.00	816.	128.34	1.2663
18.65	-24.00	797.	128.06	1.2369
20.30	-26.00	778.	127.77	1.2075
21.98	-28.00	760.	127.47	1.1798
22.84	-29.00	752.	127.31	1.1665
23.71	-30.00	743.	127.16	1.1531
24.58	-31.00	735.	127.00	1.1398
25.47	-32.00	726.	126.84	1.1264
26.37	-33.00	717.	126.69	1.1131
27.28	-34.00	709.	126.52	1.0997
28.20	-35.00	700.	126.36	1.0864
29.13	-36.00	691.	126.19	1.0730
30.08	-37.00	683.	126.03	1.0597
31.03	-38.00	674.	125.86	1.0463
32.00	-39.00	666.	125.68	1.0330
32.98	-40.00	657.	125.51	1.0196
33.97	-41.00	648.	125.33	1.0063

Attachments B

1

MOTOR CONDITIONS FOR
TEST CONFIGURATION
OF 9-20-90

```
**********************************************************
*                                                        *
*  NASA-LEWIS THERMOCHEMISTRY PROGRAM (SDA03) 12/10/83   *
*            SCIENTIFIC PROGRAMMING VERSION              *
*            MTI/ELKTON DIVISION 843309 VOD              *
*                                                        *
**********************************************************

SYNOPSIS...
      CONDITIONS AT CHEMICAL EQUILIBRIUM ARE UNIQUELY DEFINED
      BY SPECIFYING REACTANT COMPOSITION AND ANY COMBINATION OF
      TWO THERMODYNAMIC CONDITIONS. FOUR TYPES OF PROBLEMS ARE
      SOLVED BY SDA03...
         1) ADIABATIC CHEMICAL EQUILIBRIUM FOR ASSIGNED THERMODYN-
            AMIC STATES (TP,HP,SP,TV,UV,SV)
         2) THEORETICAL ROCKET PERFORMANCE (1D FLOW,ZERO PARTICLE
            LAGS,ETC) FOR EQUILIBRIUM AND/OR FROZEN COMPOSITION DURING
            ADIABATIC EXPANSION DOWN A NOZZLE. HERE THE TWO THERMODYN-
            AMIC CONDITIONS (P,T) ARE CONSTRAINED...
             1) IN THE CHAMBER...BY INGRED HEAT OF FORM AND P OR T OR R
             2) AT THE THROAT...NOTING THAT M=1 AND S=SC.
             3) AT SPECIFIED AREA OR PRESSURE RATIOS...NOTING THAT S=SC
         3) CHAPMAN-JOUGUET DETONATIONS, OR
         4) SHOCK TUBE PARAMETERS.
      SDA03 IS A COPY OF THE NASA-LEWIS CODE (SP-273) WITH MANY
      I/O IMPROVEMENTS AND 5 ADDED MODELS...
         0) BASIC CODE (REF...SALITA, MEMO 2814-83-M075, 5/13/83)
         1) HAWKINS LOSS CORRELATIONS ACTIVATED BY ILOSS=1 (REF...SAME)
         2) HERMSEN COMBUSTION EFFICIENCY CALCULATION ACTIVATED BY ILOSS=2
            (REF...SALITA, MEMO 2814-83-M107, 8/2/83)
         3) AFTER-BURNING CALCULATION ACTIVATED BY UAMB
            (REF...SALITA, MEMO 2814-83-M125, 9/20/83)
         4) VICTOR/BUECHER PLUME FLOWFIELD CALCULATION ACTIVATED BY NIX (REF...SAME)
         5) TRANSPORT PROPERTIES FROM SPP/SVEHLA (REF...SALITA, MEMO 2814-83-M147, 11/17/83)

CASE = THERMOCHEMICAL STUFF TPH-3433 FOR ICE PENETRATOR DHD 9-24-90

INPUT...

      REACTANTS
      HC            14.38
      AP            83.50
      THERMAX        0.2
      TP-90B         1.90
      CC-2            .02

      NAMELISTS
       &INPT2 MOLMAS=2,IPRINT=0,IPLOT=0,ILOSS=0,P=400.   &END
       &RKTINP SUPAR=4.0        &END
      STOP

REACTANTS
*********

               INGREDIENT DATA MARKED WITH * OBTAINED FROM MASTER FILE
```

2

```
TP-90B      1.900 O 17.0000 H 36.0000 O  6.0000     0.0        0.0    -320820.   0.970     *
CC-2        0.020 C  5.2652 H 10.2190 O  1.8163 CR 0.1036      0.0    -162920.   0.956     *

FUEL   ENTHALPY   (CAL/GRAM)    AT  77.0 DEG F = -530.54          CPPROP (CAL/GM-K)=  0.2700
                                AT  77.0 DEG F = -530.54

OXIDIZ ENTHALPY   (CAL/GRAM)    AT  77.0 DEG F =    0.0           CPOX   (CAL/GM-K)=  0.2420
                                AT  77.0 DEG F =    0.0

NAMELISTS
*********
&INPT2
KASE=       1,IDEBUG=      0,IPRINT=      0,MOLMAS=      2,IPLOT=      0,ILOSS=      0,TRNSPT=T,PSIA=T,NSQM=
F,MMHG=F,INHG=F,SIUNIT=F,RKT=T,PHI=F,IONS=F,TP=F,HP=F,SP=F,TV=F,UV=F,SV=F,FA=F,FPCT=F,IP=      0,ERATIO=F,OF=F,DETN=F,SHOCK=F,
TRACE=  .0        ,SO=  .0         ,SO=  .0          ,CR=  .0         ,UAMB=  -10.0000000   ,P=  400.000000   ,
 .0        , .0        , .0        , .0        , .0        , .0        , .0        ,
 .0        , .0        , .0        , .0        , .0        , .0        , .0        ,
 .0        , .0        , .0        , .0        , .0        , .0        , .0        ,
 .0        , .0        , .0        , .0        ,T=  .0     , .0        , .0        ,
 .0        , .0        , .0        , .0        , .0        , .0        , .0        ,
 .0        , .0        , .0        , .0        , .0        , .0        , .0        ,
 .0        , .0        , .0        , .0        , .0        , .0        , .0        ,
 .0        , .0        ,V=  .0     , .0        , .0        , .0        , .0        ,
 .0        , .0        , .0        , .0        , .0        , .0        , .0        ,
 .0        ,RHO=  400.000000       , .0        , .0        , .0        , .0        ,
 .0        , .0        , .0        , .0        , .0        , .0        , .0        ,
 .0        , .0        , .0        , .0        , .0        , .0        ,MIX=  .0   ,
 .0        , .0        , .0        , .0        , .0        , .0        , .0        ,MIX=
 .0        , .0        , .0        , .0        , .0        , .0        , .0        ,
 .0        , .0        , .0        , .0        , .0        , .0        , .0        ,
      0,HTEMP=  .0     , .0        , .0        , .0        , .0        , .0        ,
 .0        , .0        , .0
 .0        , .0        ,RRAZ=F
&END.

NO INPT2 VALUE GIVEN FOR OF, EQRAT, FA, OR FPCT
```

111 SPECIES BEING CONSIDERED IN THIS SYSTEM (I.E. CONTAINING ONLY THOSE ELEMENTS APPEARING IN THE INGREDIENTS)

C1(G)	C1(S)	C1CL1(G)	C1CL1N1(G)	C1CL1O1(G)
C1CL2(G)	C1CL2O1(G)	C1CL3(G)	C1CL4(G)	C1H1(G)
C1H1CL1(G)	C1H1CL3(G)	C1H1N1(G)	C1H1N1O1(G)	C1H1O1(G)
C1H2(G)	C1H2CL2(G)	C1H2O1(G)	C1H3(G)	C1H3CL1(G)
C1H4(G)	C1N1(G)	C1N1O1(G)	C1N2(G)	C1O1(G)
C1O2(G)	C2(G)	C2CL2(G)	C2CL4(G)	C2CL6(G)
C2CR3(S)	C2H1(G)	C2H1CL1(G)	C2H2(G)	C2H4(G)
C2H4O1(G)	C2N1(G)	C2N2(G)	C2O1(G)	C3(G)
C3CR7(S)	C3O2(G)	C4(G)	C4N1O4(G)	C4N1O4(L)
C4N2(G)	C5(G)	C6CR23(S)	CL1(G)	CL1H1(G)
CL1H1O1(G)	CL1H4N1(S)	CL1H4N1O4(S)	CL1N1O1(G)	CL1N1O2(G)
CL1O1(G)	CL1O2(G)	CL2(G)	CL2O1(G)	CR1(G)
CR1(L)	CR1(S)	CR1CL2(G)	CR1CL2(L)	CR1CL2(S)
CR1CL3(G)	CR1CL4(G)	CR1CL4(L)	CR1N1(G)	CR1N1(S)
CR1O1(G)	CR1O2(G)	CR1O3(G)	CR1O3(L)	CR2CL3(S)
CR2N1(S)	CR2O3(L)	CR2O3(S)	H1(G)	H1N1(G)
H1N1O1(G)	H1N1O2(G)	H1N1O3(G)	H1O1(G)	H1O2(G)
H2(G)	H2N1(G)	H2N2(G)	H2O1(G)	H2O1(L)
H2O2(G)	H3N1(G)	H4N2(G)	H4N2(L)	N1(G)
N1H1O2(G)	N1O1(G)	N1O2(G)	N1O3(G)	N2(G)
N2C1(G)	N2O1(G)	N2O3(G)	N2O4(G)	N2O4(L)
N2O4(S)	N2O5(G)	N3(G)	O1(G)	O2(G)
O3(G)				

SPECIES DATA FROM SNNEW ... THRU REVISION 55 (MAR 1979)

```
&RKTINP
EQL=T,FROZ=T,SUBAR=  .0           , .0            , .0            , .0            , .0            , .0
  .0             , .0           , .0            , .0            , .0            , .0            , .0           ,SUPAR=
  4.00000000     , .0           , .0            , .0            , .0            , .0            , .0           ,
  .0             , .0           , .0            , .0            , .0            , .0            ,PCP=  .0       ,
  .0             , .0           , .0            , .0            , .0            , .0            , .0           ,
  .0             , .0           , .0            , .0            , .0            , .0            , .0           ,
  .0             , .0           , .0            , .0            , .0            , .0            , .0           ,TCEST=
  3800.00000     ,NFZ=          1
&END

     *****FUEL FRACTION FF=  1.0000                        OF =  0.0      *****

                              EFFECTIVE FUEL          EFFECTIVE OXIDANT          MIXTURE
ENTHALPY                          HPP(2)                   HPP(1)                 HSUBO
(KG-MOL)(DEG K)/KG          -0.26698560E+03          0.0                    -0.26698560E+03

KG-ATOMS/KG                   BOP(I,2)                 BOP(I,1)                   BO(I)
      C                     0.11395492D-01           0.0                     0.11395492D-01
      H                     0.45889312D-01           0.0                     0.45889312D-01
      N                     0.72186246D-02           0.0                     0.72186246D-02
      O                     0.28987734D-01           0.0                     0.28987734D-01
      CL                    0.71070380D-02           0.0                     0.71070380D-02
      CR                    0.20760260D-06           0.0                     0.20760260D-06

POINT      C         H         N         O        CL        CR        ITN       T
  1     -13.906    -9.632   -13.573   -18.102   -20.299   -17.489    16.000 2714.542
  2     -13.695    -9.746   -13.689   -19.037   -20.809   -17.658     4.000 2474.721
PC/PT= 1.768257     T =   2474.72
  2     -13.693    -9.747   -13.690   -19.047   -20.815   -17.652     2.000 2472.418
PC/PT= 1.778049     T =   2472.42
  2     -13.693    -9.747   -13.690   -19.047   -20.815   -17.652     1.000 2472.399
PC/PT= 1.778131     T =   2472.40
  3     -11.182   -10.173   -14.179   -25.978   -24.130   -15.387     4.000 1535.171
ADD CR2O3(S)
  3     -11.182   -10.173   -14.179   -25.978   -24.130   -16.324     1.000 1535.183
  3     -11.112   -10.180   -14.188   -26.152   -24.209   -16.417     3.000 1521.211
  3     -11.113   -10.180   -14.188   -26.152   -24.209   -16.417     1.000 1521.233
```

5

THEORETICAL ROCKET PERFORMANCE ASSUMING EQUILIBRIUM COMPOSITION DURING EXPANSION

PC = 400.0 PSIA
CASE NO.= 1

	CHEMICAL FORMULA				WT FRACTION (SEE NOTE)	ENERGY CAL/MOL	STATE	TEMP DEG K	DENSITY G/CC	GFW
FUEL	C 7.13400	H 10.71500	N 0.07760	O 0.15170	0.143800	-6750.000		0.0	0.9084	100.002
FUEL	CL 1.00000	H 4.00000	N 1.00000	O 4.00000	0.835000	-70690.000		0.0	1.9500	117.489
FUEL	C 1.00000				0.002000	0.0		0.0	2.2600	12.011
FUEL	C 17.00000	H 36.00000	O 6.00000		0.019000	-320820.062		0.0	0.9700	336.473
FUEL	C 5.26520	H 10.21900	O 1.31630	CR 0.10380	0.000200	-162919.937		0.0	0.9560	99.999

O/F= 0.0 PERCENT FUEL= 100.0000 EQUIVALENCE RATIO= 1.4055 PHI= 0.0 REACTANT DENSITY (GM/CC)= 1.6469

EQUIV FORM= C 1.13955 H 4.58893 N 0.72186 O 2.89877 CL 0.71070 CR 0.00002

MOLE FRACT= C 0.11328 H 0.45616 N 0.07176 O 0.28815 CL 0.07065 CR 0.00000

MIX PROPS	CHAMBER	THROAT	EXIT
PC/P	1.0000	1.7781	24.441
P, ATM	27.218	15.307	1.1136
T, DEG K	2714.5	2472.4	1521.2
RHO, G/CC	2.9279-3	1.8133-3	2.1495-4
H, CAL/G	-530.54	-654.05	-1079.90
S, CAL/(G)(K)	2.5219	2.5219	2.5219
M, MOL WT	23.960	24.033	24.094
(DLV/DLP)T	-1.00283	-1.00129	-1.00001
(DLV/DLT)P	1.0621	1.0304	1.0002
CP, CAL/(G)(K)	0.5645	0.5053	0.4257
GAMMA (S)	1.1946	1.2084	1.2404
SON VEL,M/SEC	1060.8	1016.6	806.9
MACH NUMBER	0.0	1.000	2.657

		THROAT	EXIT
AE/AT		1.0000	4.0000
CSTAR, FT/SEC		4908.2	4908.2
CF		0.6796	1.4332
IVAC LB-SEC/LB		169.46	243.60
IMAT LB-SEC/LB		103.67	218.63

MASS FRACTIONS (IF GE 5.E-06)

C1CL1O1(G)	0.00001	0.00000	0.0
C1O1(G)	0.22844	0.22184	0.18474
C1O2(G)	0.14571	0.15296	0.21125
CL1(G)	0.00554	0.00279	0.00001
CL1H1(G)	0.25336	0.25623	0.25911
CL1H1O1(G)	0.00001	0.00000	0.0
CL2(G)	0.00004	0.00002	0.00000
CR1CL2(G)	0.00003	0.00002	0.00001
CR1CL3(G)	0.00001	0.00000	0.00000
CR1O1(G)	0.00001	0.00000	0.0
CR1O2(G)	0.00001	0.00000	0.0
CR2O3(S)	0.0	0.0	0.00001
H1(G)	0.00017	0.00008	0.00000
H1O1(G)	0.00208	0.00078	0.00000
H2(G)	0.01045	0.01068	0.01330
H2O1(G)	0.25478	0.25342	0.23045
H1O1(G)	0.00025	0.00007	0.00000
[illegible]	0.10000	0.10107	0.10111

6

CONDENSED MF		0.0	0.0	0.00001
BETA(DIF-LH)		0.21119	0.21127	0.21130
GAS DEN G/CC		2.9279-3	1.8133-3	2.1495-4
GAS MOLEC WT		23.960	24.033	24.094
(DLH/DLT)	P	-0.06208	-0.03037	-0.00015
(DLH/DLP)	T	0.00283	0.00129	0.00001
(DLT/DLPC)	PC/P	0.00912	0.00447	-0.00105
(DLA/DLPC)	PC/P	0.99314	0.99668	1.00106
(DLI/DLPC)	PC/P	0.0	0.00251	0.00064
(DLC/DLPC)	PC/P		0.00081	

TOTAL MASS FRACTION OF CONDENSED SPECIES IN CHAMBER= 0.0

7

FROZEN TRANSPORT PROPERTIES CALCULATED FROM EQUILIBRIUM CONCENTRATIONS (A LA SPF) ...

AT MOST, 20 SPECIES ARE CONSIDERED IN THIS CALCULATION.
FOR REFERENCE, THEIR CHAMBER PROPERTIES ARE ...

SPECIES	VISCOSITY	CONDUCTIVITY	SIGMA	EPS/K	TSTAR	OMEGA	CP/R
CL1H1(G)	0.18357E-05	0.15804E-01	3.339	344.7	7.8751	0.8562	4.4418
H2O1(G)	0.17482E-05	0.44151E-01	2.641	809.1	3.3550	1.0101	6.5916
H2(G)	0.78103E-06	0.11979E+00	2.827	59.7	45.4697	0.6601	4.3704
N2(G)	0.15717E-05	0.17590E-01	3.798	71.4	38.0186	0.6775	4.4362
C1O1(G)	0.16063E-05	0.18073E-01	3.690	91.7	29.6024	0.7022	4.4610
C1O2(G)	0.15639E-05	0.18187E-01	3.941	195.2	13.9065	0.7926	7.4573
H1O1(G)	0.17539E-05	0.31828E-01	3.147	79.8	34.0168	0.6890	4.3616
CL1(G)	0.17888E-05	0.95328E-02	3.613	130.8	20.7534	0.7400	2.5319
H1(G)	0.64556E-06	0.11942E+00	2.708	37.0	73.3660	0.6154	2.5002
CL2(G)	0.16273E-05	0.75795E-02	4.217	316.0	8.5903	0.8444	4.6912
N1O1(G)	0.17875E-05	0.18905E-01	3.492	116.7	23.2608	0.7293	4.4944
O2(G)	0.18968E-05	0.19748E-01	3.467	106.7	25.4409	0.7200	4.7349
C1(G)	0.14662E-05	0.23375E-01	3.385	30.6	88.7105	0.5986	2.5766
N1(G)	0.14738E-05	0.19672E-01	3.298	71.4	38.0186	0.6775	2.5076
O1(G)	0.17331E-05	0.20280E-01	3.050	106.7	25.4409	0.7200	2.5117
C1H4(G)	0.10869E-05	0.55247E-01	3.758	148.6	18.2674	0.7572	12.0841

CHAMBER ...GAS TEMPERATURE (K) = 2714.5
MIXTURE VISCOSITY (LBF-SEC/FT2) = 0.16951E-05
MIXTURE CONDUCTIVITY (LBF/SEC-DEGR) = 0.32291E-01
GAS FROZ SPECIF HEAT (CAL/GM -DEGK) = 0.44688
MIXTURE PRANDTL NUMBER = 0.58699

EXIT ...GAS TEMPERATURE (K) = 1521.2
MIXTURE VISCOSITY (LBF-SEC/FT2) = 0.11280E-05
MIXTURE CONDUCTIVITY (LBF/SEC-DEGR) = 0.20246E-01
GAS FROZ SPECIF HEAT (CAL/GM -DEGK) = 0.40622
MIXTURE PRANDTL NUMBER = 0.56629

SCALING OF VISCOSITY TO OTHER TEMPERATURES ... VISO = 0.16951E-05 (T/ 2714.5)** 0.70338

6

```
                                        FROZEN EXPANSION

PC =   400.0 PSIA
 CASE NO.=      1                                                   WT FRACTION    ENERGY    STATE   TEMP    DENSITY     DFH
                                                                    (SEE NOTE)     CAL/MOL           DEG K    G/CC
          CHEMICAL FORMULA                                           0.143800     -6750.000           0.0    0.9084   100.002
FUEL     C  7.13400  H 10.71500  N  0.07760  O  0.15170              0.835000    -70690.000           0.0    1.9500   117.489
FUEL     CL 1.00000  H  4.00000  N  1.00000  O  4.00000              0.002000         0.0             0.0    2.2600    12.011
FUEL     C  1.00000                                                  0.019000   -320820.062           0.0    0.9700   336.473
FUEL     C 17.00000  H 36.00000  O  6.00000                          0.000200   -162919.937           0.0    0.9560    99.999
FUEL     C  5.26520  H 10.21900  O  1.31630  CR 0.10380

    O/F=  0.0       PERCENT FUEL= 100.0000    EQUIVALENCE RATIO= 1.4055    PHI= 0.0      REACTANT DENSITY (GM/CC )=  1.6469

    EQUIV FORM= C    1.13955   H    4.58893   N    0.72186   O    2.89877   CL   0.71070   CR   0.00002

    MOLE FRACT= C    0.11328   H    0.45616   N    0.07176   O    0.28815   CL   0.07065   CR   0.00000
 MIX PROPS        CHAMBER    THROAT     EXIT
PC/P               1.0000    1.7915    25.192
P, ATM             27.218    15.193    1.0804
T, DEG K           2714.5    2434.2    1445.5
RHO, G/CC        2.9279-3  1.8226-3  2.1826-4
H, CAL/G          -530.54   -654.92  -1072.59
S, CAL/(G)(K)      2.5219    2.5219    2.5219
M, MOL WT          23.960    23.960    23.960
CP, CAL/(G)(K)     0.4469    0.4432    0.3992
GAMMA (S)          1.2279    1.2322    1.2622
SON VEL,M/SEC      1075.4    1020.2     795.7
MACH NUMBER        0.0        1.000     2.677

AE/AT                        1.0000    4.0000
CSTAR, FT/SEC                4866.3    4866.3
CF                           0.6878    1.4359
 IVAC LB-SEC/LB              188.46    241.19
 IMAT LB-SEC/LB              104.03    217.18

 STOP
 *********
```

THIOKOL CORPORATION
ELKTON DIVISION
ELKTON, MARYLAND

RAPID THERMAL ICE PENETRATOR

TEST PLAN 2833-1485

Abstract: A gas generator will be test fired to demonstrate its ability to penetrate polar ice.

PREPARED BY Jay Blevins DATE July 30, 1990
J. D. Blevins, Test Engineer

APPROVED BY David M. Dunlap DATE 8-28-90
D. Dunlap, Design Engineer

APPROVED BY Michael G Kramer DATE 8/28/90
M. Kramer, Program Manager

CUSTOMER APPROVED James K Andersen DATE 8/30/90
Ocean Systems Research

TABLE OF CONTENTS

1.0 SCOPE

1.1 The scope of this document is to define the requirements for testing a solid fuel polar ice penetrator.

1.2 Test item description. The penetrator will be a end burning solid fuel gas generator assembled in accordance with Drawing E43894-01 and designated as Thiokol motor type TE-M-913-2. It is approximately 27 inches long and 4 inches in diameter. It is equipped with an aft end igniter and five nozzles.

1.3 Test Arrangement. The test arrangement will provide a guide and restraint for the gas generator above the ice pack. The ice pack will consist of an ice block approximately 4 feet thick. Weight of the system will advance the burning gas generator into the ice as the melted material is removed.

2.0 EQUIPMENT REQUIRED

2.1 Ice Block - A block of ice approximately 30 inches diameter by 48 inches long.

2.3 Motor mount and guide - supplied by testing per Figure 1.

2.4 Standard Video - Primary data will be standard closed circuit video recorded on tape for observation.

2.5 Gas Generator - E43894-01

2.6 High speed cameras (2)

2.7 High speed video (2 cameras)

2.8 Fans

2.9 Templac (150° To 300°F)

3.0 SAFETY

3.1 All operations shall be conducted in accordance with the Testing Department Safety Manual, E63-84.

A. Educate personnel to establish personal grounding habits prior to handling explosive components.

B. To avoid the possibility of accidental ignition due to electrostatic discharge, the test item must be maintained at zero voltage potential relative to any handling equipment, test stand, or personnel by use of grounding straps connected to a verified earth ground.

C. If conductive plastic (Velostat) is used to cover the test item, the plastic must be connected to earth ground by means

D. Nonmetallic explosive components, such as propellant cups, shall be installed in Velostat conductive bags prior to environmental, structural, or static test efforts.

E. Eliminate the use of nonconductive bags in all operations involving propellants, flammable solvents, flammables, dusts, fine micron powders, igniters, and ignition systems. Use only conductive Velostat.

F. In those test operations where tarps, canvasses,or other nonconductive environmental coverings must be utilized, the electrostatic voltmeter surveys of paragraph J must be conducted to evaluate the hazards.

G. Utilize "make before break" procedures in all motor, hoist, test stand, and/or test fixture grounding operations. That is, prior to disconnecting one ground cable (break), a second ground cable must be connected (make). This operation shall be routinely followed during handling and transport operations.

H. Connect a ground cable to all hoist hooks unless they are marked as designated grounds.

I. Provide ground straps between test stands and/or fixtures, hoists, and explosive items being lifted.

J. Use electrostatic voltmeters routinely to evaluate potential static problems prior to beginning hazardous operations. Technicians using the voltmeters shall have touched a ground bar moments prior to using the voltmeters.

When the measured electrostatic potential is above 5000 volts, it must be assumed that a potentially hazardous condition exists. The following steps shall be taken to safely discharge the voltage:

Provide for an ionized atmosphere between the static accumulating source and a fixed ground -- the most practical and safest device for this is a radioactive alpha particle source. Such a device is available from the Safety Department. Continue ionization techniques until meter readings indicate neutralized conditions.

Use of grounding devices -- electrical conductors from the accumulated charge to a suitable electrical ground will safely reduce and dissipate the accumulated charge; in this context, a suitable ground is one which meets the National Electric Code acceptance limit of 10 ohms, maximum.

In the event a charge between 5000 and 10000 volts is measured, a special insulated bleeder cable, which has a 1 megohm resistor installed between two insulated alligator clips may be used to safely bleed the voltage to ground. In those instances where an ionized atmosphere is used to neutralize the charge, the insulated bleeder cable may be used at voltages less than 10000 volts.

If repeated electrostatic testing shows that certain operations result in static buildup, the following actions may be taken in addition to grounding and ionization techniques.

Control of environmental conditions -- high temperature and high humidity reduce accumulation of electrostatic charge while cool temperatures and low humidity intensify the accumulation of electrostatic charge.

Use of static collectors -- grounded metallic combs, brushes, or tinsel bars must not touch the surface to be discharged but should be located within 1/4 to 1 inch of the surface.

K. Study the published plans showing facility "designated grounds", ground wires, work bench ground systems, and grounding bars for each building, test facility, and test bay in the Testing Department. Utilize grounding point lugs on all explosive components, when available. Contact the test engineer if a grounding point is not clear.

L. Static control wrist straps shall be utilized during all igniter assembly operations. The straps must be attached to the work bench or test bay ground wire prior to initiating efforts on the igniter. Facility ground cables shall be routinely utilized on all items containing electrical initiation systems.

M. The following procedures shall be followed for installation of propellant-containing components into thermal conditioning chambers:

<u>NOTE:</u> Small metallic case and other small hand-carried motors shall be exempt from the facility ground cable requirements when being carried from a thermal room or chamber to a grounded test stand or from a truck to the thermal room.

A facility ground cable must be attached to the rocket motor (component) prior to movement to the chamber.

Ensure the thermal chamber is grounded.

If a metal case rocket motor is to be positioned on the metal floor of the chamber, place the component into the chamber and remove the facility ground cable from the component.

Prior to removal from the chamber, re-attach the facility ground cable and then remove the motor (component).

If the metal case rocket motor (component) is to be placed on a wooden pallet (or other nonconductive surface), a metallic mesh (screen) shall be placed over the surface with assurance of a proper ground prior to installing the rocket motor (component).

Install the rocket motor (component) into the chamber and remove the facility ground cable from the component.

Prior to removal from the chamber, re-attach the facility ground cable and then remove the component from the chamber.

If the rocket motor (component) is to be installed in a conditioning "room", the rocket motor (component) must be positioned on conductive shelving. Verify that conductive shelving has been grounded.

In the event wooden shelving (or other nonconductive surface) is utilized, the nonconductive surface shall be covered with metallic mesh (screen) prior to installing the rocket motor (component).

Prior to removal from the conditioning "room", re-attach the facility ground cable and then remove the motor (component).

Non-metallic cases (components) shall be routinely checked using an electrostatic voltmeter and the above facility ground cable procedures utilized. In addition, a ground cable internal to the chamber or room must be attached to the grounding lug on the non-metallic case (component).

4.0 PRETEST PREPARATION

4.1 The support system (shown in Figure 1) will be mounted to a monorail support at C36 test bay (as assigned).

4.2 The ice block will be frozen in C-9 six (6) inches at a time.

4.2.1 Thermocouples will be enbedded in the ice as it is frozen per E43896.

4.3 The ice block will be obtained from the freezer using a fork lift.

4.3.1 The ice block will be weighed before installation in test bay.

4.4 The gas generator will be painted with stripes of templac paint as shown in Figure 2.

4.5 Provide a breakaway system for the ingiter leads to allow the test item to spin freely.

4.6 The test item will be fitted with an 1196 squib if not already installed.

5.0 OPERATIONS

5.1 The gas generator head cap will be attached to the lower end of the restrain - guide system as shown in Figure 1 using (TBD) cap screws.

5.2 The assembly will be lifted as high as required to clear the ice block and supports

5.3 Place concrete blocks in position to support the ice pallet under the guide.

5.4 Using a fork lift, position the ice mass under the guide system and gas generator.

5.5 Lower the gas generator into position above the ice (ice cube spacers will be installed under the nozzle cap to maintain correct spacing).

5.6 Install fans to clear away smoke and steam to provide a better view for cameras.

5.7 Verify that pretest photographs have been completed.

5.8 Verify that video and/or cameras are prepared for the test.

5.9 At the direction of the test director arm the gas generator and clear the area.

5.9.1 The igniter leads must be positioned to break free of the test item to allow free spin.

5.10 Verify that the gas generator functions.

5.11 Maintain area control until all safety checks are completed.

CAUTION! The combination of exhaust gases and water from the ice melt will be highly acidic and can cause irritation if contacted.

6.0 INSTRUMENTATION OPERATIONS

6.1 Provide control and conditioning equipment for the following data parameters:

Parameter	Number	Range	Recording Method
Ignition Current	1	0-10 amps	Analog/Digital
Temperature	8	0-1000°	Analog/Digital

6.1.1 Provide method to cut ignition lines after ignition.

6.1.2 Provide 10 amperes to one 1196 squib or equivalant. (approximately 1 ohm maximum resistance).

6.2 Record data on analog at 10 inches per second.

6.3 Perform dry run before motor and ice pack are installed.

6.4 At the direction of the test director initiate the firing sequence and record temperature data as long as thermocouple circuits are maintained. (Thermocouple leads may be broken by spinning gas generator.)

7.0 PHOTOGRAPHIC - VIDEO REQUIREMENTS

7.1 Standard Video - Primary data will be standard closed circuit video recorded on tape for observation.

7.2 Still Photographs - Still photographs will be provided in black and white 8 1/2 " X 11" format to document the test results and test arrangement.

7.3 High speed video - use two (2) cameras; one above and one beside the test assembly.

7.4 Arrange cameras for over all coverage to show melt through.

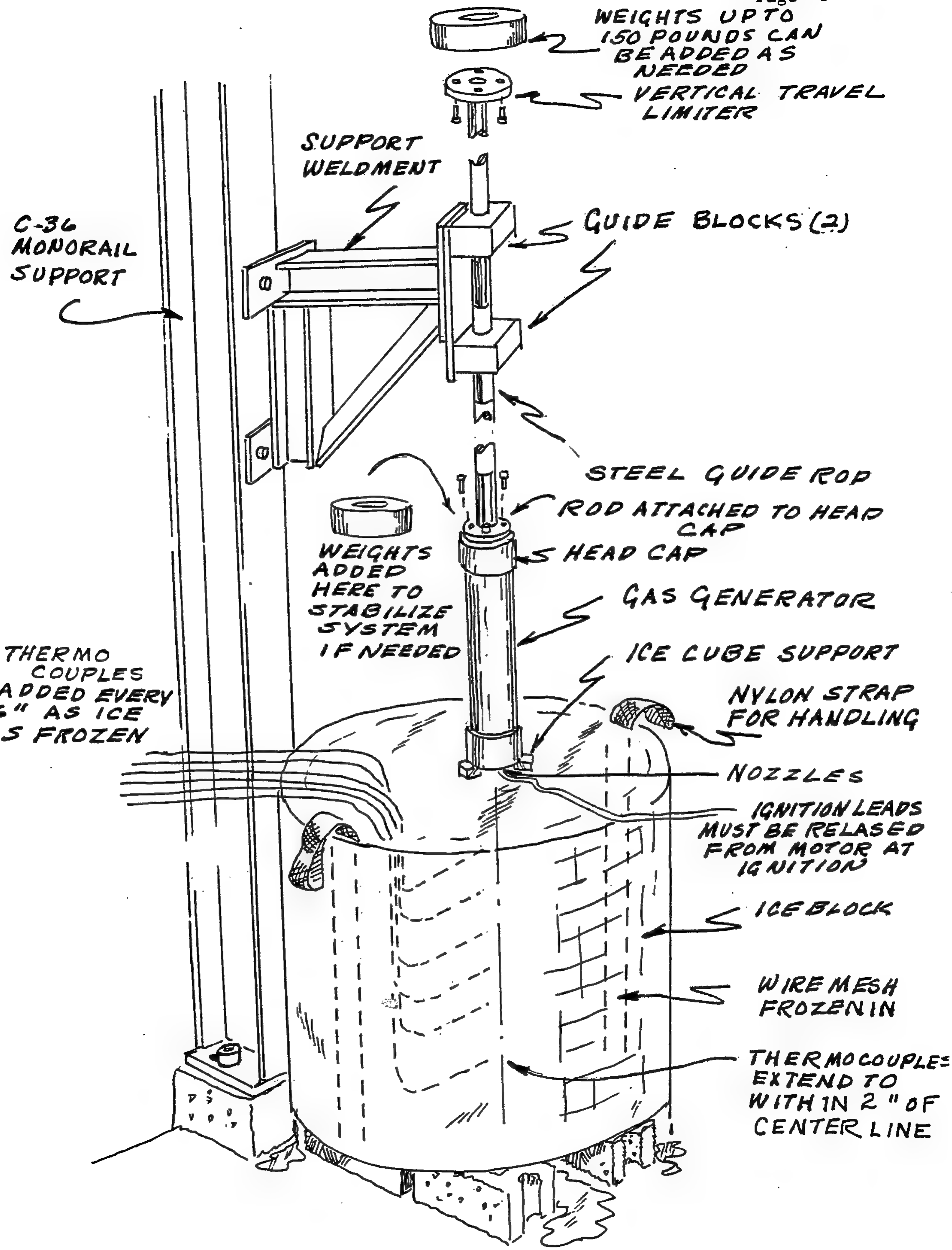
WEIGHTS UP TO 150 POUNDS CAN BE ADDED AS NEEDED
VERTICAL TRAVEL LIMITER
SUPPORT WELDMENT
C-36 MONORAIL SUPPORT
GUIDE BLOCKS (2)
STEEL GUIDE ROD
ROD ATTACHED TO HEAD CAP
HEAD CAP
WEIGHTS ADDED HERE TO STABILIZE SYSTEM IF NEEDED
GAS GENERATOR
ICE CUBE SUPPORT
THERMO COUPLES ADDED EVERY 6" AS ICE IS FROZEN
NYLON STRAP FOR HANDLING
NOZZLES
IGNITION LEADS MUST BE RELASED FROM MOTOR AT IGNITION
ICE BLOCK
WIRE MESH FROZEN IN
THERMOCOUPLES EXTEND TO WITHIN 2" OF CENTER LINE

FIGURE 1

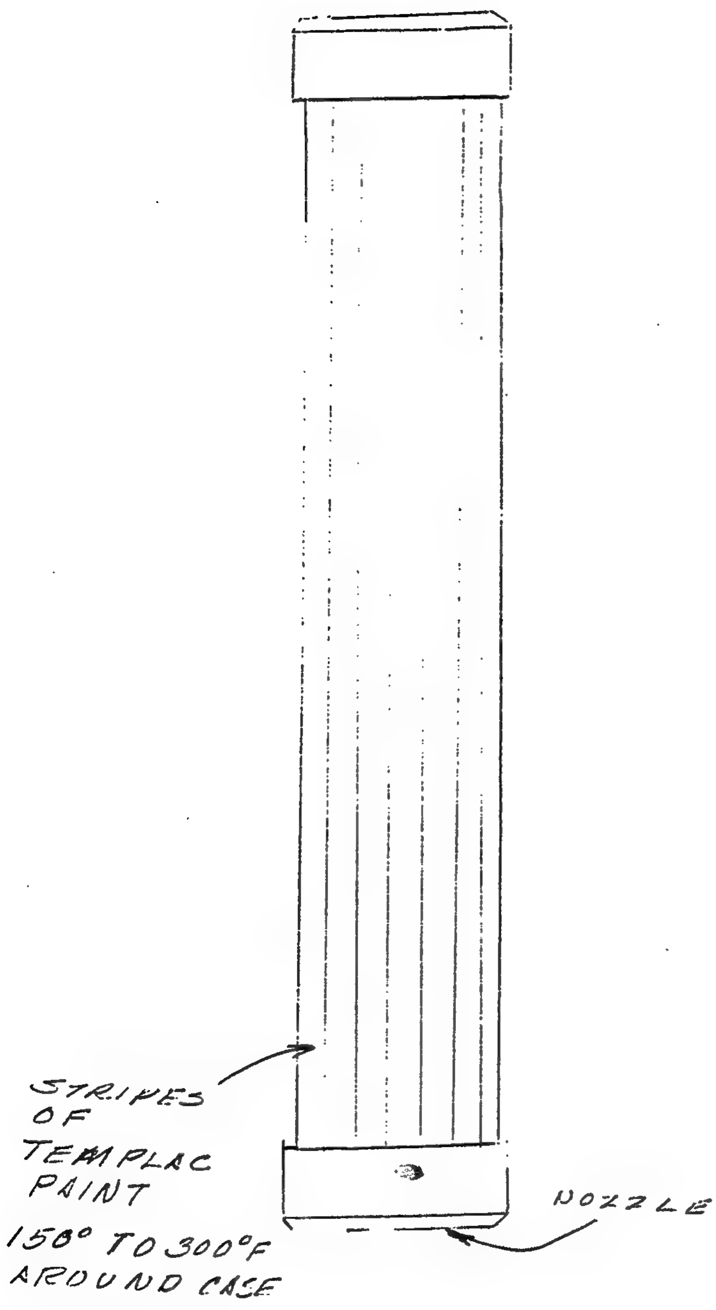

FIGURE 2

ICE PENETRATION TEST NUMBER 1

(SEPTEMBER 20, 1990)

TEST REPORT

OCTOBER 31, 1990

THIOKOL CORPORATION

ELKTON DIVISION

PROJECT ENGINEER Daniel M. Dunlap

PROGRAM MANAGER Donald E. Osborne

TABLE OF CONTENTS

LIST OF FIGURES

LIST OF TABLES

I INTRODUCTION

On 20 September the first in a series of two penetration tests was conducted. This test was done to:

1) assess the feasibility of using a solid propellant rocket motor for rapid ice penetration;

2) determine the efficiency of the penetration using four inch diameter hardware in a heavy weight configuration;

3) gather sufficient data, most notably penetration rate, to be able to size a flightweight configuration capable of penetrating 10 feet of ice in an arctic environment.

The motor cross-section is shown in figure 1, and figure 2 is a sketch of the test arrangement.

II SUMMARY

The heavyweight test motor successfully penetrated the full thickness of the ice block (41 inches) in less than the total burn time of the motor. First evidence of flame below the ice occurred at 28.3 seconds into the burn, with full motor penetration 9 seconds later. The total motor burn time was 45.5 seconds. The hole in the ice was approximately conical in shape, with considerable channeling and flow induced cavities on the hole wall. The top of the hole was approximately 7 inches in diameter, with a 5 inch diameter hole at the exit point.

III CONCLUSION/RECOMMENDATIONS

This test has demonstrated rapid penetration of ice by using a solid propellant rocket motor. For this particular design, the motor appears capable of penetrating about 50% more ice. Although designed to spin, very little spin was seen in the test. This is likely due to the inert weight placed on top of the assembly compressing the bearing and adding to the inertia of the test system. Two changes are recommended for the next test. The first is to reduce the inert weight placed on the assembly by 40 lbm, and the second is to increased the ice thickness to approximately 60 inches.

IV DISCUSSIONS

Table I presents the pertinent design and performance data for the motor used for the penetration test. The motor was designed to burn nominally for about 43 seconds at 400 psia, giving a propellant mass flow to the ice block of about 0.193 lbm/second. Due to slight nozzle insert erosion and a burn rate scale factor of less than 1, the total burn time was actually about 45.5 seconds, with an average pressure of about 370 psia and an average mass flow rate of about 0.182 lbm/second. The pre-test predicted and post-test reconstructed pressure and thrust traces are shown in figures

3 and 4. The post-test reconstructed traces (labeled ACTUAL) were derived based on the measured throat diameters before and after, as well as the burn time determined from the video. The motor pressure level was then inferred from these data.

Figure 5 presents two sets of data, the penetration rate as derived from the high speed video, and the time when heat was first detected by the thermocouples placed in the ice block. There are a number of interesting points to note about these data: 1) After about 5 seconds of burn, the penetration rate stays constant at about 1.29 inches/second, although there are a few points were the descent is both more and less rapid. This is true until flame breaches the ice bottom surface at 28.3 seconds. 2) The thermocouple data indicate that the flame front precedes the advancing penetrator by roughly a constant amount, between 4 and 6 inches. The last data point plotted (at about 17 1/2 seconds) is an indication of the unevenness of the flame propagation through the cracking ice, for this seems to be about 9 inches ahead of the penetrator. 3) The first indication of flame below the ice was at 28.3 seconds, when the penetrator had descended only 36 1/2 inches. From this point on, the penetration rate was naturally slower, about 0.5 inch/second, until final ice breakthrough at 37.3 seconds. 4) The penetrator burned freely below the ice (on the ground) from 37.5 seconds until burnout at 45.5 seconds.

Table II lists the data points taken from analysis of the high speed video; these are the data plotted in figure 5. The thermocouple data are plotted in Appendix A.

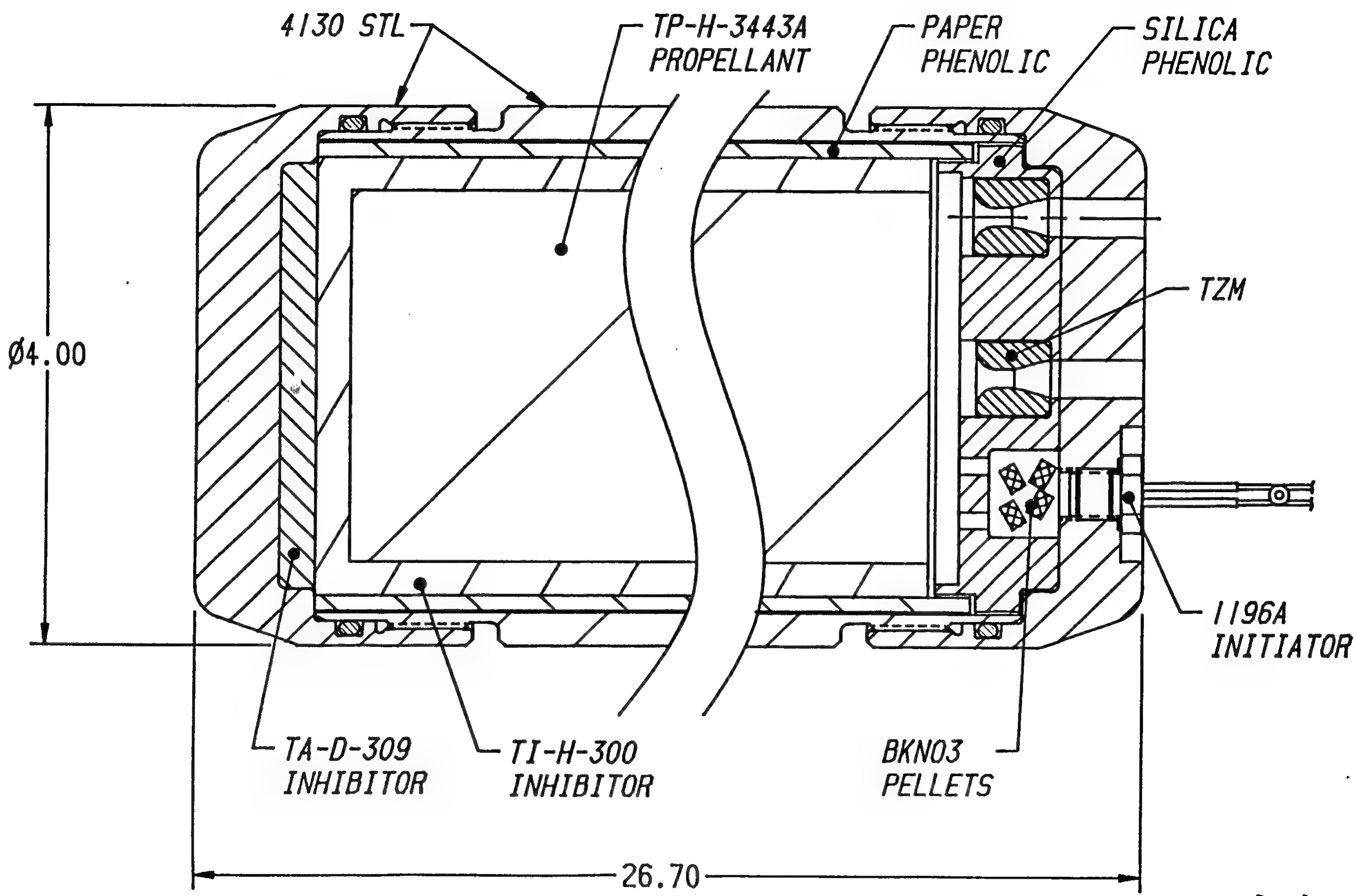

FIGURE 1. MOTOR CROSS-SECTION

DMD
8-22-90

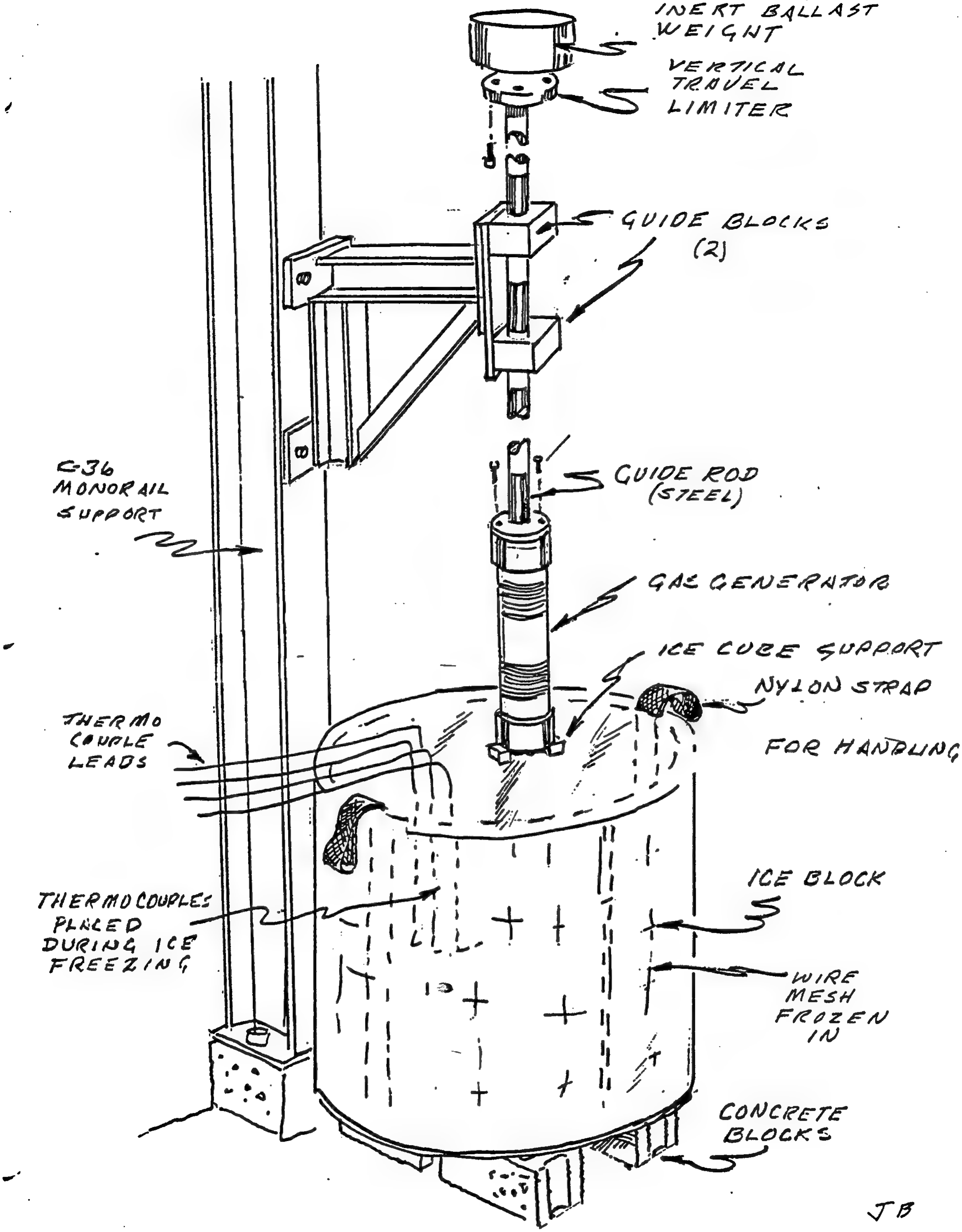

FIGURE 2: TEST ARRANGEMENT

Ice Penetrator

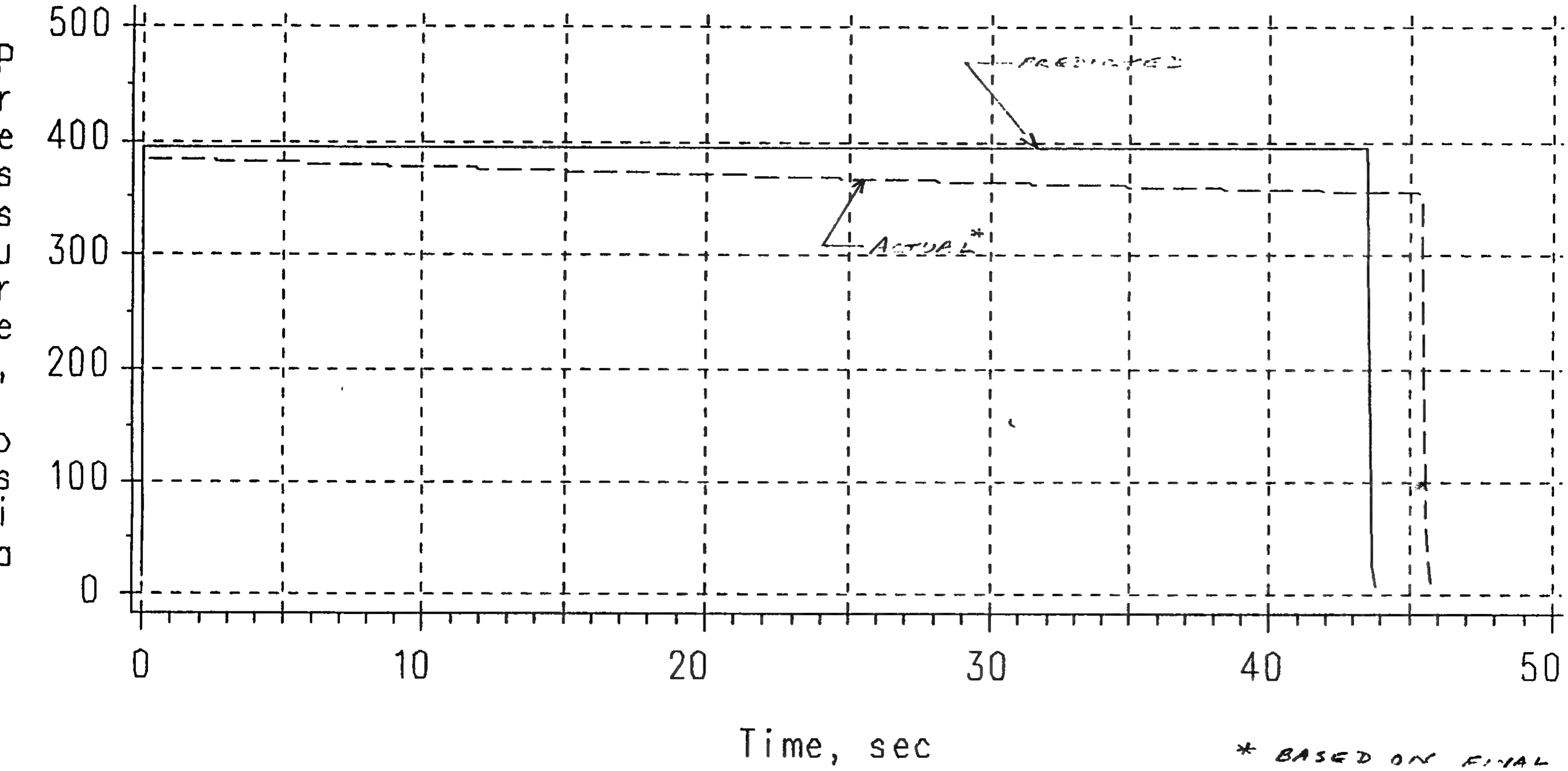

* BASED ON FINAL THROAT AREA AND BURN TIME. NO MEASUREMENT MADE

hiokol Corporation
kton Division

Prel. Design —dmd—
26OCT90 11:56

FIGURE 3. MOTOR CHAMBER PRESSURE

Ice Penetrator

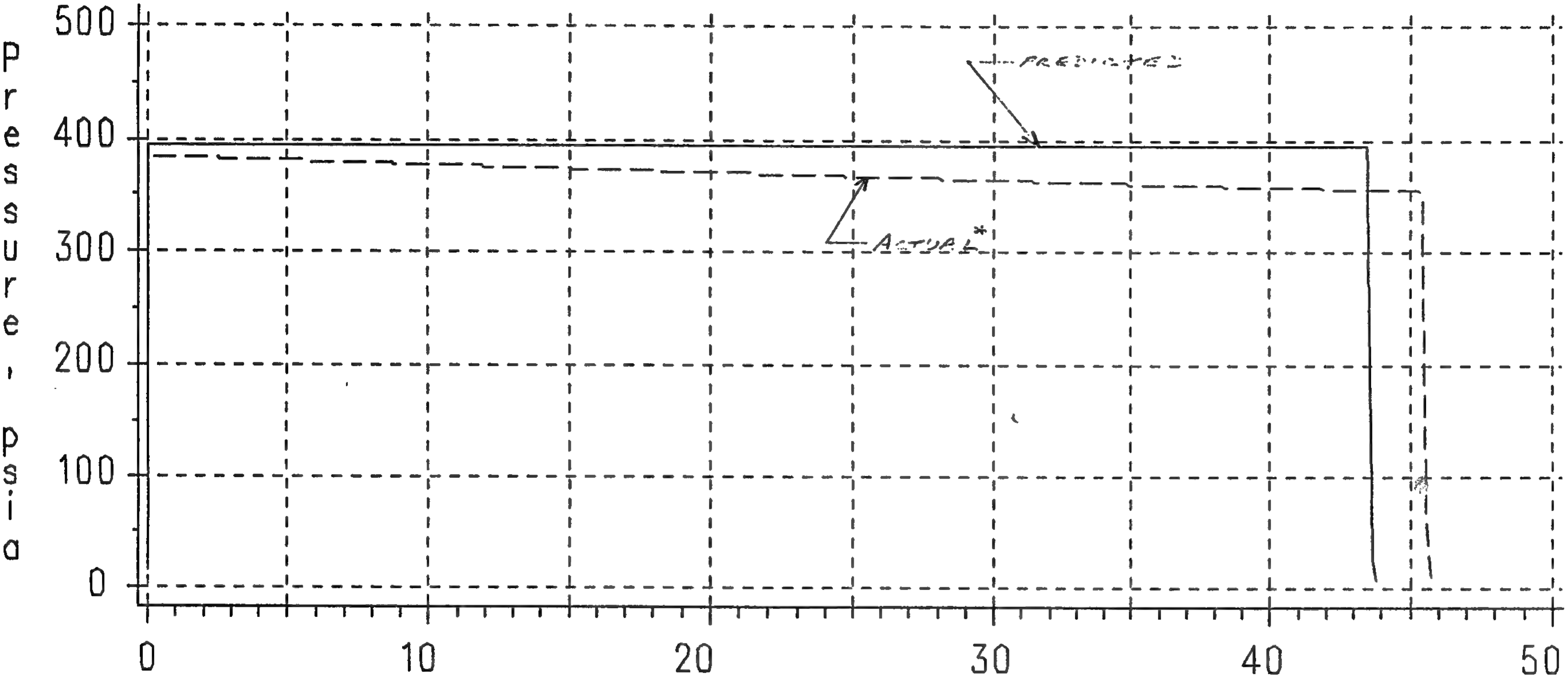

* BASED ON FINAL THROAT AREA AND BURN TIME. NO MEASUREMENT MADE

hiokol Corporation
kton Division

Prel. Design —dmd—
26OCT90 11:56

FIGURE 3. MOTOR CHAMBER PRESSURE

Ice Penetrator

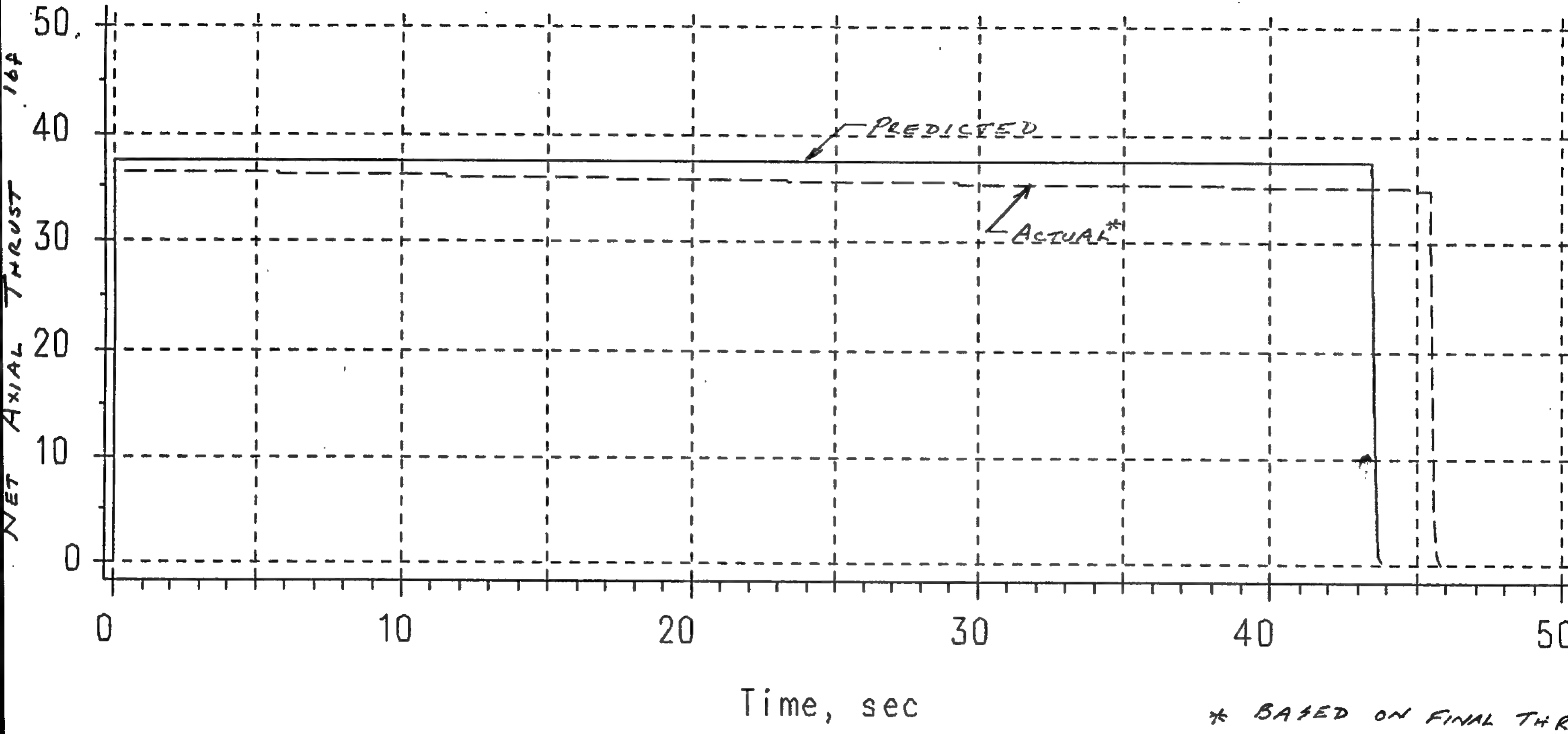

* BASED ON FINAL THROAT AREA AND BURN TIME
NO MEASUREMENT MADE

hiokol Corporation
lkton Division

Prel. Design –dmd–
26OCT90 13:11

FIGURE 4 NET AXIAL THRUST

Ice Penetrator

TEST 9-20-90

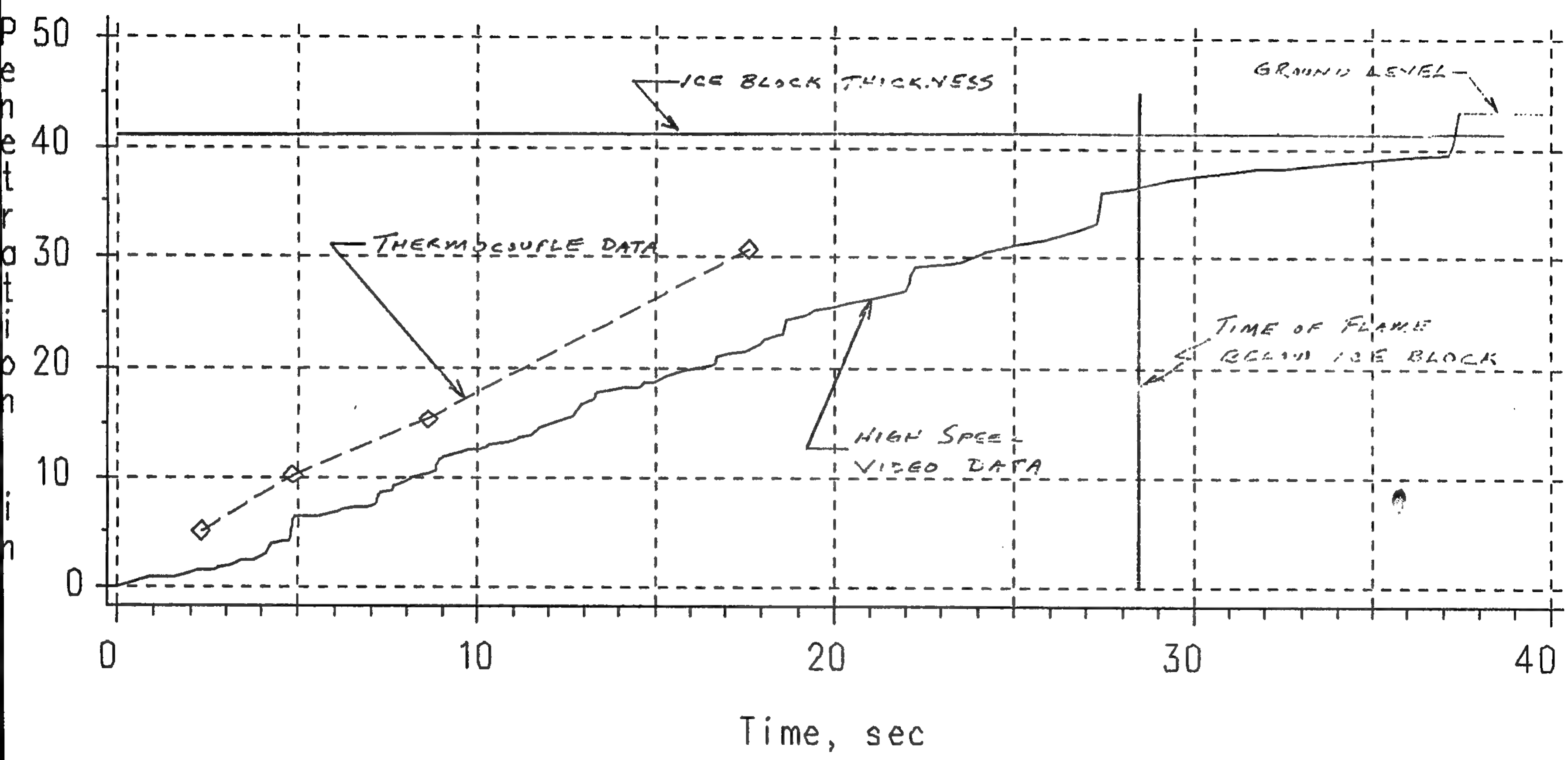

hiokol Corporation
lkton Division

Prel. Design –dmd–
8OCT90 14:16

FIGURE 5. ICE PENETRATION DATA

TABLE I

ICE PENETRATOR DESIGN AND PERFORMANCE DATA

DESIGN DATA

Outside Diameter, in	4.0
Overall Length, in	26.7
Propellant Weight, lbm	8.28
Total Motor Weight, lbm	36.5
*Total Test Arrangement Weight, lbm	130.3
Nozzle Throat Diameter, in (ea of 5, initial)	0.140/0.138/0.142/0.140/0.141
Nozzle Exit Diameter, in	0.280
Total Throat Area, (init/final) in^2	0.0772/.0812
Effective Expansion Ratio, (init/final)	3.98/3.79

PERFORMANCE DATA

Avg Chamber Pressure	psia	370
Net Avg Axial Thrust	lb_f	36
Burn Time	sec	45.5
**Chamber Temperature	°F	4425
**Nozzle Exit Pressure	psia	16.4
**Nozzle Exit Static Temperature	°F	2280
**Nozzle Exit Velocity	ft/s	7035
**Gas Viscosity (chamber/exit)	lb_f-sec/ft^2	$1.695 \times 10^{-6}/1.128 \times 10^{-6}$
**Gas Conductivity (chamber/exit)	lb_f-sec/°R	$3.229 \times 10^{-2}/2.025 \times 10^{-2}$
**Gas Specific Heat (chamber/exit)	BTU/lbm -°F	0.447/0.406
**Maximum Available Heat Content	BTU	18630

*Includes 21 lbm rod, 4 lbm adaptor, 68.8 lbm weight
**THEORETICAL

TABLE II

Ice Penetrator Test 9/20/90
Penetration Data From High Speed
Video Analysis

Time, sec	Penetration Distance, in
0.000	0.00
0.840	0.90
1.560	0.90
1.780	1.20
2.216	1.50
2.616	1.65
2.784	1.80
3.152	2.10
3.448	2.40
3.784	2.55
4.128	3.15
4.176	3.45
4.264	3.90
4.392	4.05
4.624	4.20
4.728	4.20
4.792	4.65
4.816	5.10
4.840	5.55
4.864	6.00
4.872	6.30
5.024	6.30
5.104	6.30
5.280	6.45
5.552	6.45
5.776	6.60
6.048	6.75
6.232	7.05
6.536	7.20
6.848	7.35
7.088	7.50
7.136	7.65
7.152	7.80
7.168	7.95
7.184	8.25
7.200	8.40
7.232	8.55
7.592	8.85
7.640	9.15
7.656	9.30
7.840	9.45
8.112	9.90
8.272	10.05
8.584	10.35
8.776	10.50
8.808	10.65
8.824	10.95
8.848	11.25
8.880	11.55
8.888	11.70

TABLE II (CONT)

Time, sec	Penetration Distance, in
9.000	11.85
9.280	12.00
9.528	12.30
9.760	12.45
10.016	12.60
10.192	12.75
10.312	12.90
10.824	13.20
11.016	13.50
11.176	13.65
11.472	13.95
11.736	14.55
12.064	15.00
12.696	15.60
12.960	16.65
13.288	17.10
13.312	17.25
13.336	17.55
13.360	17.70
13.736	18.00
14.104	18.15
14.544	18.30
14.718	18.60
14.989	18.75
15.360	19.35
15.816	19.65
16.568	20.10
16.696	20.40
16.720	20.55
16.752	21.00
17.104	21.30
17.544	21.45
17.992	22.20
18.080	22.65
18.528	23.10
18.576	23.10
18.672	24.45
19.240	24.90
19.512	25.20
19.856	25.50
20.440	25.95
21.144	26.40
22.008	27.00
22.088	27.75
22.152	28.35
22.272	29.10
23.208	29.40
23.560	29.70
24.184	30.45
24.936	31.05
25.808	31.65
26.728	32.40
27.264	33.15
27.328	33.75
27.368	34.65

ICE PENETRATION TEST NUMBER 2

(OCTOBER 12, 1990)

TEST REPORT

NOVEMBER 2, 1990

THIOKOL CORPORATION

ELKTON DIVISION

PROJECT ENGINEER ____________________

PROGRAM MANAGER ____________________

I INTRODUCTION

On 12 October 1990 the second in a series of two penetration tests was conducted. This followed the successful test of 20 September 1990, discussed in the test report dated 10-31-90. This test was done to gather additional data on penetration efficiency. The motor configuration is identical to that of the first test (shown in figure 1), with only the test configuration (figure 2) changing somewhat. The thickness of the ice block was increased from 41 inches to 62 inches, and the inert weight placed on top of the assembly was reduced from 68.8 lbm to 30 lbm. The ice thickness was increased because test #1 penetrated the full 41 inches before motor burnout. The weight was reduced to investigate its affect on both the motor spin rate and the penetration rate.

II SUMMARY

The motor burned exactly like the first test for 45.5 seconds, in which time it penetrated through 54.5 inches, and then settled through another 1.9 inches after burn while the case cooled down. At 30.5 seconds a gas leak occurred through the seam of the ice block, reducing somewhat the penetration efficiency. The motor had a spin rate that ranged from about 30 to 80 rpm, the maximum occurring at about 28 seconds into the burn. The hole in the ice was again roughly conical, with a 7 inch diameter hole at the top and about a 4 1/2 inch diameter hole at the bottom. The hole wall surface was somewhat smoother than the first test, probably due to the motor spinning, although there is no quantitative evidence of this.

III CONCLUSION/RECOMMENDATION

The penetration rate and efficiency of this test was nearly identical with the test of 20 September 1990, including the slower penetration before a hole is established in the ice (before 5 seconds). Had the seam between ice blocks not failed, approximately 2.5 to 3 more inches of ice would likely have been penetrated, which would still have been about 2 or 3 inches short of the full ice thickness. The fact that the motor had a sustained spin rate seemed not to affect the penetration rate, although this was likely obscured by having less inert weight on the system. These two factors are obviously interrelated.

The thermocouples placed in the ice block yielded no usable data, and any succeeding tests should be run without their inclusion.

IV DISCUSSION

Table I presents the performance and design data for the motor used with this penetration test. Most of the data are exactly the same as the first test, with the exception of the actual propellant weight (8.24 vs 8.28 lbm), and the throat diameters. The motor burned for 45.5 seconds at an average pressure of about 370 psi, and a mass flow rate of about 0.182 lbm/sec. The pre and post-test thrust and pressure traces are show in figures 3 and 4.

Figure 5 is an overlay of the penetration data from both tests. The similarity of the traces shows good repeatability. Both show a rather slow start to the penetration until 5 seconds as the motor gasses are being dissipated at the ice surface. In test two the penetration rate between 5 and 30 seconds (until gas breach of the ice block was seen) was 1.29 inches/second, the same rate that test 1 exhibited over the period 5 until 28.3 seconds (when gas breached below the ice surface). After 30 seconds the penetration rate drops to about 1.11 inches/second when some of the energy escapes through the side of the ice block. After motor burnout at 45.5 seconds, some penetration continues as the hot motor case settles into the ice.

Table II is a digital listing of the penetration as taken from analysis of the high speed video.

Because the volume of ice carved out by the penetrator is difficult to estimate or predict, a method for calculating overall penetration efficiency was derived based on the motor diameter only. This is based on the concept of the "perfect" hole, i.e. one having the same diameter as the penetrator. Table III compares the efficiency of both tests based on the perfect hole concept, and the energy that was expended from the motor in creating the hole. The actual energy used in test 1 was calculated by using only that burn time necessary to make the hole, not the total burn time. This was calculated by determining the time at which the 41 inch ice block would have been penetrated had the flame not breached the lower surface reducing the efficiency of penetration. Extension of the slope of the curve before 28.3 seconds intersects the 41 inch point point at about 32.3 seconds. Therefore, the fraction of available energy used is 32.3/45.5 or .71.

Both tests give an overall efficiency of about 20% using this method. This calculation is however crude, for no attempt is made to include the effects of nozzle configuration, mass flow, spin rate, total weight or burn time. The 20% efficiency factor is therefore applicable only to this design, but could be used as a starting place for further predictions.

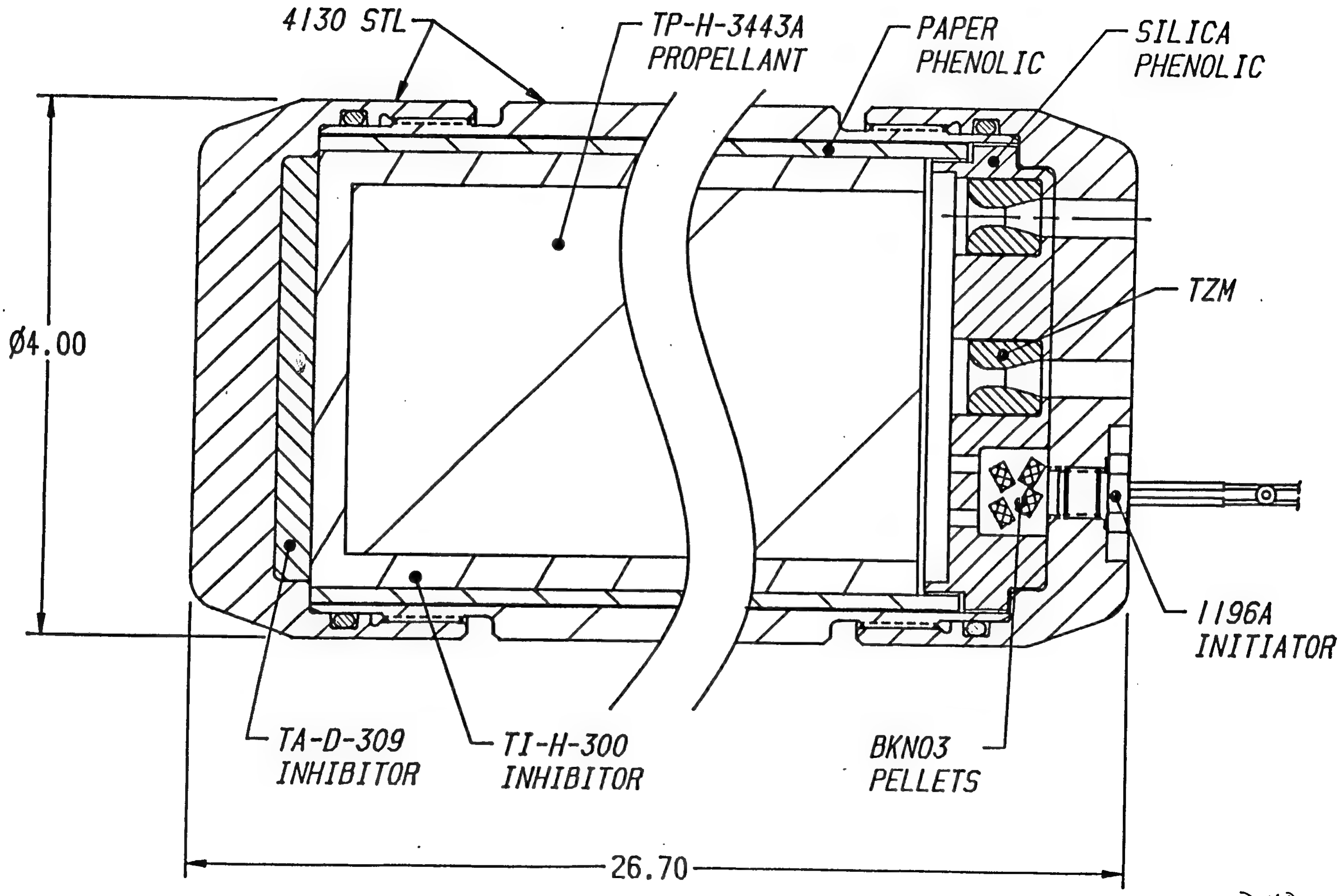

FIGURE 1. MOTOR CROSS-SECTION

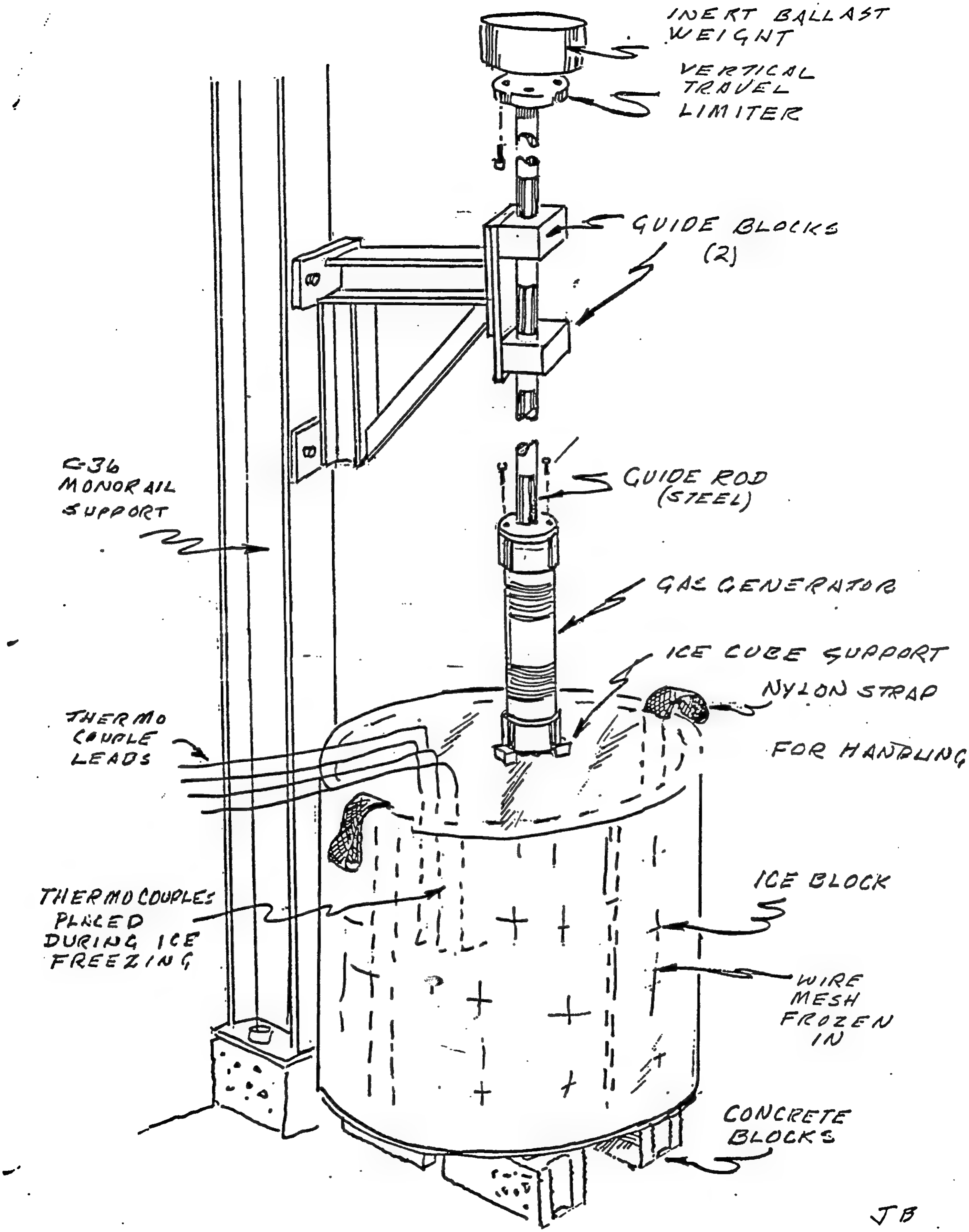

FIGURE 2: TEST ARRANGEMENT

Ice Penetrator

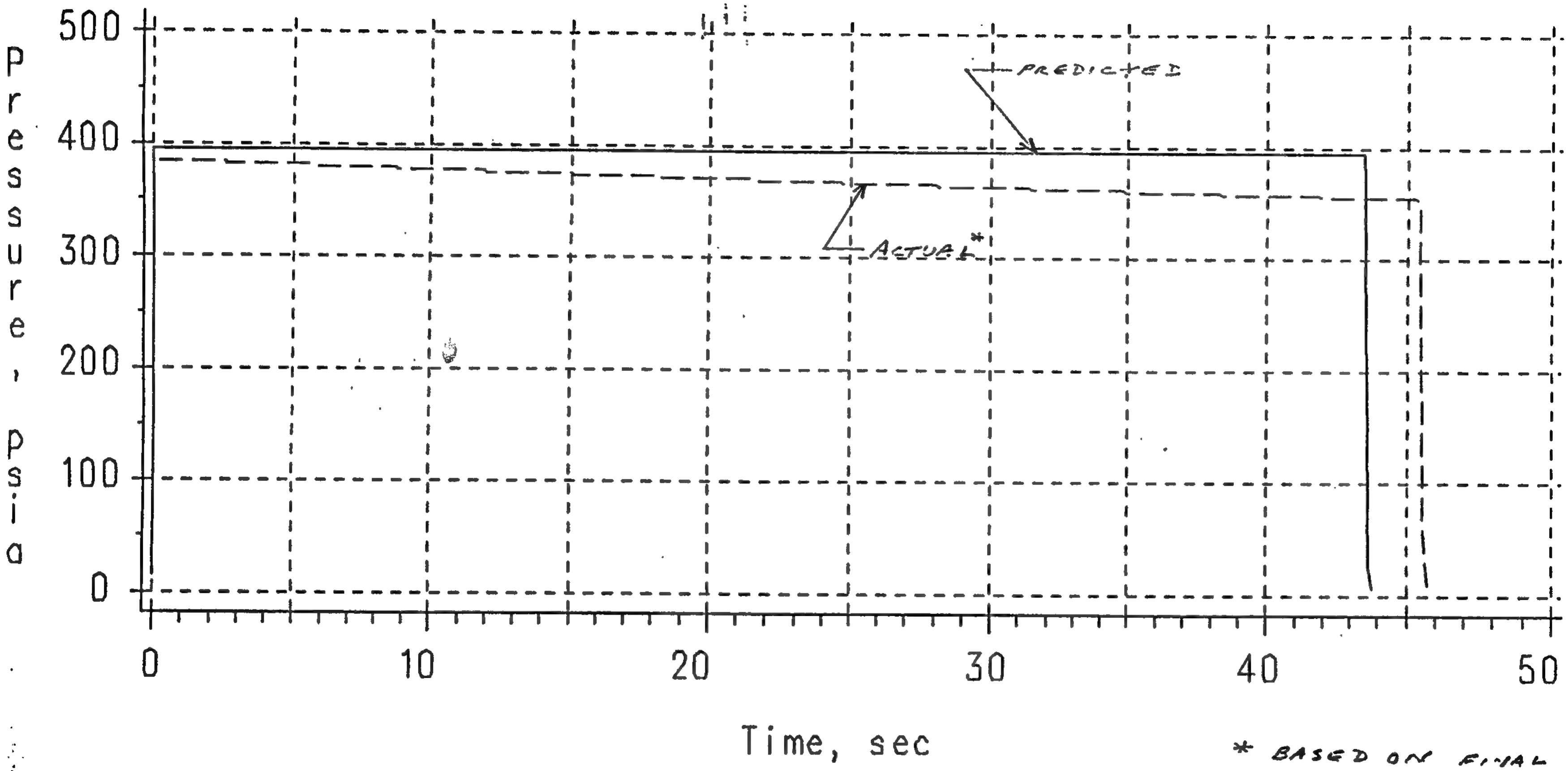

* BASED ON FINAL THROAT AREA AND BURN TIME. NO MEASUREMENT MADE

iokol Corporation
ton Division

Prel. Design —dmd—
26OCT90 11:56

FIGURE 3. MOTOR CHAMBER PRESSURE

Ice Penetrator

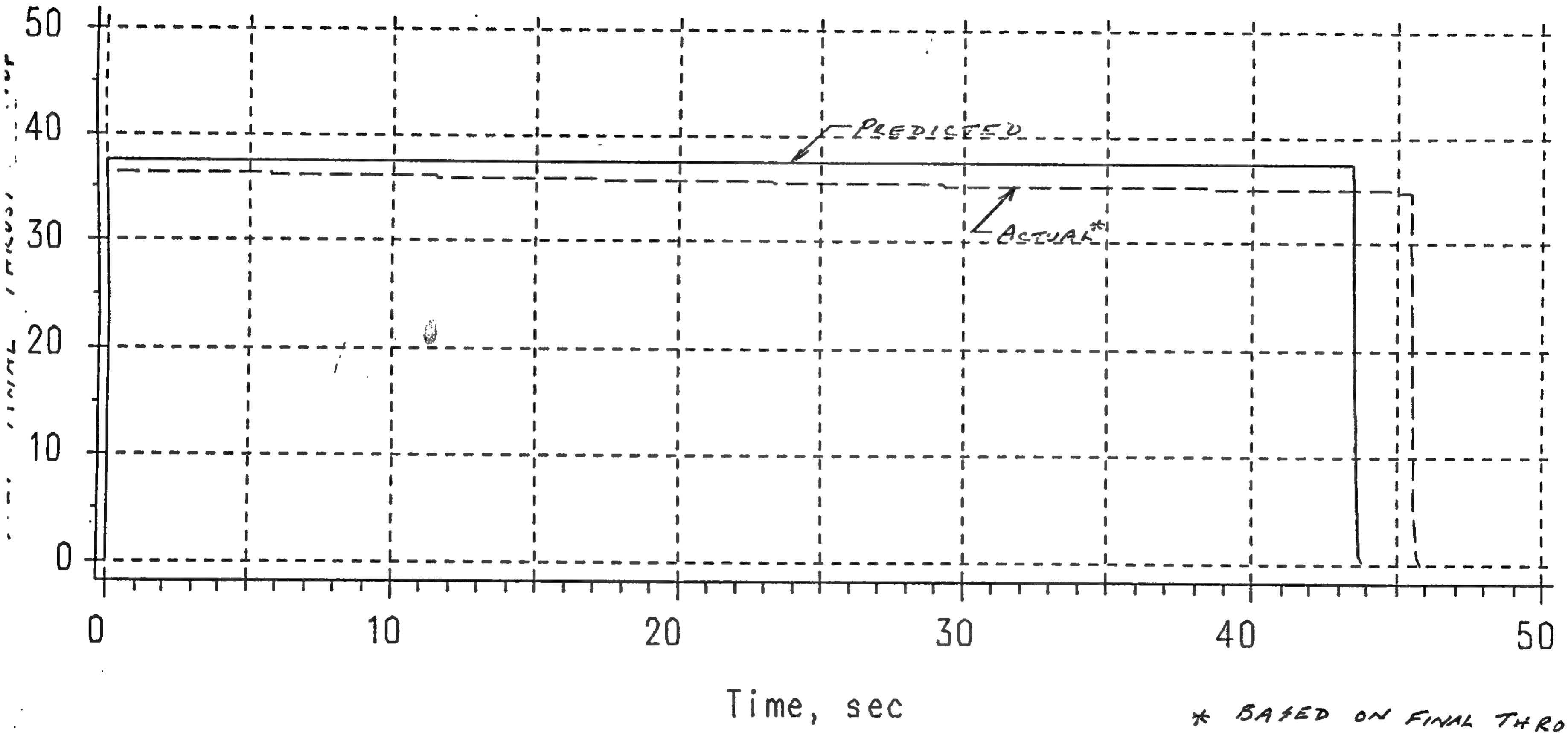

* BASED ON FINAL THROAT AREA AND BURN TIME
NO MEASUREMENT MADE

ıiokol Corporation
‹ton Division

Prel. Design —dmd—
26OCT90 13:11

FIGURE 4 NET AXIAL THRUST

Ice Penetrator

TEST RESULTS

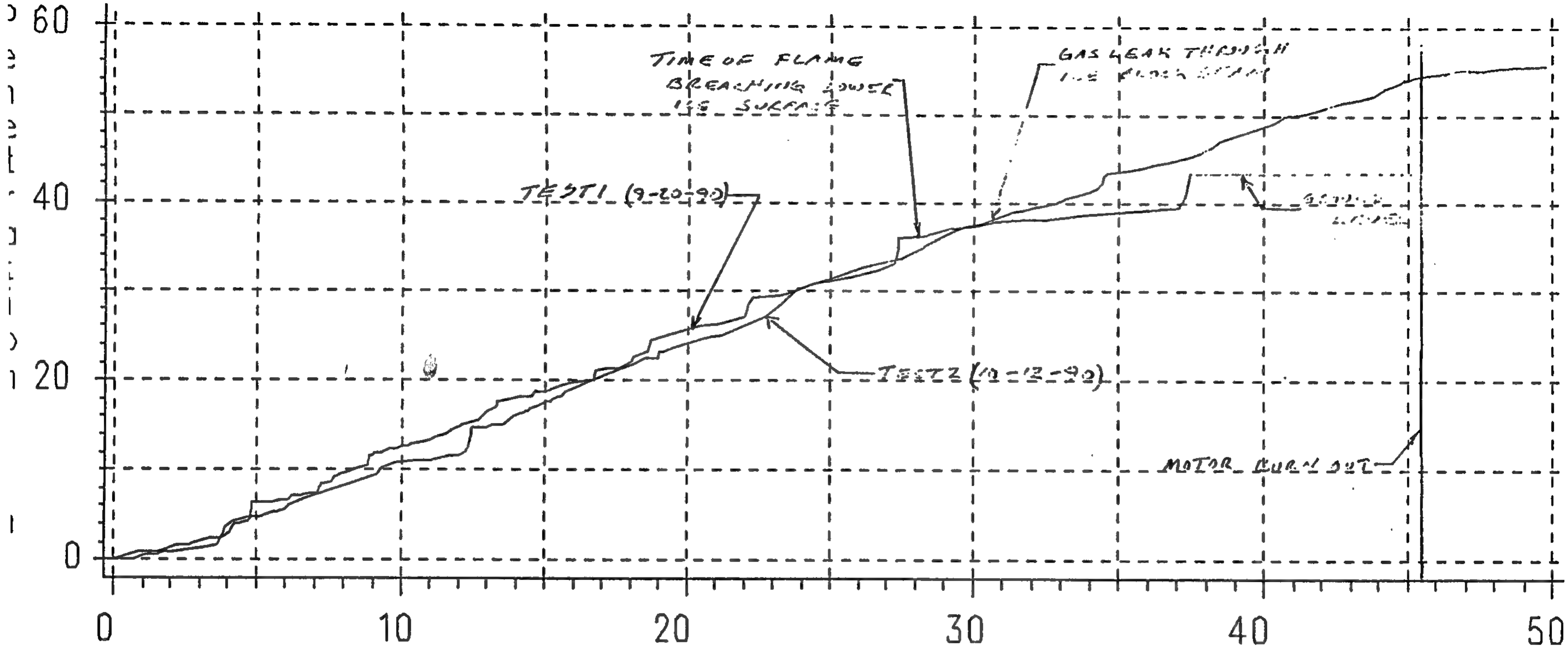

hiokol Corporation

kton Division

Prel. Design —dmd—

19OCT90 9:25

FIGURE 5. PENETRATION RATE COMPARISONS

TABLE I

ICE PENETRATOR DESIGN AND PERFORMANCE DATA

DESIGN DATA

Outside Diameter, in	4.0
Overall Length, in	26.7
Propellant Weight, lbm	8.24
Total Motor Weight, lbm	36.5
*Total Test Arrangement Weight, lbm	91.5
Nozzle Throat Diameter, in (ea of 5, initial)	0.140/0.139/0.139/0.139/.0141
Nozzle Exit Diameter, in	0.280
Total Throat Area, (init/final) in^2	0.0765/0.0806
Effective Expansion Ratio, (init/final)	4.02/3.82

PERFORMANCE DATA

Avg Chamber Pressure	psia	370
Net Avg Axial Thrust	lbf	36
Burn Time,	sec	44.5
**Chamber Temperature	°F	4425
**Nozzle Exit Pressure	psia	16.4
**Nozzle Exit Static Temperature	°F	2280
**Nozzle Exit Velocity	ft/s	7035
**Gas Viscosity (chamber/exit)	lb_f-sec/ft^2	$1.695 \times 10^{-6}/1.128 \times 10^{-6}$
**Gas Conductivity (chamber/exit)	lb_f-sec/°R	$3.229 \times 10^{-2}/2.025 \times 10^{-2}$
**Gas Specific Heat (chamber/exit)	BTU/lbm -°F	0.447/0.406
**Maximum Available Heat Content	BTU	18540

*Includes 21 lbm rod, 4 lbm adapter, 30.0 lbm weight
**Theoretical

TABLE II

Ice Penetrator Test 10/12/90
Penetration Data From High Speed
Video Analysis

Time, sec	Penetration Distance, in
0.000	0.0000
0.456	0.0000
0.664	0.1579
0.928	0.3158
1.144	0.4737
1.512	0.6316
1.760	0.7895
2.120	0.9474
2.560	1.1053
3.136	1.2632
3.648	1.5789
3.800	2.6842
3.920	3.7895
4.152	4.2632
4.528	4.5789
4.768	4.7368
5.120	4.8947
5.320	5.0526
5.568	5.2105
5.720	5.3684
5.928	5.6842
6.096	6.0000
6.328	6.3158
6.656	6.7895
9.120	9.6316
9.248	9.9474
9.328	10.2632
9.800	10.7368
10.536	11.0526
11.000	11.2105
11.392	11.3684
11.632	11.5263
11.936	11.6842
12.240	12.1579
12.264	12.3158
12.336	13.1053
12.360	13.4211
12.376	13.7368
12.392	13.8947
12.400	14.2105
12.416	14.5263
12.488	14.8421
12.728	14.8421
12.944	14.8421
13.128	15.0000
13.200	15.0000
13.464	15.1579
13.752	15.7895
13.816	15.9474
13.912	16.1053
14.104	16.2632
14.176	16.4211
14.280	16.5789

TABLE II (CONT)

Time, sec	Penetration Distance, in
14.368	16.7368
14.440	16.8947
14.704	17.2105
15.008	17.6842
15.168	17.6842
15.232	18.0000
15.424	18.3158
15.480	18.3158
15.648	18.6316
17.016	20.5263
18.144	21.7895
18.456	22.2632
18.944	22.4211
18.984	23.0526
19.088	23.2105
19.536	23.6842
20.152	24.3158
20.704	24.7895
21.232	25.1053
22.672	27.1579
23.304	28.5789
23.848	30.3158
23.952	30.3158
24.344	30.7895
25.232	31.5789
26.048	32.5263
26.440	33.0000
27.496	33.7895
28.328	34.8947
28.696	35.6842
29.360	36.7895
29.744	37.2632
30.272	37.7368
30.904	38.3684
31.344	38.8421
31.760	39.1579
32.072	39.4737
32.488	39.7895
32.744	39.9474
33.120	40.4211
33.504	40.8947
33.960	41.3684
34.192	41.5263
34.432	42.3158
34.488	43.1053
34.624	43.4211
35.248	43.7368
35.768	44.0526
36.352	44.3684
36.752	44.6842
37.384	45.3158
37.840	45.7895
38.136	46.2632
38.440	47.0526
39.128	47.8421
39.776	48.6316

TABLE II (CONT)

Time, sec	Penetration Distance, in
40.280	49.2632
40.672	49.8947
41.352	50.3684
42.152	51.1579
42.680	51.4737
43.216	51.7895
43.768	52.4211
44.136	53.0526
44.352	53.5263
44.752	54.0000
45.224	54.4737
45.696	54.6316
46.432	54.9474
47.096	55.2632
47.592	55.2632
48.200	55.4211
49.768	55.8947
50.736	55.8947
53.408	56.2105
56.472	56.3684

dmd 10-19-90

TABLE III

PENETRATION EFFICIENCY CALCULATION

PERFECT HOLE CONCEPT	TEST 1 9-20-90	TEST 2 10-12-90
Hole Diameter, in	4	4
Hole Depth, in	41	56.4
Hole Volume, in^3	515	710
Weight of Ice Removed, lbm	17.1	23.5
*Net Heat Rqd To Melt, BTU	2730	3752
ENERGY EXPENDED		
Propellant Energy Content, BTU/lbm	2250	2250
Propellant Weight, lbm	8.28	8.24
Total Available Energy, BTU	18630	18540
**Fraction of Energy Used	0.71	1.0
ENERGY EFFICIENCY		
Energy Rqd/Energy Used (X100), %	20.6	20.2

* $\Delta H = C_p \Delta T W_{ti} + H_f W_{ti}$
Where C_p = .49 BTU/lbm-°F
ΔT = 32 °F
W_{ti} = ice weight
H_f = 144 BTU/lbm

** Based on burn time used during melting. For test 1 it is 32.3/45.5

TABLE 7 (CONT)

Time, sec	Penetration Distance, in
27.416	36.00
28.400	36.45
29.256	37.05
30.072	37.50
30.784	37.80
31.768	38.10
32.488	38.25
33.776	38.70
35.976	39.15
37.136	39.45
37.232	40.20
37.296	40.80
37.376	42.30
37.440	43.50

dmd 10-8-90

APPENDIX A

DISTRIBUTION

TE-M-913-2 - RAPID THERMAL ICE PENETRATOR

J. D. BLEVINS	G-28	(1)
D. M. DUNLAP	G-22	(1)
M. G. KRAMER	G-29	(1)
D. E. OSBORNE	G-29	(3)
FILE	G-28	(1)

Jay Blevins
Sept. 25. 1990

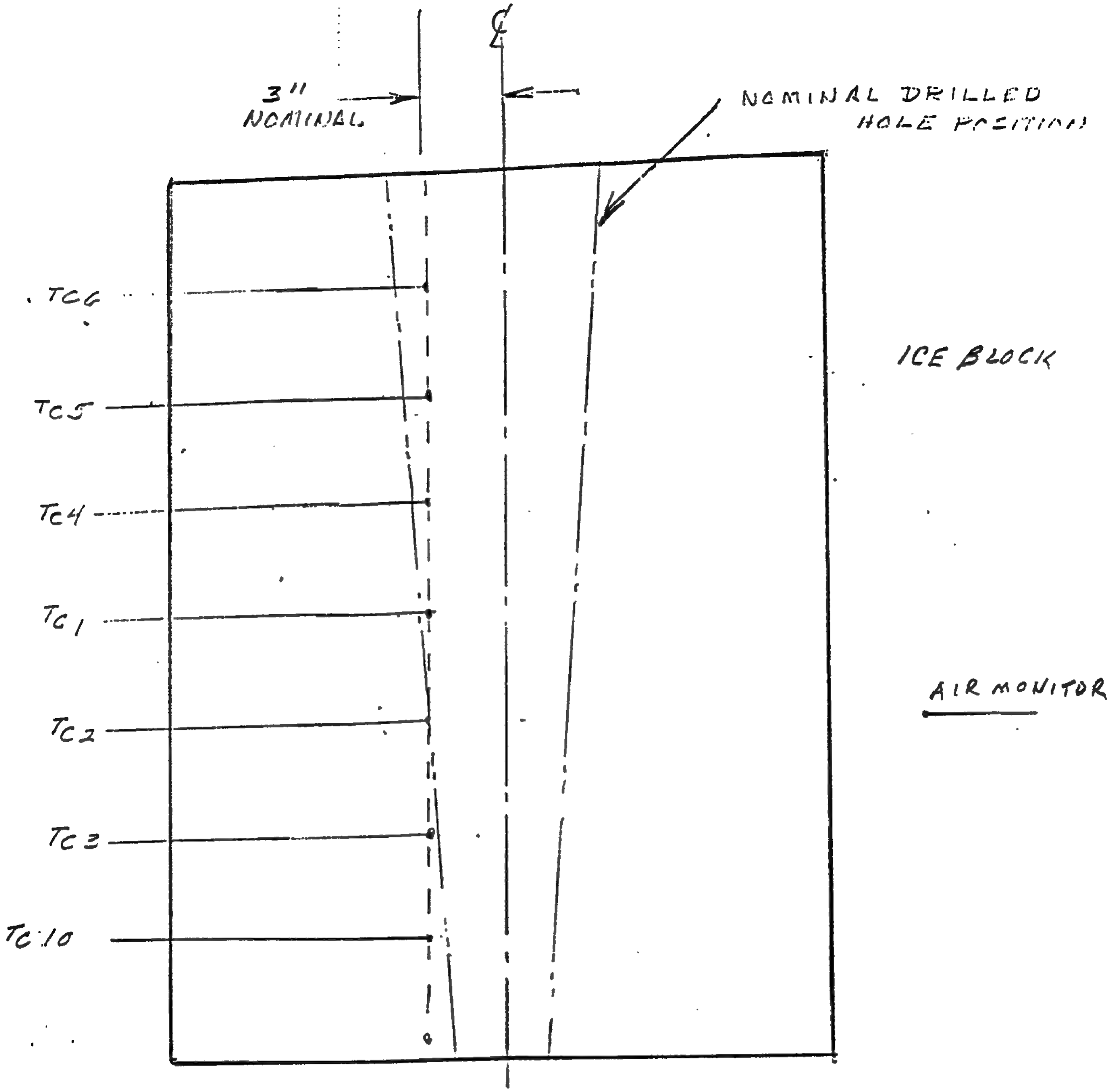

RAPID THERMAL ICE PENETRATOR

THERMOCOUPLE LOCATIONS

A

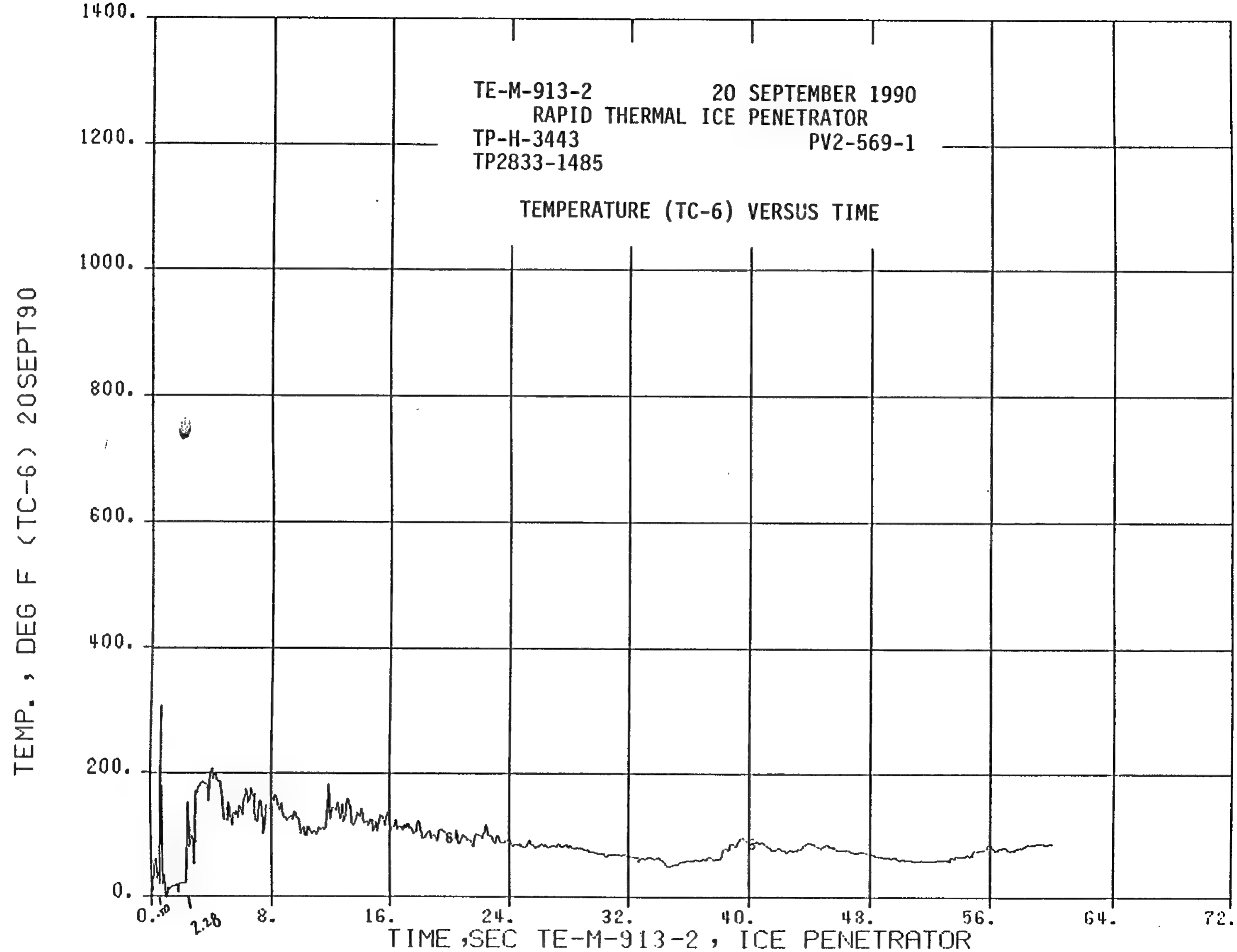

CMSBATCH 09/21/90

B

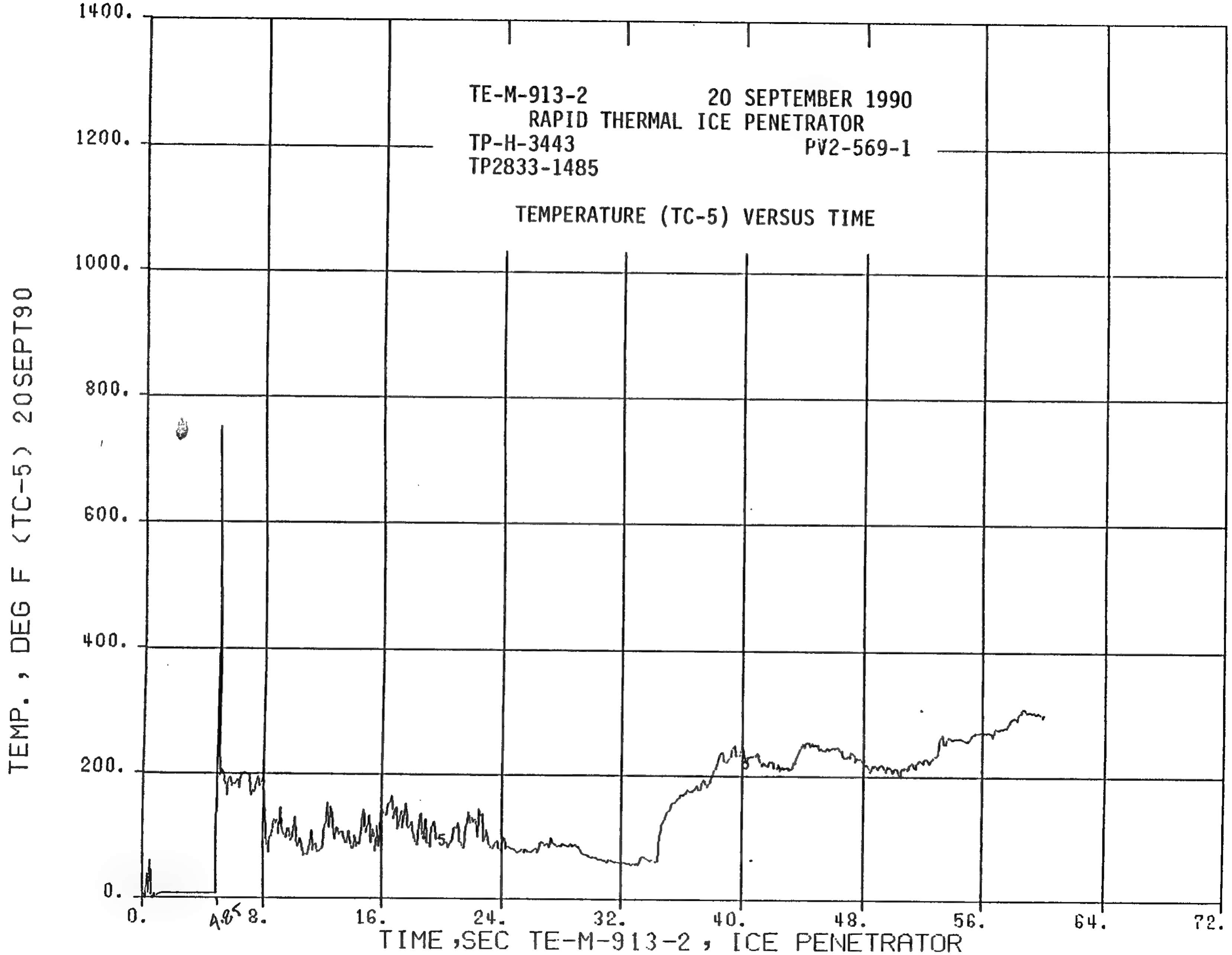

CMSBATCH 09/21/90

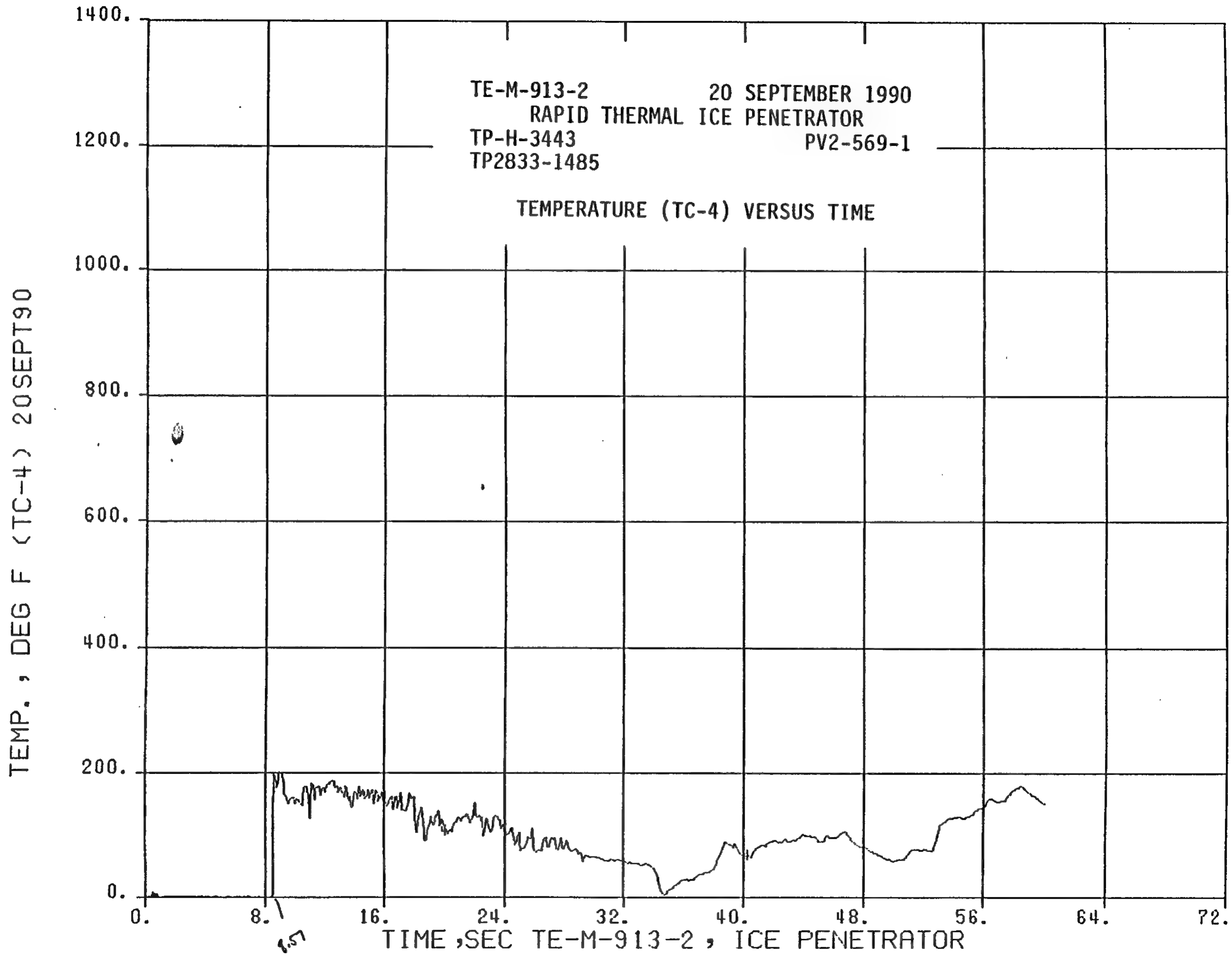

CMSBATCH 09/21/90

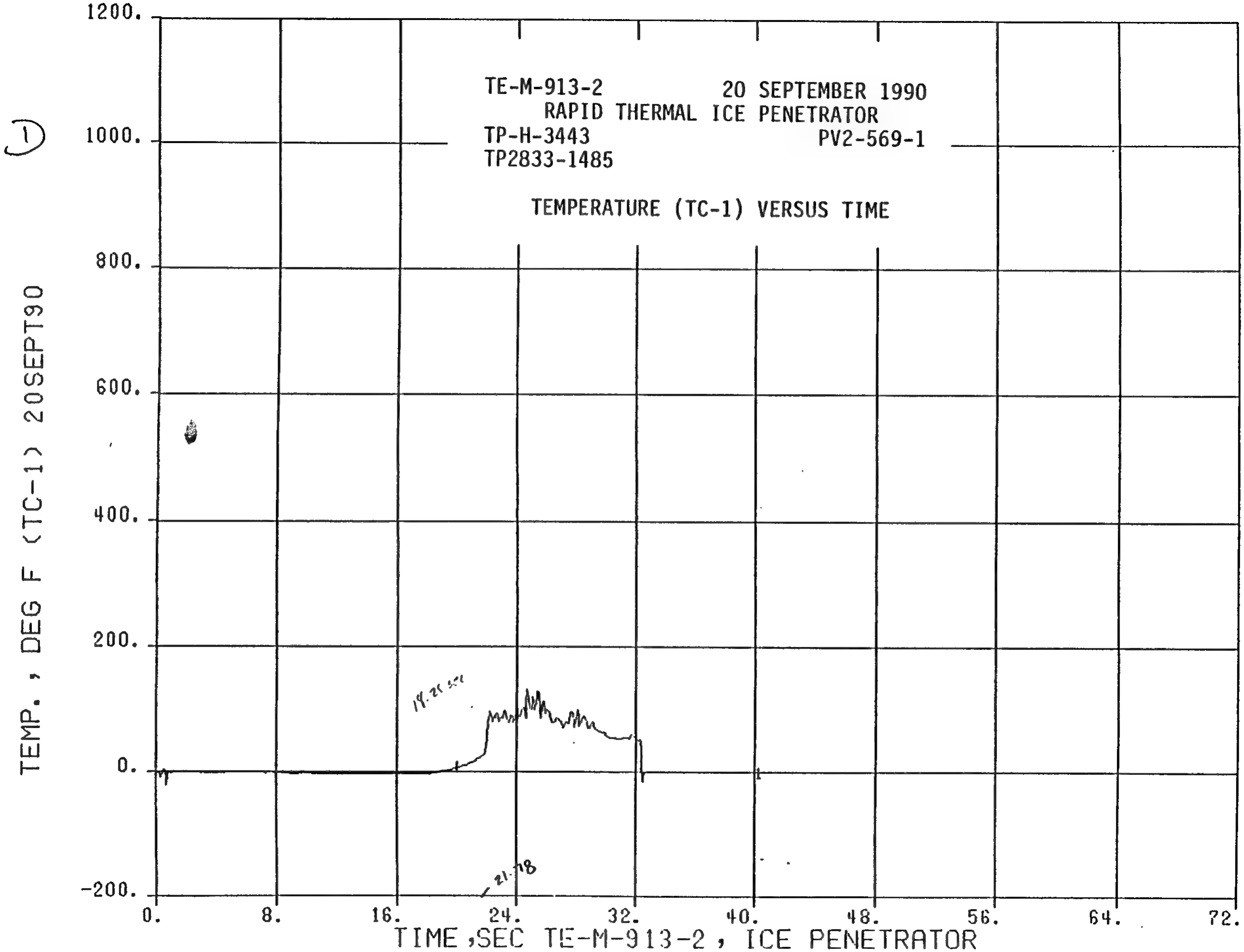

CMSBATCH 09/21/90

E

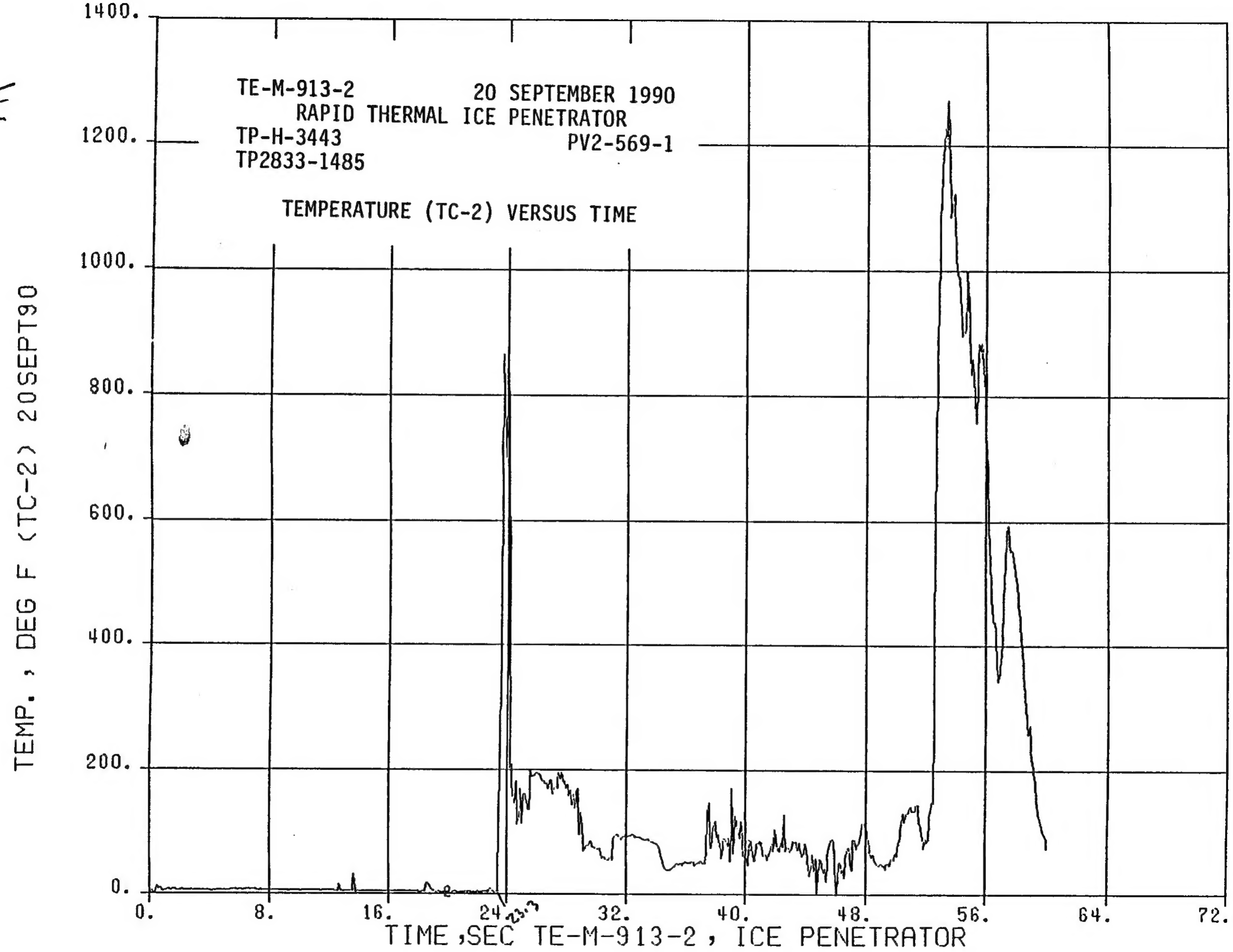

CMSBATCH 09/21/90

F

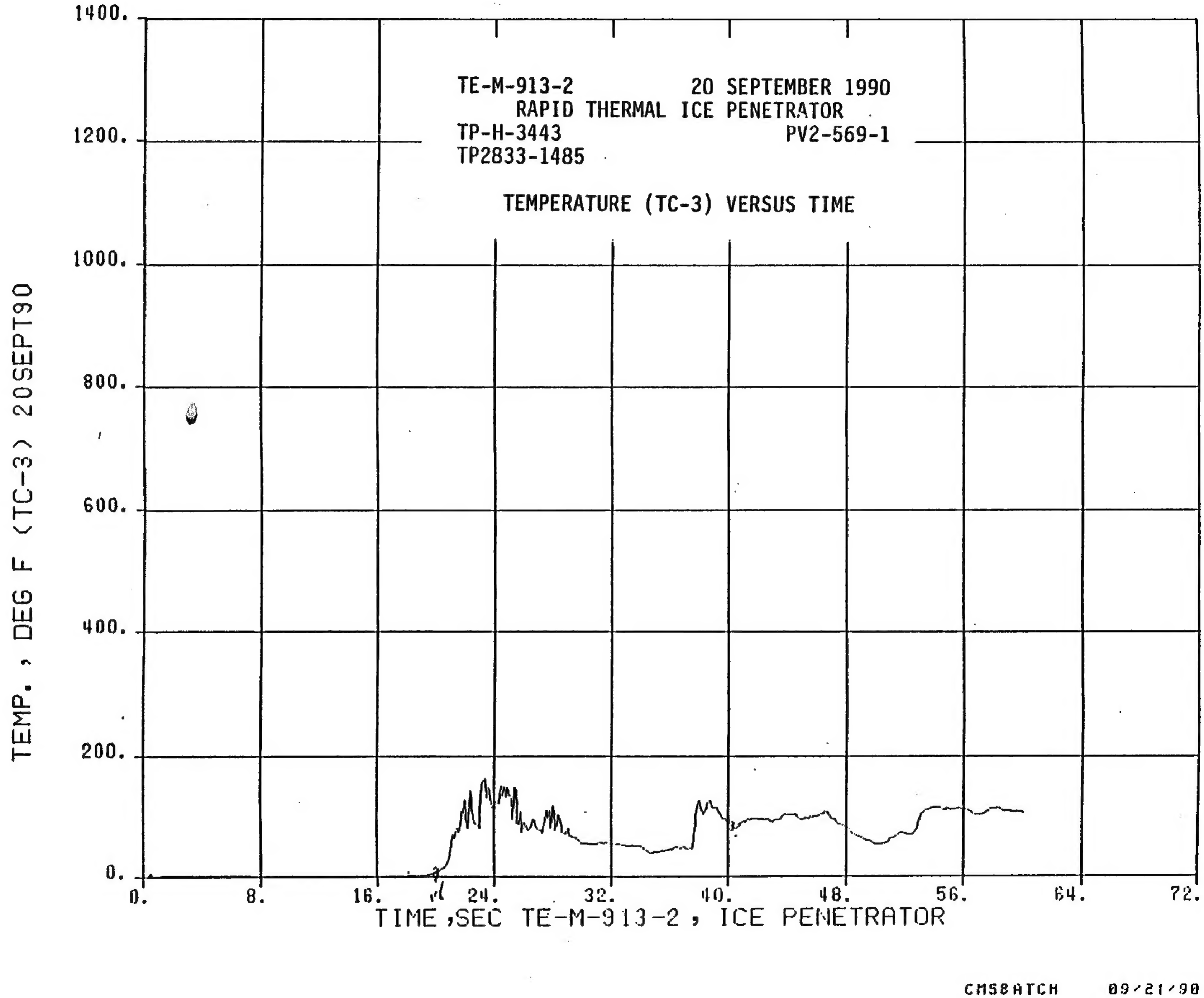
TE-M-913-2
20 SEPTEMBER 1990
RAPID THERMAL ICE PENETRATOR
TP-H-3443
PV2-569-1
TP2833-1485
TEMPERATURE (TC-3) VERSUS TIME
TEMP. , DEG F (TC-3) 20SEPT90
1400.
1200.
1000.
800.
600.
400.
200.
0.
0.
8.
16.
24.
32.
40.
48.
56.
64.
72.
TIME ,SEC TE-M-913-2 , ICE PENETRATOR
CMSBATCH 09/21/90

A!R

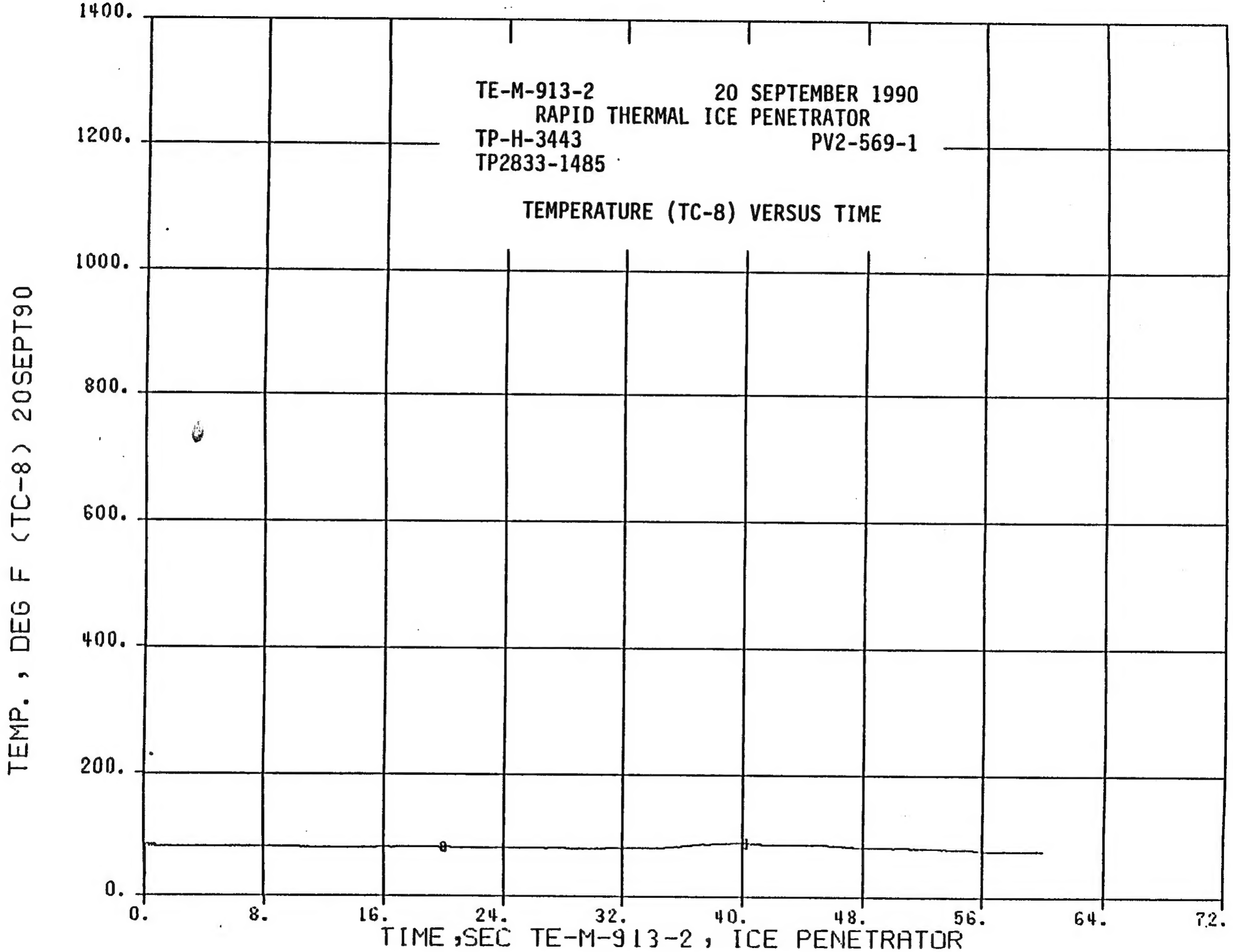

CMSBATCH 09/21/90

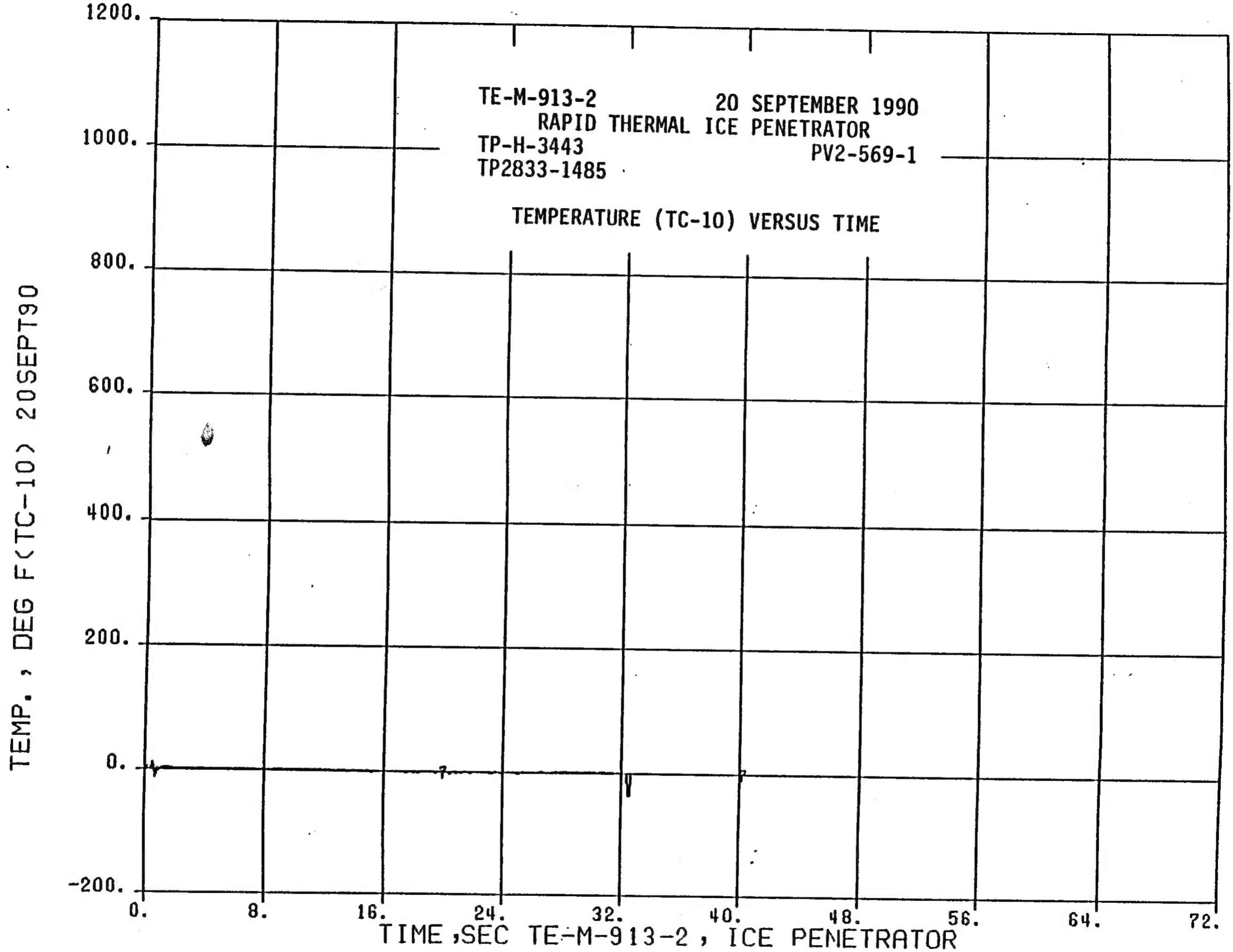

CMSBATCH 09/21/90